Australian Rainfall & Runoff

Revision Projects

PROJECT 7

Baseflow for Catchment Simulation

P7/S1/004

DECEMBER 2009

ENGINEERS
AUSTRALIA
Water Engineering

**AUSTRALIAN RAINFALL AND RUNOFF
REVISON PROJECT 7: BASEFLOW FOR CATCHMENT SIMULATION**

STAGE 1 REPORT – VOLUME 1 - SELECTION OF APPROACH

DECEMBER, 2009

Project Project 7: Baseflow for Catchment Simulation	**AR&R Report Number** P7/S1/004
Date 17 December 2009	**ISBN** 978-085825-9218
Contractor Sinclair Knight Merz	**Contractor Reference Number** VW04648
Authors Rachel Murphy, Zuzanna Graszkiewicz, Peter Hill, Brad Neal, Rory Nathan, Tony Ladson	**Verified by**

ACKNOWLEDGEMENTS

Contractor Details

Sinclair Knight Merz (SKM)
PO Box 2500
Malvern
Victoria 3144

Tel: (03) 9248 3100
Fax: (03) 9500 1180
Web: www.skmconsulting.com

FOREWORD

AR&R Revision Process

Since its first publication in 1958, Australian Rainfall and Runoff (AR&R) has remained one of the most influential and widely used guidelines published by Engineers Australia (EA). The current edition, published in 1987, retained the same level of national and international acclaim as its predecessors.

With nationwide applicability, balancing the varied climates of Australia, the information and the approaches presented in Australian Rainfall and Runoff are essential for policy decisions and projects involving:
- infrastructure such as roads, rail, airports, bridges, dams, stormwater and sewer systems;
- town planning;
- mining;
- developing flood management plans for urban and rural communities;
- flood warnings and flood emergency management;
- operation of regulated river systems; and
- estimation of extreme flood levels.

However, many of the practices recommended in the 1987 edition of AR&R are now becoming outdated, no longer representing the accepted views of professionals, both in terms of technique and approach to water management. This fact, coupled with greater understanding of climate and climatic influences makes the securing of current and complete rainfall and streamflow data and expansion of focus from flood events to the full spectrum of flows and rainfall events, crucial to maintaining an adequate knowledge of the processes that govern Australian rainfall and streamflow in the broadest sense, allowing better management, policy and planning decisions to be made.

One of the major responsibilities of the National Committee on Water Engineering of Engineers Australia is the periodic revision of AR&R. A recent and significant development has been that the revision of AR&R has been identified as a priority in the Council of Australian Governments endorsed National Adaptation Framework for Climate Change.

The Federal Department of Climate Change announced in June 2008 $2 million of funding to assist in updating Australian Rainfall and Runoff (AR&R). The update will be completed in three stages over four years with current funding for the first stage. Further funding is still required for Stages 2 and 3. Twenty one revision projects will be undertaken with the aim of filling knowledge gaps. The 21 projects are to be undertaken over four years with ten projects commencing in Stage 1. The outcomes of the projects will assist the AR&R editorial team compiling and writing of the chapters of AR&R. Steering and Technical Committees have been established to assist the AR&R editorial team in guiding the projects to achieve desired outcomes.

Project 7: Baseflow for Catchment Simulation

An important aspect of flow estimation as distinct from flood estimation is the relative importance of the baseflow component of a hydrograph. Whereas the quickflow component is the most significant component of a hydrograph for flood estimation and the baseflow component is neglected, this is not always the case for general flow estimation. In recent years the need to estimate small flood flows (in-bank floods) has arisen and, therefore, estimation of baseflow needs to be considered within Australian Rainfall and Runoff.

This project focuses on the development of appropriate techniques for estimating the baseflow component of a hydrograph. It is expected that both statistical and deterministic approaches be developed to meet the various needs of the industry.

This project will result only in preliminary guidance in a form suitable for inclusion in Australian Rainfall and Runoff. It is expected that further developments will occur post this edition of Australian Rainfall and Runoff.

The aim of Project 7 is to identify and test techniques for estimation of the baseflow component of a flood hydrograph for situations where the baseflow cannot be neglected as a significant component of the flood hydrograph.

Mark Babister
Chair National Committee on Water Engineering

Dr James Ball
AR&R Editor

AR&R REVISION PROJECTS

The 21 AR&R revision projects are listed below:

ARR Project No.	Project Title	Starting Stage
1	Development of intensity-frequency-duration information across Australia	1
2	Spatial patterns of rainfall	2
3	Temporal pattern of rainfall	2
4	Continuous rainfall sequences at a point	1
5	Regional flood methods	1
6	Loss models for catchment simulation	2
7	Baseflow for catchment simulation	1
8	Use of continuous simulation for design flow determination	2
9	Urban drainage system hydraulics	1
10	Appropriate safety criteria for people	1
11	Blockage of hydraulic structures	1
12	Selection of an approach	2
13	Rational Method developments	1
14	Large to extreme floods in urban areas	3
15	Two-dimensional (2D) modelling in urban areas.	1
16	Storm patterns for use in design events	2
17	Channel loss models	2
18	Interaction of coastal processes and severe weather events	1
19	Selection of climate change boundary conditions	3
20	Risk assessment and design life	2
21	IT Delivery and Communication Strategies	2

AR&R Technical Committee:

Chair   Associate Professor James Ball, MIEAust CPEng, Editor AR&R, UTS
Members   Mark Babister, MIEAust CPEng, Chair NCWE, WMAwater
             Professor George Kuczera, MIEAust CPEng, University of Newcastle
             Professor Martin Lambert, FIEAust CPEng, University of Adelaide
             Dr Rory Nathan, FIEAust CPEng, SKM
             Dr Bill Weeks, FIEAust CPEng, DMR
             Associate Professor Ashish Sharma, UNSW
             Dr Michael Boyd, MIEAust CPEng, Technical Project Manager *

Related Appointments:
Technical Committee Support: Monique Retallick, GradIEAust, WMAwater
Assisting TC on Technical Matters: Michael Leonard, University of Adelaide

* EA appointed member of Committee

PROJECT TEAM

Project Team Members:

- Dr Rory Nathan (AR&R TC Project Manager and SKM)

- Rachel Murphy (SKM)

- Zuzanna Graszkiewicz (SKM)

- Peter Hill (SKM)

- Brad Neal (SKM)

- Dr Tony Ladson (SKM)

- Jason Wasik (SKM)

- Chriselyn Meneses (SKM)

This report was independently reviewed by:

- Erwin Weinmann
- Trevor Daniell (University of Adelaide)

EXECUTIVE SUMMARY

ARR Update Project 7 aims to develop a method for estimating baseflow contribution to different sized flood events across Australia. This report summarises the work undertaken as a part of Phase 1 of the overall project. It focuses on the physical processes of groundwater-surface water interaction, theoretical approaches to baseflow separation, and the testing of these methods to various case study catchments across Australia. The aim of these case studies is to develop a suitable approach for more widescale application.

Streamflow can be considered to comprise of two main components based on the timing of response in a river after a rainfall event. Water that enters a stream rapidly is termed "quickflow" and is sourced from direct rainfall onto the river surface and rainfall-runoff across the land surface. Water which takes longer to reach a river is termed "baseflow" and is sourced primarily from groundwater discharge into the river. Different locations have varying degrees of baseflow contribution to streamflow based on regional hydrogeological conditions.

This current study seeks to develop a consistent approach to incorporating baseflow into design flood estimates. Baseflow has been the subject of much investigation in the past and a range of techniques are available to estimate its behaviour. The focus of this study is to quantify the magnitude of baseflow associated with flood events, regardless of the source of the water or the detailed and often complex physical processes which generate it. For this reason, the study has utilised automated baseflow separation techniques as an investigative tool, rather than more detailed models or field based chemical traces studies of groundwater and surface water interaction.

The magnitude of the peak and the shape of a baseflow hydrograph in flood events is subjective because baseflow is not readily measureable. However, some common features capture the general understanding of the physical processes in action:

- Low flow conditions prior to the commencement of a flood event typically consist entirely of baseflow;
- The rapid increase in river level relative to the surrounding groundwater level results in an increase in bank storage. The delayed return of this bank storage to the river causes the baseflow recession to continue after the peak of the total hydrograph.
- Baseflow will peak after the total hydrograph peak, due to the storage-routing effect of the sub-surface stores;
- The baseflow recession will most likely follow an exponential decay function (a master recession curve); and
- The baseflow hydrograph will rejoin the total hydrograph as quickflow ceases.

Various techniques are available to separate baseflow from gauged streamflow data. These include graphical and automated procedures. The advantage of an automated technique is that it provides an objective, repeatable estimate of baseflow that is comparable over time and between locations. The absolute magnitude of baseflow at individual sites may vary from estimates derived using separation techniques. Studies which require accurate estimates of

baseflow magnitude should therefore be supplemented with detailed at-site investigations of both aquifer and streamflow characteristics, where available.

Historically, most baseflow separation approaches have been developed and applied to daily streamflow data. The focus of this project was on flood events, so it was necessary to identify a method that is suitable for the analysis of hourly streamflow data. A number of different baseflow separation methods were reviewed and trialled at several case study locations to evaluate the suitability of techniques using hourly data.

The outcomes of this testing processs identified that the most plausible baseflow hydrographs were produced when the Lyne and Hollick filter was applied using 9 passes across the hourly data with a filter parameter value of 0.925. Based on analysis at case study catchments, this method produces a plausible baseflow hydrograph for a range of event sizes at eight of the nine case study catchments. The results obtained at one case study site in Western Australia were considered less plausible, and require further analysis. Regionalisation of the method may help to establish an approach that is more suitable across all catchment conditions.

The outcomes from the case study analysis demonstrate that the baseflow contribution to the total flood peak varies depending on event size and location. The proportional contribution of baseflow to the event peak tends to decrease as the magnitude of the total flood event increases. This trend was observed for three different measures of baseflow calculated in this study:

- Event BFI (the ratio of the event baseflow volume to the event streamflow volume);
- Ratio of the baseflow under the streamflow peak to the peak streamflow; and
- Ratio of the peak baseflow to the peak streamflow.

The variability associated with the estimates of baseflow relative to the total streamflow generally decreased with ARI both at individual sites and between sites. Further investigations in Phase 2 of the project may help to explain the reasons for the variability in baseflow contribution to flood peak for low ARIs.

The magnitude of baseflow generally increased as the size of the total flood event increased. This trend was observed when considering the magnitude of the baseflow at the time of the streamflow peak and also the peak baseflow. The magnitude of the baseflow was often easier to predict than other measures of baseflow, with less uncertainty than the results for the proportional contribution to floods.

Catchment characteristics will be extracted for each catchment and summarised in a database and supporting report (SKM, in preparation).

Phase 2 of the study will further refine the recommended baseflow separation approach so that it is applicable across Australia. The adopted technique will be applied to events extracted from hourly data at approximately 250 catchments. An existing automated approach will be refined to better handle the large volumes of data to be processed.

In the next stage of the study, it is intended that the extracted catchment characteristics will be utilised to establish regional prediction equations that will enable the user to estimate baseflow contribution to a design flood event of any size in any region of Australia. Guidelines will then be

prepared to describe the relevant procedures for this application, and will enable incorporation of the method into Australian Rainfall and Runoff.

Table of Contents

1.   Introduction

Guidelines for rainfall-based design flood estimation are contained in Australian Rainfall and Runoff (Institution of Engineers, 1999). The procedure for estimating a design flood hydrograph with specified annual exceedance probability (AEP) for a catchment starts with a design rainfall of the desired AEP. As indicated in Figure 1, the probability of the calculated design flood peak will depend upon the choice of the critical storm duration, areal reduction factor, storm temporal pattern, design losses, runoff routing model, model parameters, and baseflow.
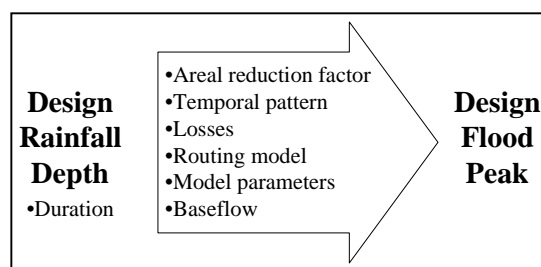
Figure 1 Event Based Design Flood Estimation

Each of these components has a distribution of possible values, so the probability of the calculated flood peak should theoretically account for the effect of the combined probabilities. In the light of the current lack of information on the true distribution of each of the components, and the complexity involved, the recommendation in Australian Rainfall and Runoff is to take some 'central' or 'typical' value for each of the key inputs. Of all of the inputs shown in Figure 1, there is least guidance available in Australian Rainfall and Runoff on appropriate values for the baseflow contribution to design flood estimates.

Book V, Section 2 of Australian Rainfall and Runoff (Cordery, 1998) provides methods for estimating surface runoff during flood events, but does not currently provide any guidance on estimating the component of the flood hydrograph sourced from baseflow. Baseflow is generally a minor component in extreme flood events, but can potentially be significant in smaller flood events. This is particularly the case where the catchment geology consists of high yielding aquifers with large baseflows.

The focus of Australian Rainfall and Runoff Update Project 7 (Baseflow for Catchment Simulation) is to recommend practical yet technically robust preliminary advice on the estimation of baseflow in design flood events for inclusion in Australian Rainfall and Runoff. This report presents the findings of Stage 1 of the project, and summarises data collection and demonstration of the method for baseflow separation to eight case study catchments. The following provides a summary of the report structure:

- Section 2 describes the physical processes associated with baseflow.
- Section 3 summarises the theory of baseflow separation.
- Section 4 outlines the selected baseflow separation technique.
- Section 5 describes the catchment selection process. Further details on this will be provided in a separate report that will accompany the catchment characteristics database (SKM, in preparation).

- Section 6 summarises the data analysis approach.

- Section 7 presents the results of baseflow analysis at each of the case study catchments.

- Section 8 compares the baseflow analysis between catchments.

- Section 9 outlines the next steps in ARR Update Project 7.

- Section 10 provides conclusions from this first stage of the study.

- References and Acknowledgements are provided at the conclusion of the report.

- Appendices provide further information on the comparison of various baseflow separation techniques and baseflow analyses at case study catchments.

It is not expected that the user will need to undertake the analysis contained in this report; rather, the details of this report are relevant to the development of a suitable method for user application.

Stage 2 of the project will be undertaken following the completion of Stage 1, and will cover the
1) Development of prediction equations in case study catchments;
2) Application of the prediction equations across Australia; and
3) Testing of the recommended procedures.
The ultimate objective of the project is to develop prediction equations that will allow the user to estimate baseflow contribution to design flood events at a particular location from a small number of easily measured variables.

2.   Physical Processes Associated with Baseflow

The hydrological cycle consists of constant movement of water within the Earth's environment, comprising processes such as evapotranspiration, precipitation, surface runoff, subsurface flow and groundwater movement. Using the radiant energy from the sun, water is evaporated from water bodies, such as oceans, rivers and lakes, and the land surface, including vegetation, to the atmosphere and is recycled back in the form of rain or snow. When this precipitation falls to the land surface it can move via a number of different interconnected pathways. Precipitation can be intercepted by vegetation, can directly enter surface water bodies or can infiltrate into the ground to replenish soil moisture. Excess water percolates to the saturated zone of the soil profile, from where it moves downward and laterally to sites of groundwater discharge. The rate of infiltration varies with land use, soil characteristics and the duration and intensity of the rainfall event. If the rate of precipitation exceeds the rate of infiltration runoff across the land surface can occur. Water reaching streams, both by surface runoff and groundwater discharge eventually moves to the sea where it is again evaporated to perpetuate the hydrological cycle.

Hence, streamflow can be considered to comprise of two main components based on the timing of response in a river after a rainfall event. Water that enters a stream rapidly is termed "quickflow" and is sourced from direct rainfall onto the river surface and rainfall-runoff across the land surface. Water which takes longer to reach a river is termed "baseflow" and is sourced primarily from groundwater discharge into the river. Groundwater movement is typically a slow process, as a result of the processes described below.

Different locations have varying degrees of baseflow contribution to streamflow based on regional hydrogeological conditions. These can result in streams varying between gaining (receipt of groundwater flow) and losing (discharge to groundwater system) conditions over time and space. Hence, understanding the local characteristics is imperative for detailed analysis of baseflow conditions as many of the automated baseflow separation approaches do not distinguish between these physical states.

Conceptually, groundwater-surface water interaction processes are increased during a flood event, with significantly greater volumes both in the river and the surrounding landscape. Simplistically, a flood event causes a fast but temporary increase in stream water level that moves rapidly downstream under the force of gravity. This increase in water level can lead to a change in hydrostatic pressure between the river and the groundwater in the surrounding bank. In a gaining stream, depending on the hydrostatic pressure in the surrounding aquifer, this can stimulate the movement of flow from the stream to the bank. As the flood peak subsides, water moves back to the stream and the hydrostatic pressure in the river reduces. This temporary storage of water during flood events is known as bank storage. It acts to attenuate the peak of the flood wave by reducing the magnitude and delaying the timing of the total flow peak. The local hydrogeological conditions combined with the specific flood conditions dictate the significance of this process. The interaction of these processes is complex and automated baseflow separation algorithms do not attempt to take these conditions into account.

Commonly, groundwater discharge from aquifers is assumed to represent the baseflow contribution to streamflow. This assumption requires the aquifer to have a groundwater hydrostatic pressure higher than the stream hydrostatic pressure, be regularly (seasonally)

recharged and be made up of materials that support the storage and transmission of flow to the stream (Smakhtin, 2001). In some instances, these assumptions may not reflect the local hydrogeological conditions and other factors may affect the baseflow regime, by mimicking or interfering with the signal usually associated with baseflow. These factors may include:

- Connection with additional water stores – snowpack, bank storage, deeper aquifers and connected lakes can impact on the baseflow regime at a given location contrary to the conditions described above.

- Flow regulation from upstream reservoirs – reservoirs that release outflows that are different to inflows will produce a low flow signal that can be misinterpreted as baseflow at downstream flow gauges. Neal et al (2004) adopted a criterion that not more than 10% of the catchment should be upstream of flow regulating structures when selecting streamflow gauges for regional baseflow assessment, which should be regarded as an upper limit for local investigations.

- Catchment farm dams – high concentrations of catchment farm dams could also influence baseflow but only where the dams are located on-stream or where they interact with groundwater. Many off-stream dams are clay lined specifically to avoid interaction with groundwater.

- Major diversions – diversions for consumptive use, such as irrigation channels and urban diversions, can decrease low flows and hence appear to reduce estimates of baseflow. Allowances can be accurately made for those diversions where they are metered.

- Urbanisation – In urban areas, activities such as excess garden or sports field watering can increase low flows during summer that appear similar to baseflow in streamflow data (Daamen et al, 2006).

- Return flows – Water can be returned to rivers from sewage treatment plants or from industry. Power stations in particular often discharge cooling tower water to streams. This will increase low flows and appear similar to baseflow.

- River evaporation and evapotranspiration – Evaporation from the river surface and plant water uptake will generally be a negligible influence on streamflows for catchments less than 1000 km^2. For larger catchments, baseflow expressed at an upstream location may be reduced at the streamflow gauging station because of reach losses, particularly during summer low flow conditions when baseflow is most evident.

In catchments where in-stream flows are significantly affected by some of the above influences, it may be difficult to separate baseflow. This is discussed further in the following sections.

3. Baseflow Separation Theory

The following section summarises the theory behind baseflow separation. This information is presented to provide context for the selection of the method applied in the catchment analysis (Section 7). It is not anticipated that ARR users will be required to separate baseflow in their analysis; rather, the final outcomes of this project will provide users with a method to estimate baseflow contribution to flood events based on readily available catchment characteristics. The contents of this report represent the first phase of the development of this method.

3.1. Components of streamflow

Streamflow is made up of a number of components including baseflow, which is sourced from groundwater aquifers, and quickflow, which is sourced from surface runoff. The boundary between each of these sources of water is difficult to distinguish in practice. River channel precipitation and evapotranspiration also occurs, but is generally small and indistinguishable from other components of streamflow.

Strict definitions of baseflow are difficult to formulate but in general terms baseflow represents river flow sourced from groundwater aquifers.

Groundwater and surface water interaction can occur from the stream to groundwater, vice versa or in both directions at different times, depending on river and groundwater levels and hydrogeologic conditions. Baseflow separated from streamflow data at a gauging station location represents the estimate of baseflow from all of the catchment upstream of that gauging station. In practice, only part of the upstream river reaches may be receiving baseflow, whilst other reaches may be losing water to groundwater. The baseflow observed at the streamflow gauge represents the net effect of these upstream processes.

The time lag for the expressions of each of these components of streamflow after rainfall can vary considerably. Quickflow occurs immediately after rainfall, with interflow taking slightly longer to travel through the unsaturated soil profile, while baseflow may take several hours to several days or years to respond to rainfall.

3.2. General characteristics of baseflow

The shape of a baseflow hydrograph is partly subjective, although some common features should be captured in the baseflow curve, as presented by Nathan and McMahon (1990) and Brodie and Hostetler (2005):

- Low flow conditions prior to the commencement of a flood event consist entirely of baseflow;
- The rapid increase in river level relative to the surrounding groundwater level results in an increase in bank storage. The delayed return of this bank storage to the river causes the baseflow recession to continue after the peak of the total hydrograph;
- Baseflow will peak after the total hydrograph due to the storage-routing effect of the sub-surface stores;
- The baseflow recession will most likely follow an exponential decay function (a master recession curve) except in ephemeral streams; and
- The baseflow hydrograph will rejoin the total hydrograph as quickflow ceases.

3.2.1. Recession analysis

Following a flood event, the streamflow hydrograph typically diminishes quite steeply but slows over time. This results in a reasonably flat component of the hydrograph at the end of the runoff event, which is comprised primarily of baseflow and continues until another runoff event occurs.

At a given location, comparison of a number of recession curves will typically highlight a consistent shape that follows an exponential decay response. This characteristic response is termed the master recession curve, which represents the average catchment flow recession unaffected by precipitation (Figure 2). The master recession curve can be represented by the relationship

$$Q = Q_0 k^t$$

<div align="right">**Equation 1**</div>

Where Q_0 =Initial streamflow

            k = Recession constant

            t = time

The master recession curve can be used to estimate baseflow during periods of pure recession (no quickflow). The recession constant can be an hourly or daily value, depending on the time step of the data being analysed, and can also be used in a number of the baseflow separation methods described below. In the figure below, the master recession curve has been defined with k = 0.98 and the half flow period (HFP) = 34.
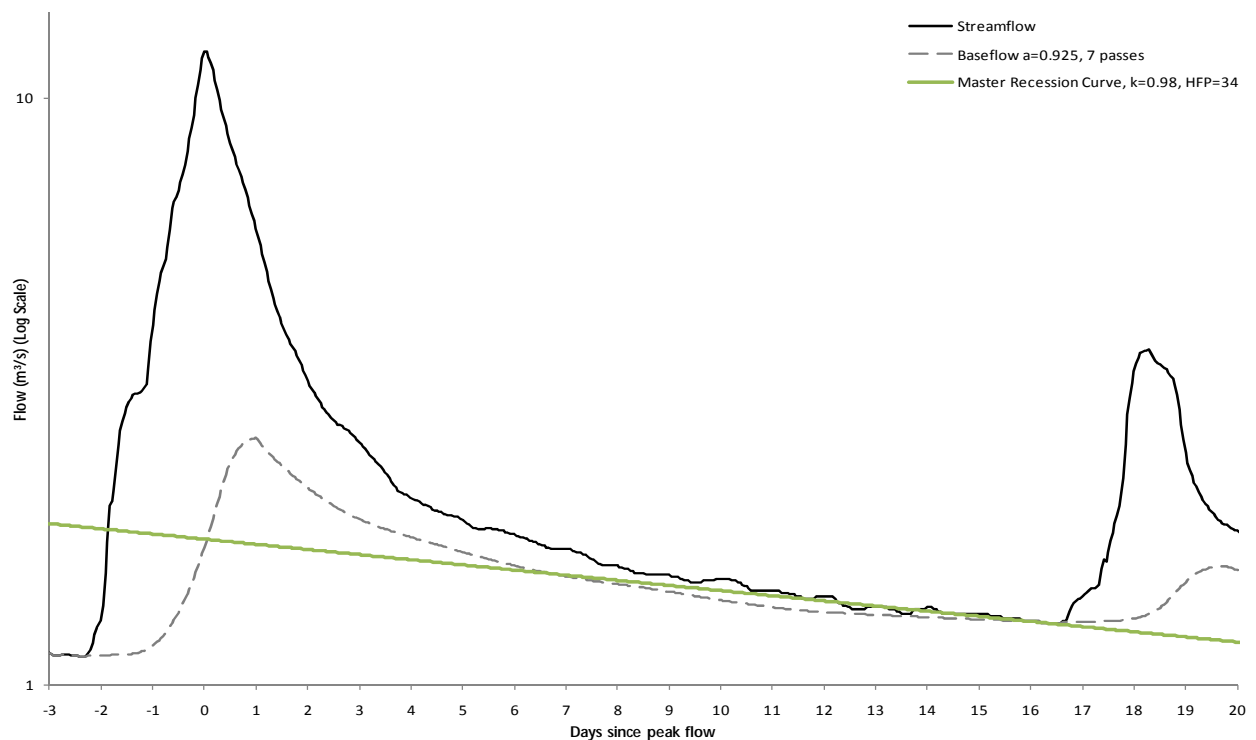
Figure 2 Example master recession curve, applied to an event observed in the Little Yarra River at Yarra Junction, Victoria (Gauge number 229214) for February, 1996

Techniques for developing a master recession curve are documented in Nathan and McMahon (1990) and Brodie and Hostetler (2005). Of these techniques, the matching strip method is reasonably robust and in wide application. The matching strip method involves lining up the tails of different hydrograph events on a logged vertical axis until they match to reveal a single slope, which defines the master recession curve. It is possible that the master recession curve can have more than one equation over different flow ranges, corresponding to different discharge rates from different aquifers connected to the stream. In some cases, this is a result of different groundwater conditions that occur during the seasons.

3.3.   Baseflow separation techniques

Various techniques are available to separate baseflow from gauged streamflow data. These include traditional graphical procedures and more recent automated procedures. It is important to note that although all baseflow separation techniques, either graphical or automated, are suitable for comparative analysis to ascertain relative baseflow contributions between sites or at the same site over time, quantitative determination of the absolute magnitude of baseflow is not achievable through baseflow separation alone. Baseflow hydrographs for detailed at-site investigation should be conditioned by local knowledge of both aquifer and streamflow characteristics, regardless of the baseflow separation technique applied.

Given the above constraints, quantification of the baseflow volume for any given flood event requires the application of a robust baseflow separation technique that identifies a reasonable baseflow hydrograph. The follow discussion presents a summary of the general characteristics of baseflow, and baseflow separation approaches that attempt to interpret these characteristics in defining a baseflow hydrograph.

Most of the approaches described below have been developed for application on daily streamflow data. Given the focus of this project on flood events, it is necessary to identify a method that is suitable for the analysis of hourly streamflow data. A number of the methods identified in the literature review were tested for this purpose. Details of these trials are provided in Appendix A.

3.3.1. Graphical procedures

Graphical procedures for separating baseflow use a variety of techniques, outlined in Viessman et.al. (1977), Maidment (1993) and Brodie and Hostetler (2005). In the simplest form, these approaches partition the baseflow on a hydrograph using a combination of segments, which may assume:

- Constant baseflow over the course of the runoff event (constant discharge method), depicted by the dashed line A-B in Figure 3;

- A linear reduction in baseflow during the rising limb of the flood event followed by a linear increase in baseflow as the flood recedes (concave method) shown by long dashed lines A-C-D in Figure 3;

- A master recession curve that describes the shape of the hydrograph once streamflow diminishes can estimate the baseflow under the flood peak. The master recession curve is projected backwards and connected to the start of the runoff event arbitrarily, as indicated by the crossed lines A-E-F in Figure 3; and

- A linear baseflow response that declines over the duration of the runoff event, demonstrated by the dashed and dotted line A-F in Figure 3.

Further graphical procedures have also been developed, each with slight variations on the characterisation of baseflow during runoff events. For example, refer to Boughton (1988) which presents ten different approaches to graphical baseflow separation that have been proposed by a number of authors since 1921.

From these graphical procedures, the approach most grounded in observed baseflow properties utilises the master recession curve at the start and end of the surface water event to define the rate of departure of the baseflow from the total flow hydrograph. Thereafter, the most realistic approach is similar to lines ACDB and AEF in Figure 3, but acknowledges that baseflow response is likely to be non-linear and that peaks and troughs will lag behind surface water peaks and troughs because baseflow is heavily damped. This most likely baseflow hydrograph is depicted by the red line in Figure 3, the curvature of which relies on subjective judgement. Tracer studies (refer to Section 3.3.4) can provide some guidance as to the expected shape of the baseflow response. The other representations presented in Figure 3 are based on simplifying assumptions that may introduce errors into the predicted estimation of baseflow (Tan et al, 2009a).

In general, graphical approaches to baseflow separation are complicated when considering continuous periods of data rather than individual events, as the presence of successive peak flow events can make it difficult to isolate baseflow contribution. Furthermore, graphical approaches to baseflow separation require manual analysis and are not easily nor quickly applied over extended periods of data (Chapman and Maxwell, 1996).
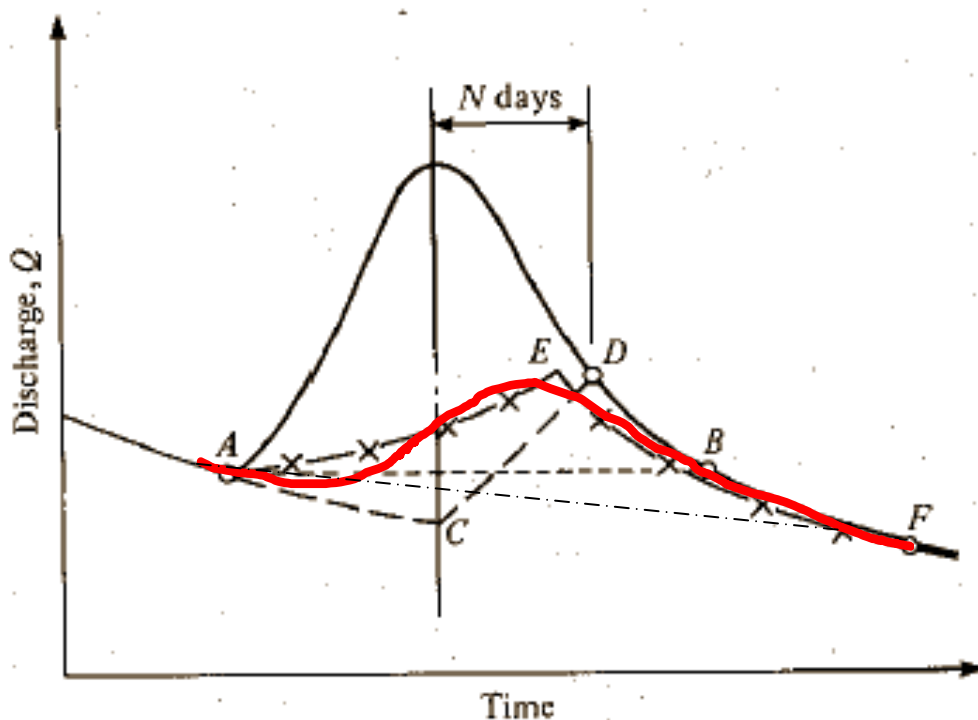
Figure 3 Baseflow separation hydrographs (Viessman et.al., 1977)

An empirical relationship defined by Linsley et al (1982) postulated that the duration of the quickflow event could be estimated based on the catchment area:

$N=0.8A^{0.2}$

<div align="right">**Equation 2**</div>

where N is the number of days from the storm event crest and A is the catchment area in km^2.

This method provides an approximation for the end of the streamflow event based on readily available catchment details, and can help to identify the relevant end-point to apply in the graphical separation approaches described above. This approach calculates a consistent event duration regardless of the antecedent conditions and event magnitude, which may not be representative in all conditions. It should be noted that Book V, Section 2 of Australian Rainfall and Runoff (Cordery, 1998) recommends against the use of empirical formulae such as this, given the lack of evidence supporting the relationship for Australian conditions.

3.3.2. Automated procedures

Automated procedures predominantly involve the use of digital filters that have their basis in signal analysis and processing, and apply mathematical rules to separate baseflow. As such, these approaches do not consider the physical processes that occur during runoff events in order to isolate baseflow. Rather, automated approaches aim to establish a simple, repeatable process to estimate baseflow from streamflow time series data.
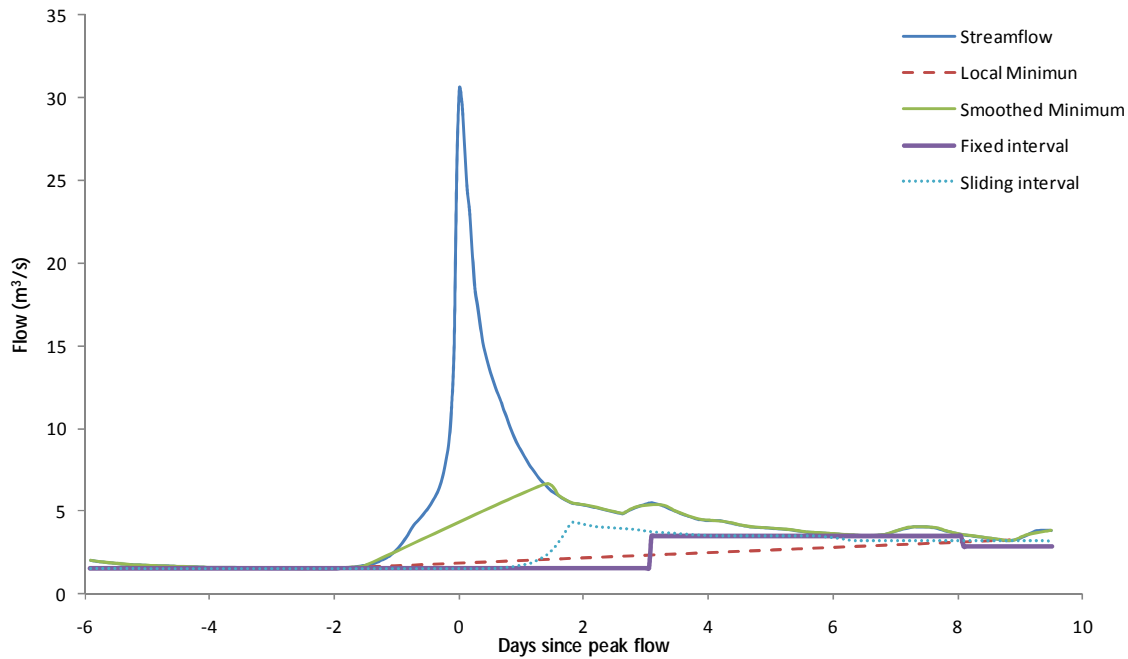
Automated baseflow separation techniques are documented in a number of publications, including Grayson et.al. (1996), Nathan and McMahon (1990) and Brodie and Hostetler (2005).

Simple filtering methods include those that analyse discrete periods of the streamflow timeseries to identify particular characteristics in the streamflow data which are used to estimate baseflow. Characteristics of interest include:

- The local minima within periods of streamflow (the period is equal to double the quickflow duration, calculated using the empirical relationship described by Equation 2), which are connected via straight lines to approximate the baseflow timeseries (local minimum method).

- The minimum streamflow within non-overlapping periods of 5 days duration, of which the turning points are connected using straight lines to estimate baseflow (smoothed minima technique).

- The minimum streamflow within discrete intervals of fixed duration (equal to double the quickflow duration), which is assigned to all time intervals within the duration to estimate the baseflow timeseries (fixed interval method).

- The minimum streamflow record within a fixed period (equal to double the quickflow duration), which is assigned to the median time value in the period and repeated on each time step to estimate the baseflow timeseries (sliding interval method).

These approaches each generate a time series that can include step changes in baseflow over time (for instance, refer to Figure 4, which presents the baseflow as calculated using these four different approaches for site 229214 in the Yarra River basin, Victoria), in response to the 'blocky' discretisation of data for analysis. Other algorithms for baseflow separation are available

to generate a smoother baseflow response, and these represent approaches that are relevant when considering an extended period of streamflow data.

Figure 4 Simple automated baseflow separation techniques, applied to an event observed in the Little Yarra River at Yarra Junction, Victoria (Gauge number 229214) for September 1984

Chapman (1991) and Chapman and Maxwell (1996) describe an approach that utilises the recession constant of the hydrograph, which represents the ratio of the flow to the proceeding flow during a period of no direct runoff (quickflow). This filter (Equation 3, shown in simplified form) is based on the assumption that the baseflow is a weighted average of the quickflow and the baseflow at the previous time interval and only requires a single pass through the data.

$$q_b(i) = \frac{k}{(2-k)} q_b(i-1) + \frac{(1-k)}{(2-k)} q(i), \text{ subject to } q_b(i) \leq q(i)$$

Equation 3

Where $q_b(i)$ = the filtered baseflow response for the ith sampling instant

                   $q(i)$ = the original streamflow for the ith sampling instant

                   k = filter parameter equivalent to the recession constant

The recession constant in this algorithm can be estimated by analysing the shape of the recession period of the runoff hydrograph and through the development of a master recession curve. Approaches to calculate the constant are widely available, although many these are not generally easily automated. Nathan and McMahon (1990) describe two common methods that have been applied in an automated manner: the correlation method (Langbein, 1938) and the matching strip method (Snyder, 1939). More recently, Mandeville (2004) developed the reservoir inflow sequence (RIS) approach which reduces the subjectivity associated with master recession curve fitting. These methods provide guidance on the recession periods of runoff events, and do not inform the shape of the baseflow series at other times.

Additional flexibility was incorporated to Equation 3 by modifying the algorithm to include an additional parameter value (Boughton, 1993; Chapman and Maxwell, 1996). This algorithm (Equation 4) is passed through the data once.

$$q_b(i) = \frac{k}{(1+C)}q_b(i-1) + \frac{C}{(1+C)}q(i), \text{ subject to } q_b(i) \le q(i)$$

Equation 4

Where $q_b(i)$ = the filtered baseflow response for the *i*th sampling instant

$q(i)$ = the original streamflow for the *i*th sampling instant

k = filter parameter equivalent to the recession constant

C = additional parameter value to alter the shape of the baseflow separation

In this form, it has been recommended that the parameter values be selected based on inspection of the shape of the resulting baseflow separation at the end of the quickflow, particularly for large events (Chapman and Maxwell, 1996). As such, this algorithm incorporates increased complexity (with two parameter values to fit) and additional subjectivity (as the selection of appropriate parameter values is no longer directly related to known processes). This algorithm has been applied to match flow path separation data for storm events from tracer studies (Chapman and Maxwell, 1996).

An alternative approach developed by Jakeman and Hornberger (1993) formulated the IHACRES method (Equation 5). This approach employs three parameters, adding complexity to partitioning of a reasonable baseflow estimate.

$$q_b(i) = \frac{k}{(1+C)}q_b(i-1) + \frac{C}{(1+C)}[q(i) - \alpha q(i-1)], \text{ subject to } q_b(i) \le q(i)$$

Equation 5

Where $q_b(i)$ = the filtered baseflow response for the *i*th sampling instant

$q(i)$ = the original streamflow for the *i*th sampling instant

k, C and α = filter parameters

In a study which applied the above three methods to partition baseflow from streamflow data (Chapman, 1999), it was concluded that the two parameter algorithm (Equation 4) produced the most satisfactory results. However, Chapman achieved little success in applying optimisation techniques to identify suitable parameter values for this algorithm even when compared to data from tracer experiments, and noted the subjective nature of the parameter selection (specifically the C parameter) as an issue. Both Equation 3 and Equation 5 were observed to generate implausible separations for some catchments. In particular, Equation 3 has been observed to limit the BFI to 0.5, which is considered an unrealistic constraint particularly in locations where streamflow is largely fed by groundwater discharge (Tan et al, 2009b).

Alternative approaches have also been proposed that build on the digital filters presented above. Eckhardt (2005) developed a modified algorithm based on the theory that all one-parameter algorithms are special cases of a two-parameter relationship, which can be explained with the use of the recession constant (objectively defined) and the BFI_{max} (which cannot be measured).

$$q_b(i) = \frac{k(1 - BFI_{\max}) + q_b(i-1) + (1-k)BFI_{\max}q(i)}{1 - kBFI_{\max}}, \text{ subject to } q_b(i) \leq q(i)$$

Equation 6

Where $q_b(i)$ = the filtered baseflow response for the *i*th sampling instant

$q(i)$ = the original streamflow for the *i*th sampling instant for the first pass

k = filter parameter equivalent to the recession constant

BFI_{max} = maximum value of the long term ratio of baseflow to total streamflow

The subjectivity that this approach is acknowledged by the author, who attempted to find typical BFI_{max} values for various classes of catchments, but notes that the analysis is far from complete. Despite this, the Eckhardt approach has been compared to other digital filters (specifically Equation 7) with good results, and it is considered that Equation 6 can reasonably reproduce baseflows estimated from manual separation or measured through field monitoring (Lim et al, 2005).

Consequently, literature concedes that digital filter algorithms that include more than one parameter are generally associated with subjectivity in determination of their parameter values (Tan et al, 2009b). Digital filters that are controlled using a single parameter value are more widely applied for hydrograph separation, particularly where the parameter value is represented by the recession constant which can be estimated through recession analysis. Such approaches reduce the uncertainty and subjectivity in the partitioning of baseflow from streamflow.

Lyne and Hollick (1978) developed an alternative baseflow separation filter that is described in Equation 7 and is based on the assumption that the filtering of baseflow from quickflow is analogous to the approach taken in the analysis of other high frequency signals.

$$q_f(i) = kq_f(i-1) + \frac{[q(i) - q(i-1)] \times (1+k)}{2}, \text{ subject to } q_f(i) \geq 0 \text{ and } q_b(i) = q(i) - q_f(i)$$

Equation 7

Where $q_b(i)$ = the filtered baseflow response for the *i*th sampling instant

$q_f(i)$ = the filtered quickflow response for the *i*th sampling instant

$q(i)$ = the original streamflow for the *i*th sampling instant for the first pass

k = filter parameter, equivalent to the recession constant

Nathan and McMahon (1990) concluded that, when applied at a daily timestep, a filter parameter of 0.925 was most appropriate to their case study locations in southern Australia, and changing the parameter by ±3% impacted on the BFI by up to +14% and -26%. Work undertaken for the Department of Agriculture, Fisheries and Forestry (SKM, 2007) that considered 11 catchments in Victoria, NSW and Queensland identified that there was no single value of the parameter that could be used universally to match the output baseflow index from a manual baseflow separation; rather, plausible baseflow separations were obtained when parameter values within the range of 0.90 – 0.99 were applied. The selection of an appropriate parameter value for different sized storm events was considered in Tan et al (2009b), which concluded that the recession constant is independent of the storm event but sensitive to catchment characteristics.

The filter is passed through the data three times (forwards, backwards and forwards again), with the (*i-1*) sampling timestep replaced by (*i+1*) for the backwards pass. After the first forwards pass, *q(i)* is replaced by the computed baseflow from the previous pass. These passes act to smooth the data.

Chapman and Maxwell (1996) are critical of the Lyne and Hollick filter due to its inherent assumption that the baseflow is constant when there is no quickflow. Chapman (1991) observed differences in the baseflows generated using Equation 3 and Equation 7, commenting that the Chapman method appeared to produce a more plausible result. However in that study, the filter was only passed over the data a single time, in contrast to the recommended three passes. This emphasises the importance of the multiple passes on the resulting partitioned baseflow. In contrast, Tan et al (2009b) compared Equation 3 and Equation 7 for 94 hydrograph records and observed no significant difference between the BFI obtained using the two methods, particularly when the parameter value was greater than 0.98. As the k value decreases, the difference in BFI of the two approaches increases, due to the maximum BFI constraint of 50% for the Chapman algorithm. Unrealistic baseflow hydrographs were produced using Equation 3 for parameter values less than 0.96, and that approach was not recommended for catchments fed largely from groundwater.

Whilst the approaches described previously have a more theoretical basis for application to baseflow, Equation 7 has been widely applied to catchments across Australia in Nathan and McMahon (1990), Nathan and Weinmann (1993), Neal et al (2004) and SKM (2007). Furthermore, Tan et al (2009a) observed that the technique was capable of reliably reproducing the physical processes of subsurface flow. Nathan and McMahon (1990) also observed that the Lyne and Hollick filter produced more stable estimates of the BFI compared to the smoothed minima technique, and was more suitable in cases with lower baseflow contributions. The digital filter was found to be a fast and objective method of separating baseflow from a continuous data set. The approach has also been successfully compared with graphical approaches (Arnold et al, 1995), the PART model (Rutledge, 1992; Rutledge and Daniel, 1994) and measured estimates of groundwater discharge to streams (Arnold and Allen, 1999) in American catchments. Mau and Winter (1997) observed that Equation 7 compared well with manual (graphical) procedures when a reasonable filter parameter value was applied, while Tan et al (2009a; 2009b) successfully compared the approach to graphical techniques and Equation 3 for catchments in Singapore, and Mugo and Sharma (1999) applied the technique in Kenya.

More recently, Schwartz (2007) developed an alternative baseflow separation algorithm that incorporates an exponential recession on the falling limb of the hydrograph, unlike many of the approaches described above. The approach requires the application of separate algorithms for the falling and rising limb components of the streamflow time series, as per Equation 8 and Equation 9 respectively.

$$\text{For the falling limb: } q_b(i) = q_b(i-1)e^{-k}, \text{ subject to } k \geq 0$$

Equation 8

Where $q_b(i)$ = the filtered baseflow response for the ith sampling instant

k = filter parameter

$$\text{For the rising limb: } q_b(i) = q_b(i-1)\exp\left(\frac{\alpha\overline{q(\iota)}}{q_b(i-1)}\right), \text{ subject to } \alpha \geq 0$$

Equation 9

Where $q_b(i)$ = the filtered baseflow response for the ith sampling instant

$\overline{q(\iota)} = n^{-1}\sum_{j=0}^{n-1} q(i-j)$, representing the average observed discharge over the last n sampling instants

α = filter parameter affecting the responsiveness to rising streamflow

For both components of the response, an additional parameter (γ) is introduced such that

$$q_b(i) \leq \gamma q(i) \text{ except when } q_q(i) = 0 \text{ and } q_b(i) > \gamma q(i)$$

Equation 10

This method requires hydrologic judgement in parameter selection, although the author regards this as advantageous since it provides the ability to modify the resulting baseflow series based on application specific needs. This method is deemed unsuitable for applications that require consistent comparisons of baseflow between sites (Schwartz, 2007).

Frolich (1994) developed an approach that made use of the master recession curve for the receding limb of the runoff event to establish a lower limit of baseflow, and took an average of the streamflow and this lower limit to derive the baseflow series. This approach results in a baseflow series that essentially follows a similar shape to the original streamflow series.

Principles of signal processing theory were utilised by Spongberg (2000) to optimise the isolation of baseflow. Fourier transformation was applied based on the assumption that baseflow is a low frequency component and runoff is a high frequency component of the streamflow time series. The signal processing challenge is a result of the overlapping frequency content of these two series. Fourier spectral analysis, specifically frequency transfer functions, were applied as a diagnostic tool to quantify the attenuation and phase altering characteristics of isolating baseflow as a function of frequency. The author concludes that each pass of a filter, such as the Lyne and Hollick filter, attenuates the baseflow signal. In combination with this, the magnitude of the filter

parameter also impacts on the attenuation. Each pass of the filter also distorts the phase of the original streamflow time series, although reverse passes help to correct this effect. Spongberg (2000) recommends optimal application of the Lyne and Hollick filter, from a mathematical perspective, is achieved with two passes of the filter using a relatively large filter parameter value. This is considered to remove most of the runoff signal while minimising phase distortion and baseflow attenuation. However, the baseflow series that results from this approach does not exhibit the typical baseflow characteristics of a delayed peak relative to the streamflow peak. Hence, there is a compromise between achieving an optimal mathematical solution and a plausible baseflow series when applying this approach.

Typically, the algorithms presented above have been applied to daily streamflow data. For the purposes of quantifying baseflow contribution to flood events, it is necessary to consider streamflow data collected on a more frequent time step. This is necessary so as to capture the full variation in flows due to the rapid generation of runoff from rainfall within the catchment. Tularam and Ilahee (2008) considered the application of two models (consistent with Boughton, 1988) on an hourly basis, using the relationship in Equation 11.

$$q_b(i) = \alpha q(i) + (1 - \alpha)q_b(i - 1), \text{ subject to } q_b(i) \leq q(i)$$
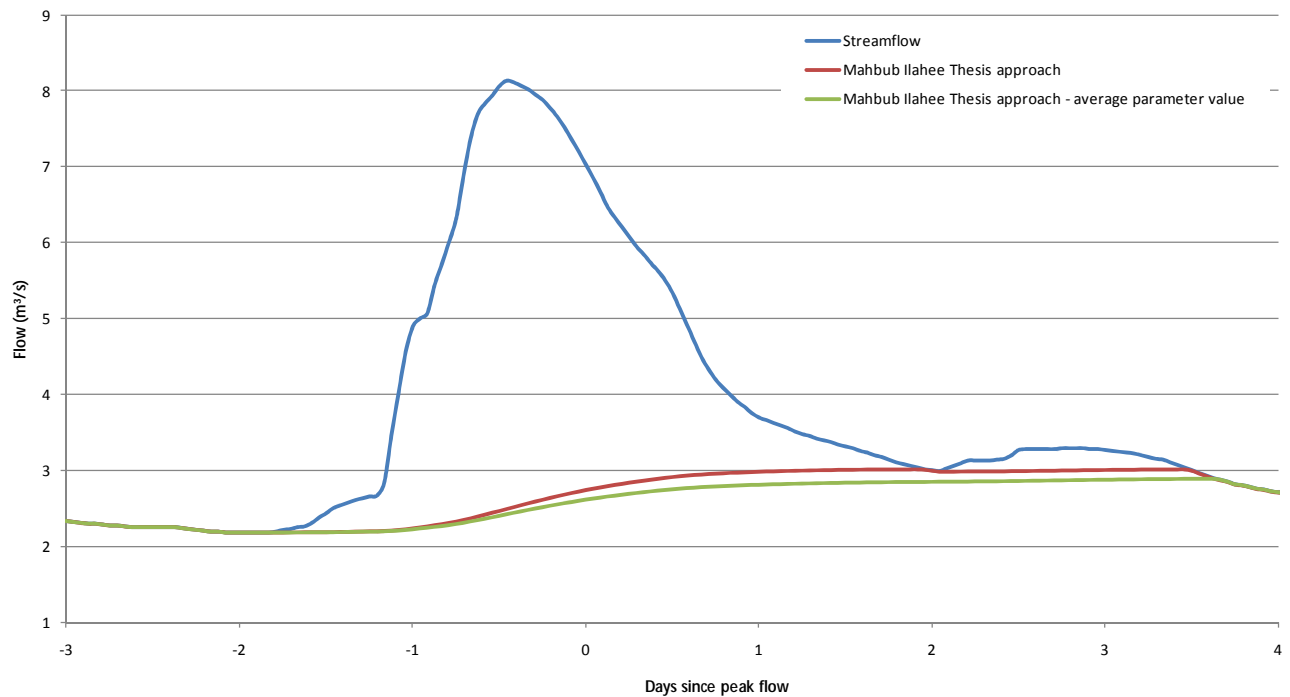
Equation 11

Where $q_b(i)$ = the filtered baseflow response for the ith sampling instant

$q(i)$ = the original streamflow for the ith sampling instant

α = filter parameter

In this assessment, the filter parameter represents a fraction of the quickflow and was selected by trial and error and sensitivity testing across a number of stream flow events. In practice, the application of this approach yields a baseflow series that appears to follow a somewhat unlikely shape, with a rapid increase around the time of the flow peak followed by a constant baseflow volume until the streamflow series is again intersected (Figure 5). In some instances, the separated baseflow intersects quite high up the streamflow hydrograph while in other instances the converse occurs, making it difficult to generate a plausible baseflow series across a range of flood event sizes,

Figure 5 Comparison of baseflow techniques for 1 in 1 year event at Little Yarra River, Victoria using hourly data

The testing of other baseflow separation processes (as described in Equation 3 to Equation 10) on an hourly basis was considered necessary to obtain a reasonable baseflow series for the purposes of this study.

3.3.3. Physically based approaches

Understanding of the general physical processes that result in baseflow is well documented. However, in most instances, detailed hydrogeological analysis has not been undertaken at study catchments to link the local conditions to the generalised theoretical concepts. Integrated groundwater and surface water process models attempt to do this, and offer an alternative approach to estimating baseflow. The explicit modelling of physical processes in models such as TOPOG and SHE can provide one of the best means of quantifying the absolute volume of groundwater flow. These models typically involve the concurrent calibration of groundwater and surface water models, allowing a good understanding of the relationships between surface and groundwater resources. Thus, baseflow can be determined based on the total stream flow and the groundwater levels, rather than subjective separation techniques.

However, these approaches are very demanding in terms of both resources and data due to the complexity of the models, and do not provide a simple method that can be rapidly applied across numerous case study locations.

More generalised theoretical approaches include that presented by Szilagyi and Parlange (1998; Szilagyi, 1999) which utilise the Boussinesq equation to describe the baseflow process. However such techniques only provide a solution for the receding limb of quickflow, and do not offer guidance on the shape of the baseflow under the flood event. Szilagyi and Parlange (1998) provide a simple option, and use straight line to connect the runoff hydrograph at the start of the event with the estimated baseflow peak. Lin et al (2007) present an alternative technique for

baseflow separation based on analytical solutions of the Horton infiltration capacity curve. The approach requires three parameter values to be determined via solution of simultaneous equations, which results in a complex method. However, the approach does reduce the subjectivity of the baseflow hydrograph rising limb that is a limitation of the method postulated by Szilagyi and Parlange (1998).

In seeking to estimate the shallow groundwater balance in a semi-arid catchment in Western Australia, Wittenberg and Sivapalan (1999) developed a method that uses baseflow recession analysis to estimate a storage-discharge relationship for the groundwater aquifer. An iterative approach is required to solve for the required parameters at different time steps, to establish seasonally appropriate parameters. Any improvement in accuracy gained from the more accurate recession characterisation would need to be considered in light of the increased computational effort to determine the appropriate parameters for each site.

Furey and Gupta (2001) proposed a physical filter based on a mass balance equation for baseflow from a hillside (Equation 12).

$$q_b(i) = (1 - \gamma)q_b(i-1) + \gamma \left(\frac{c_3}{c_1}\right)[q(i-d-1) - q_b(i-d-1)]$$

Equation 12

Where $q_b(i)$ = the filtered baseflow response for the ith sampling instant

$q(i)$ = the original streamflow for the ith sampling instant

γ, c_1 and c_3 = physically based filter parameters

d = recharge delay time

Parameter values for this approach are well defined in a physical sense. In this form, the Furey and Gupta method is considered to be more complex than most digital filters given that parameter values must be determined based on the analysis of other available data (Lin et al, 2007). Alternatively, manual manipulation of particular parameter values is suggested by the authors to improve the estimation of baseflow. The algorithm is applied forward in time, and is not subject to constraints, which results in the possibility that baseflow can exceed streamflow and be negative. Results presented in Furey and Gupta (2001) indicate that the algorithm works well over long timescales, but is frequently poor over shorter periods as the baseflow often exceeds streamflow unless the approach is constrained. A modified version of the algorithm was presented in Furey and Gupta (2003), which also provides time series estimates of soil moisture, however the baseflow estimates were observed to only marginally improve with the increased model complexity.

3.3.4. Approaches based on chemical composition

Information on stream chemical composition can be utilised to understand the source of various components of streamflow, such as, baseflow, overland flow, direct precipitation and subsurface storm flow. These approaches are based on tracing contaminant and conservative ion concentrations that occur in the various water sources, based on the assumption that the tracer concentrations are significantly different in each source.

Further details of baseflow partitioning methods that utilise chemical composition can be found in a number of references including Pilgrim et al (1979), Rice and Hornberger (1998) and Jones et al (2006).

The results of tracer studies have been used for comparison to baseflows generated through digital separation techniques, and generally, the outcomes of tracer studies have demonstrated that actual baseflow contribution is often vastly different to the baseflow series produced by partitioning the streamflow data using the methods described above. Newbury et al (1969) compared the approximations of two simple baseflow separations with the results obtained based on the dilution of the $SO_4^=$ ion. The results of this geochemical analysis produced a more sharply varying response than that estimated by the simple separation methods. Chapman and Maxwell (1996) also compared their digital filters to tracer results in a number of catchments with similar observations. Chapman and Maxwell were able to replicate the sharp tracer response by arbitrarily modifying filter parameters until a reasonable fit was achieved.

Given that such methods require extensive monitoring of field conditions and that this data does not exist historically, the use of tracer studies are not considered relevant for application in this assessment, with a simpler and more widely applicable approach more appropriate.

3.4.   Requirements of baseflow separation technique

Zhang et al (2005) identified the following three basic principles for hydrograph separation that are relevant for this current study:
1) The separated quickflow and baseflow hydrographs should follow the hydrological physical process;
2) The separated baseflow hydrograph should be consistent with the groundwater routing hydrograph; and
3) The hydrograph separation approach must have an objective and feasible procedure.

In general, the specific approach employed for the separation of baseflow from streamflow data depends on the nature of the study being undertaken. All baseflow separation techniques, either graphical or automated, are suitable for comparative analysis to ascertain the relative contributions between sites, or at the same site over time. However, in reality, accurate quantitative determination of the absolute magnitude of baseflows is not achievable without site specific knowledge of the local aquifer and streamflow characteristics, and further details of physical processes (such as those based on tracer studies).

For the purposes of understanding the contribution to a flood event, it is reasonable to approximate the baseflow volume through the application of an automated approach. In the context of this study, any number of the techniques described may be applicable for the separation of baseflow.

4. Selected baseflow separation technique

This current study seeks to develop a consistent approach to incorporating baseflow into design flood estimates. Baseflow has been the subject of much investigation in the past and a range of techniques are available to estimate its behaviour. The focus of this study is to quantify the magnitude of baseflow associated with flood events, regardless of the source of the water or the detailed and often complex physical processes which generate it. For this reason, the study has utilised automated baseflow separation techniques as an investigative tool, rather than more detailed models or field based chemical traces studies of groundwater and surface water interaction.

The literature reviewed in the previous section demonstrates that all automated baseflow separation approaches are somewhat arbitrary. However, research has also demonstrated that some approaches provide reasonable estimates of baseflow that are fit for purpose.

In order to identify an approach suitable for widescale application for this current study, a number of the methods summarised in Section 3 were tested. This section summarises the rationale used to select a baseflow separation technique for application in this study.

As identified in the literature review, most baseflow separation approaches have been developed for application on daily streamflow data. Given the focus of this project on flood events, it is necessary to identify a method that is suitable for the analysis of hourly streamflow data. A number of the methods identified in the literature review were tested for this purpose. Details of these trials are provided in Appendix A, and the key components of this analysis are summarised below.

Through the literature review process, it was observed that a small number of baseflow separation approaches were commonly applied in a number of the published studies. These include methods described by Chapman (1991; refer to Equation 3), Boughton (1993; Equation 4), Jakeman and Hornberger (1993; Equation 5) and Lyne and Hollick (1979; Equation 7). Given the limited success of some of the other methods trialled in Appendix A, it was considered relevant to focus the development of a method for hourly data around these well referenced approaches.

The Chapman, Boughton and Jakeman and Hornberger approaches were applied to daily data for the Styx River catchment in NSW, in a reproduction of the analysis presented in Chapman (1999). The outcomes of this application were consistent with those published, and demonstrated a number of features of the various approaches:

- The separated hydrographs using the Chapman and Boughton methods produce plausible results;
- The Boughton method produces the largest peaks in the baseflow hydrograph; and
- The Jakeman and Hornberger approach displays sharp peaks and rates of rise under the flood events. The baseflow recession lies well below the streamflow hydrograph.

These three methods were subsequently applied to hourly data, using consistent parameter values as fitted by Chapman and Maxwell (1999) to the daily data. The resulting hydrographs demonstrated the sensitivity of the approach to the time step of the data, and the necessity to

modify the parameter values to produce plausible outcomes using hourly streamflow records.

Through trial and error, the parameter values of the three methods were optimised to produce more realistic baseflow hydrographs using hourly data. In this process, the separated baseflow was checked for the following features:

- Rise of the baseflow hydrograph – a steep rise in baseflow at the commencement of the streamflow event may signify the inclusion of quickflow in the baseflow hydrograph;

- The timing of the peaks in the baseflow hydrograph – the baseflow hydrograph should peak after the streamflow hydrograph due to the storage-routing of the sub-surface storages;

- The steepness and magnitude of the peaks in the baseflow hydrograph should appear plausible relative to the total streamflow series;

- The baseflow recession behaviour in the log domain – the baseflow hydrograph will most likely follow an exponential decay function (a master recession curve), which should appear linear in the log domain; an d

- General baseflow hydrograph behaviour in high and low flow periods, including the extent of interflow and quickflow in the baseflow hydrograph.

The resulting hydrographs were considered more plausible than those originally obtained using the published (daily) parameter values, however some limitations were still observed (Figure 6, presented on a log scale to accentuate the features). In particular the baseflow hydrographs produced using the Boughton and Jakeman and Hornberger methods did not rejoin the streamflow hydrograph. In contrast, the Chapman approach was reasonably consistent with that obtained using the daily data.
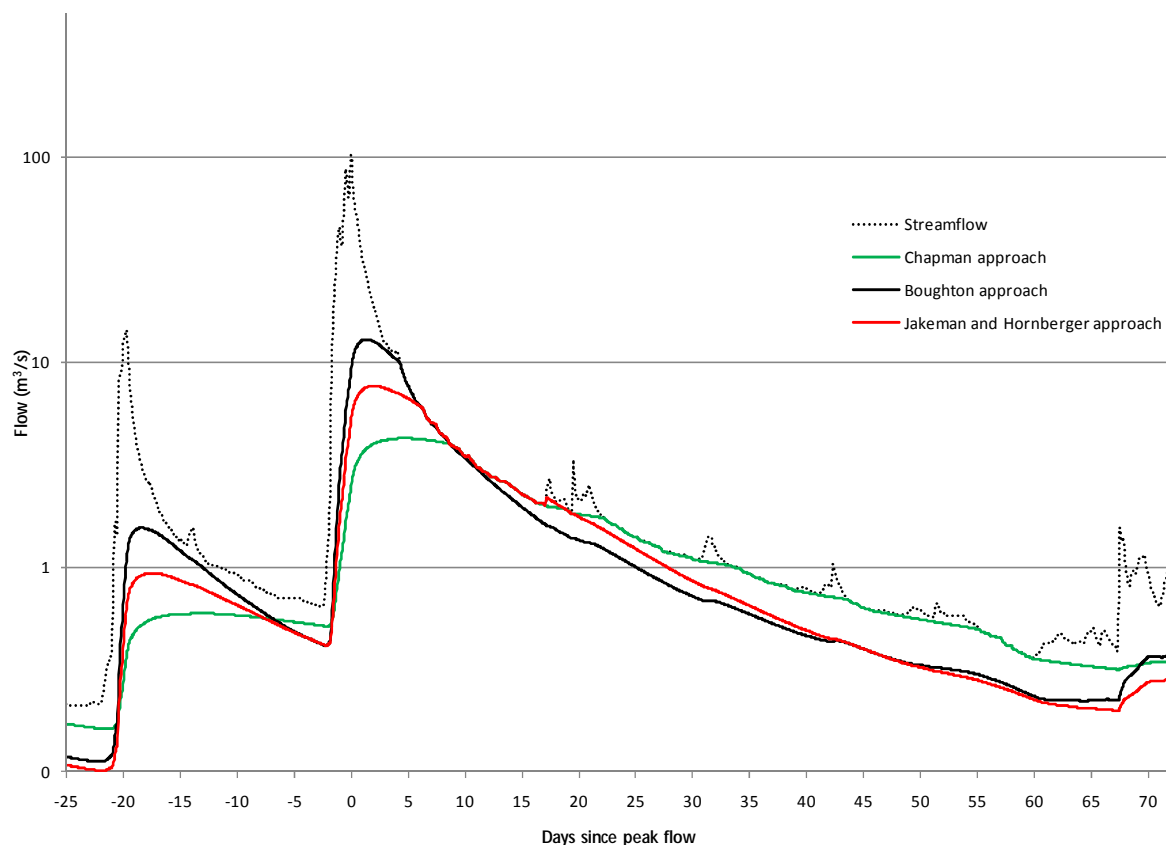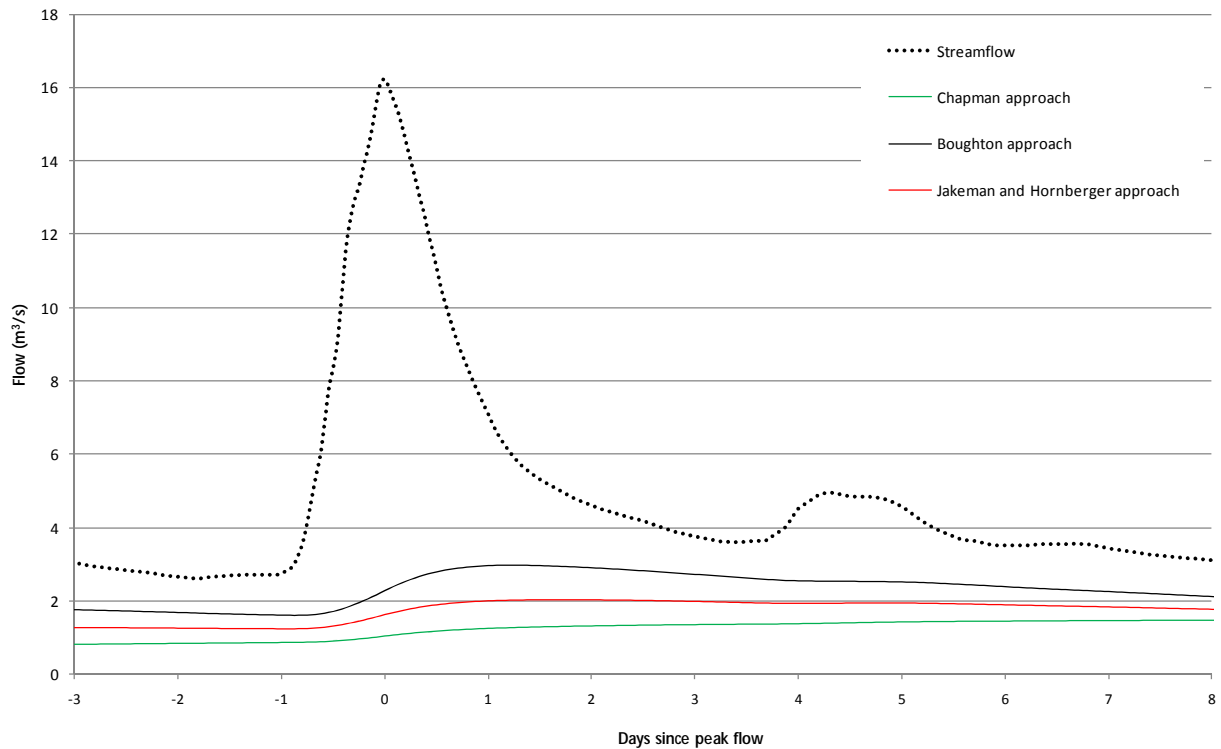

Figure 6 Baseflow separation using hourly data for the Styx River, NSW for October 1982

These methods were repeated for different events at the same location, as well as at additional locations to test whether the hourly parameter values were widely applicable without re-optimisation. The mixed results of these trials indicate:

■ The Boughton and Jakeman and Hornberger methods appear to exclude some proportion of baseflow for the full duration of the data anlaysed, as the baseflow hydrographs do not rejoin the streamflow hydrograph (Figure 7).

■ The baseflow separated using the Chapman approach appears plausible for some flow events (for example, the largest event in Figure 7), but not consistently across the entire record or at other locations. For instance, the separated baseflow series lies well below the total streamflow hydrograph for the early events in Figure 7 and the full duration of Figure 8.
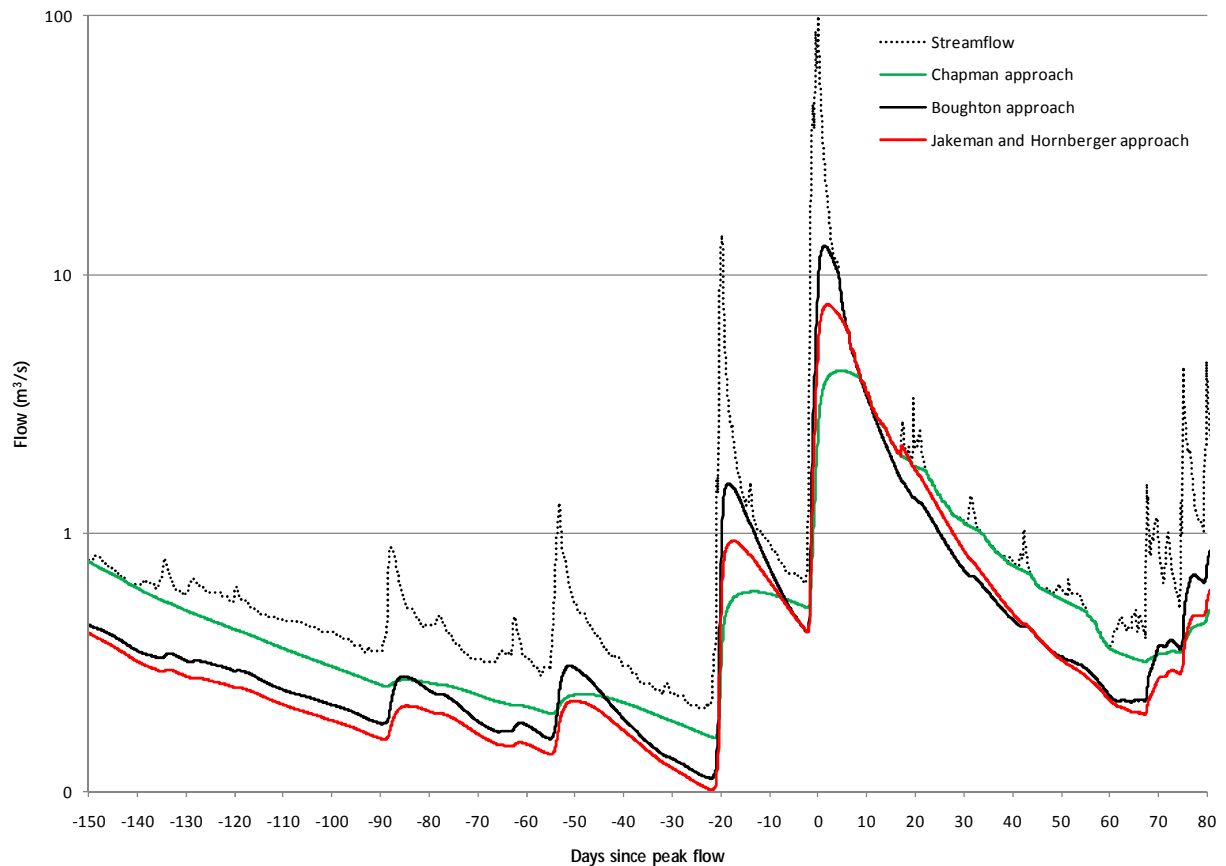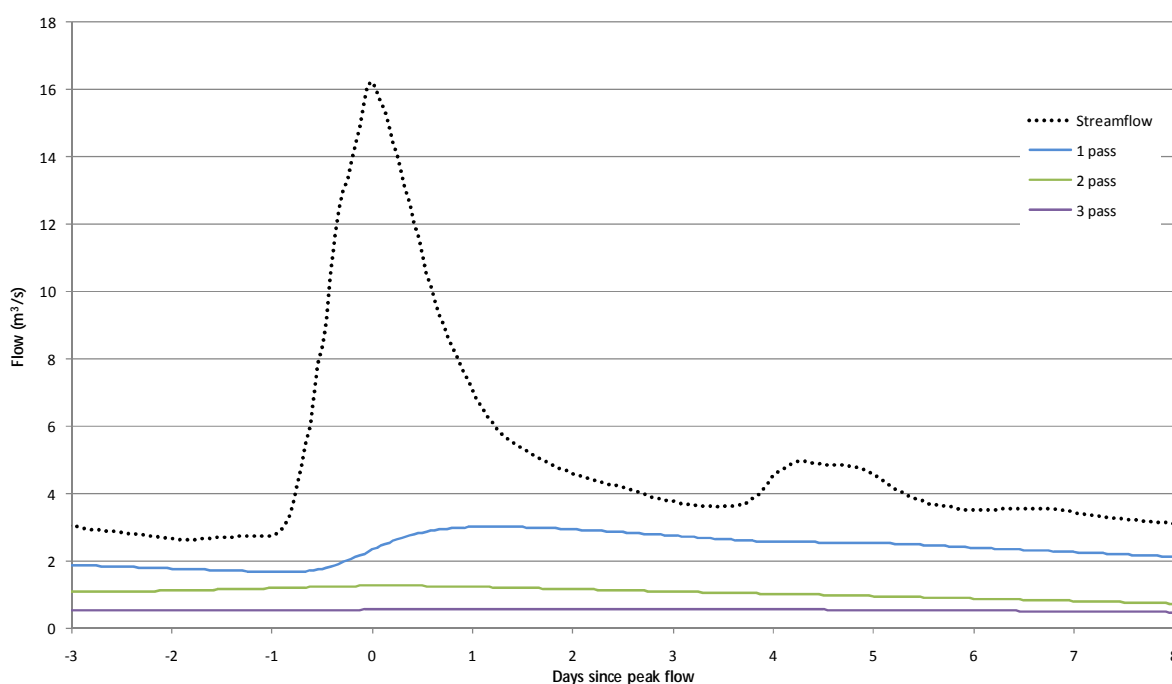

Figure 7 Baseflow separation for different events using hourly data for the Styx River, NSW for August 1982

Figure 8 Baseflow separation using hourly data for Little Yarra River, Victoria for September 1933

Further trials of these methods were undertaken, by modifying the parameter values used at different case study locations. The resulting separated baseflow series was not consistently reasonable. It was observed that when using hourly data, the parameter values that produced a reasonable approximation of baseflow were specific to the event and site of interest. Consistent with the comments in the literature review, the identification of the most suitable parameter values required manual testing and subjective judgement based on the resulting baseflow hydrograph in many instances. Furthermore, using these methods it was not possible to obtain parameter values that could be applied consistently to any number of flow events or case study sites.

While the original forms of the Chapman, Boughton and Jakeman and Hornberger methods required only a single pass of the filter forwards through the data of interest, the impact of applying additional passes was tested. This was trialled to investigate whether multiple passes of the filters would improve the separated baseflow estimation. However, consistent with the comments made by Spongberg (2000) regarding the impact of additional passes on phase distortion and baseflow attenuation, the application of additional passes of the Chapman, Boughton and Jakeman and Hornberger methods did not improve the appearance of the baseflow hydrograph. Rather, the resulting baseflow hydrograph was flattened and lowered even further (Figure 9).
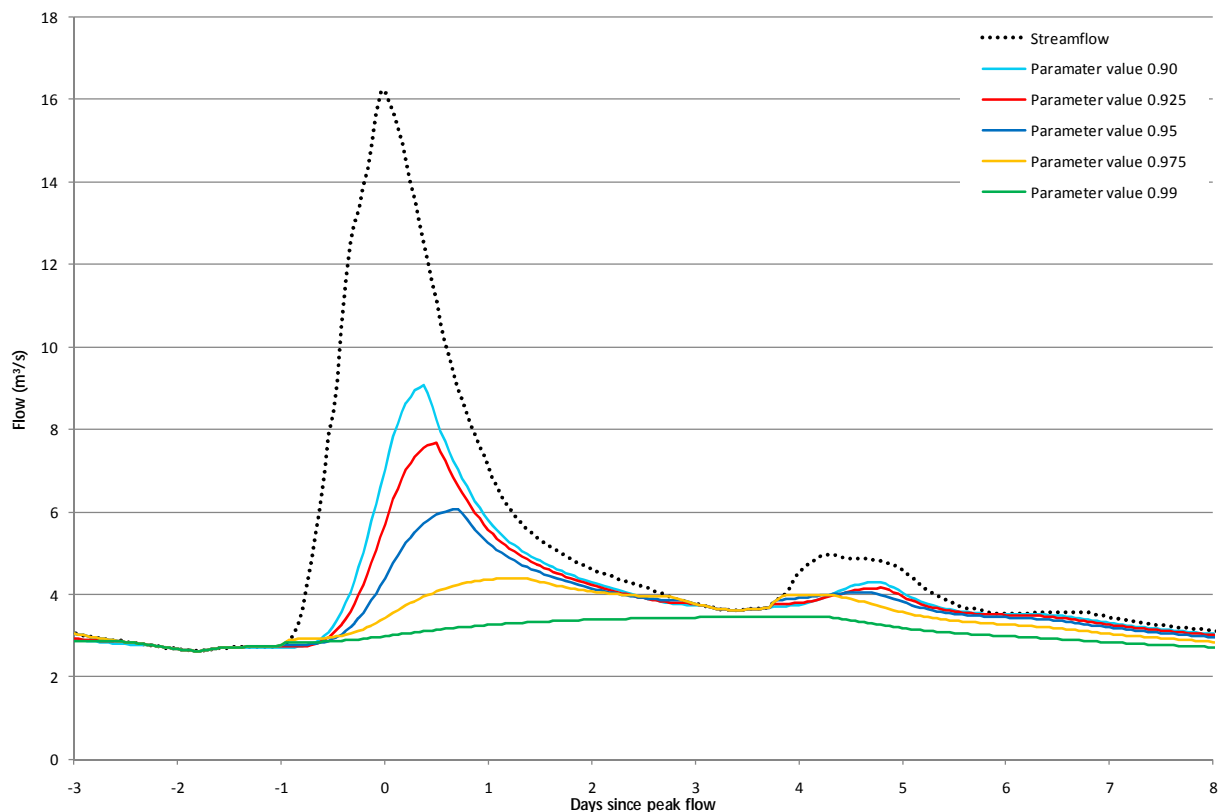
Figure 9 Baseflow separation using multiple passes of the Boughton method using hourly data for Little Yarra River, Victoria for September 1993

It is acknowledged that further manipulation of the filter parameter values would likely have yielded plausible results for individual events when the Chapman, Boughton or Jakeman and Hornberger methods were applied. However, given the large number of events and sites for analysis in this study, the limited success in being able to uniformly apply these techniques was considered a limitation preventing widescale application. The need for manual adjustment of the parameter values for different events or different locations was considered impractical when attempting to apply the approach to several hundred sites across Australia.

In other studies (Evans and Neal, 2005), it was suggested that the Lyne and Hollick filter was the most appropriate technique for both regional studies and as input into local investigations. In the case of localised investigations, manual adjustment was suggested based on site specific hydrogeological and catchment knowledge. These observations were made based on the application of the method to daily data. The suitability of the approach to hourly data is not well understood. Consistent with the analysis undertaken for other methods as described above, the Lyne and Hollick filter was applied to hourly data using the traditional approach of three passes and a filter parameter value of 0.925. As observed for the other methods, it is not suitable to simply apply the daily approach to hourly data without some modification.

Adjustment to the filter parameter value applied in the separation was tested first. A range of filter parameter values were trialled (Figure 10), with the resulting baseflow hydrographs demonstrating both plausible and unrealistic features. For instance, lower filter parameter values (such as 0.90) tended to produce high peaks in the baseflow hydrograph, indicating the incorporation of quickflow in the baseflow series. Small increases in the filter parameter value (such as a parameter value of 0.95) reduced the peaky nature of the baseflow estimate, however also resulted in the baseflow hydrograph rejoining the streamflow hydrograph before the end of the runoff event. Further increases in the parameter value (parameter value 0.99) caused the baseflow series to be smoothed significantly, to the extent that it was only after many events that the hydrographs rejoined.
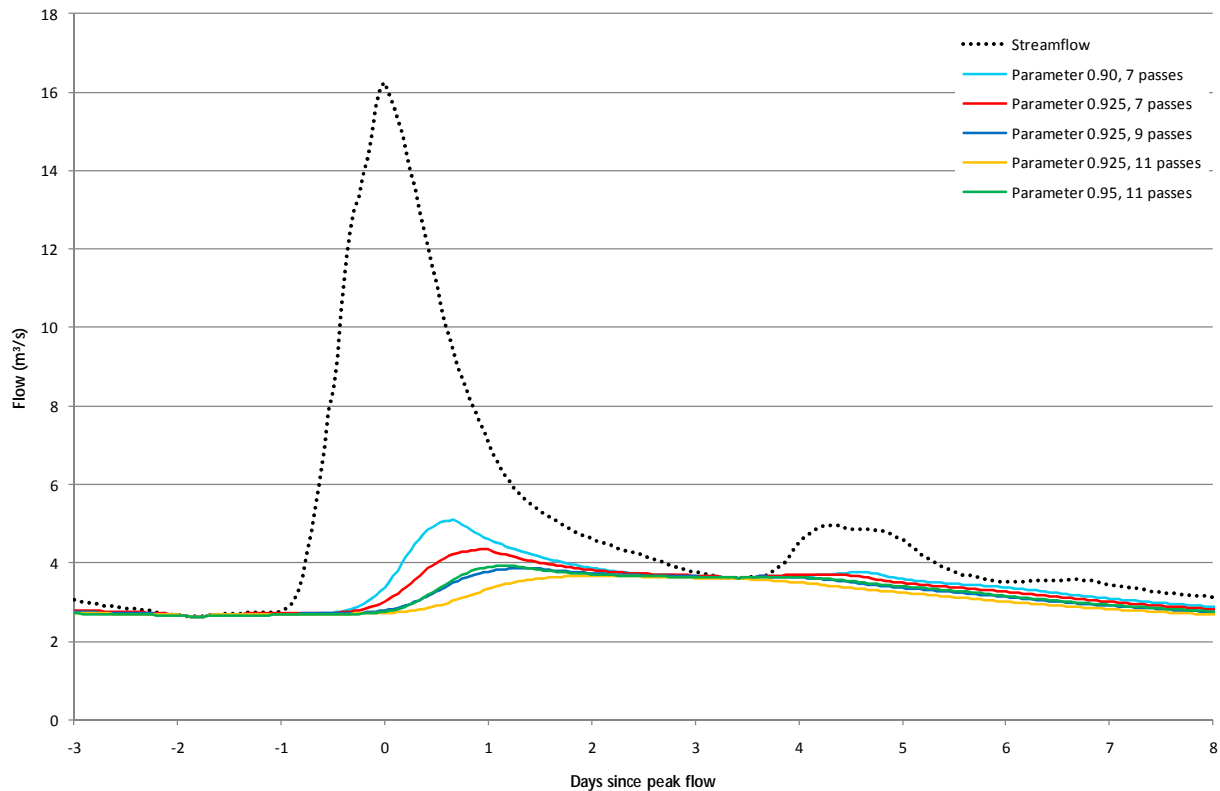
Figure 10 Baseflow separation using the Lyne and Hollick method with various filter parameter values applied to hourly data for Little Yarra River, Victoria for September 1993

Further analysis was undertaken by assessing the impact of additional passes on the resulting baseflow series (Figure 11). For this purpose a 'pass' of the filter is applied in a single direction, either forwards or backwards, through the data. Each additional pass acts to smooth the baseflow hydrograph slightly and delay the peak of the baseflow. Both of these characteristics are relevant in obtaining a plausible baseflow hydrograph, consistent with the key features listed above. However, significant attenuation of the baseflow series is obtained when a large number of passes are applied. It was considered that a more plausible baseflow series was obtained when the number of passes was increased from the 3 passes applied in the traditional approach to the Lyne and Hollick filter.
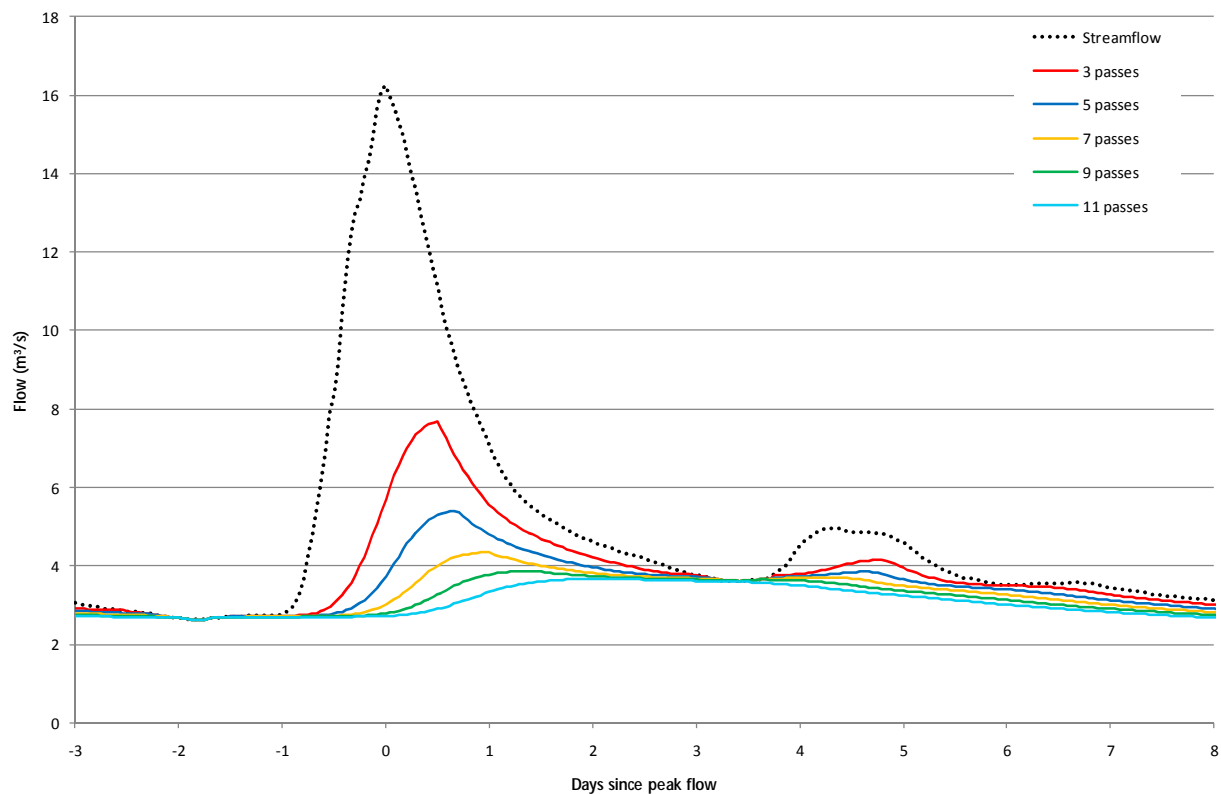
Figure 11 Baseflow separation using the Lyne and Hollick method with additional passes of the filter applied to hourly data for Little Yarra River, Victoria for September 1993

Through this testing process, it was recognised that a combination of changes to the Lyne and Hollick filter may further improve the resulting baseflow estimate. To test this concept, a number of different parameter values were applied in combination with a number of different passes of the filter over the hourly data (Figure 12). Several different combinations are presented, ranging in parameter values from 0.9 to 0.95 and from 7 to 11 passes. These combinations were selected based on investigations into various combinations, and only the options considered most plausible are presented.

Figure 12 Baseflow separation using the Lyne and Hollick method with a combination of additional passes of the filter and various parameter values applied to hourly data for Little Yarra River, Victoria for September 1993

When considered on a logarithmic scale, further details of the baseflow separation are evident. In this instance, the magnitude of the baseflow peak for the separation achieved using a parameter value of 0.9 and 7 passes was considered to include elements of the runoff event. Increasing the parameter value to 0.925 (retaining 7 passes) reduces the magnitude of the baseflow peak, however results in a baseflow hydrograph that is equal to the streamflow hydrograph at times that still experience runoff. Increasing the number of passes helps to minimise this effect, although too many passes (11 passes, parameter value 0.925) can result in a significantly attenuated baseflow estimate.

As demonstrated for this single event, different combinations of parameter values and passes can result in similar baseflow hydrographs (refer to the separations for parameter value 0.925 with 9 passes, and parameter value 0.95 and 11 passes). These estimates of baseflow were considered to be the most plausible of all the trialled approaches, as:

- The rate of rise of the baseflow peaks does not noticeably capture quickflow.
- The baseflow peak is suitably delayed after the streamflow event.
- The baseflow peaks were of reasonable magnitude.
- The recessions appear linear in the log domain
- The approaches consistently produced hydrographs with these features across other events and other sites.

Given the similarity of these two baseflow separations, and that 0.925 is widely regarded to be a reasonable baseflow filter parameter (refer Nathan and McMahon, 1990), it was considered relevant to select the method that retained most consistency with the generally accepted form of

the Lyne and Hollick filter. To this end, the recommended approach takes the same format as that described in Equation 7, however the filter is applied 9 times across the hourly data with a filter parameter value of 0.925.

This slightly modified version of the Lyne and Hollick filter has been used to partition baseflow from the hourly streamflow time series data for the catchments selected in this ARR update project. Based on analysis at case study catchments, a parameter value of 0.925 applied nine times across the hourly data produces a plausible baseflow hydrograph for a range of event sizes at eight of the nine case study catchments (refer to Section 7).

5. Catchment selection

Streamflow data is available across Australia at approximately 10,000 streamflow gauging stations, which are located in a variety of landscapes and have recorded data over different periods of record. For the purposes of this study, only a selection of these are considered relevant for the development of a national approach to estimate baseflow contribution to the design flood peak. The selection of catchments for analysis in this study was undertaken using a number of selection criteria, including:

- Degree of upstream regulation;
- Availability of hourly data;
- Length of record; and
- Missing data.

Further details on the selection of catchments for analysis will be provided in a subsequent report that will accompany the data collation and catchment characteristics database.

Data for the case study catchment analysis were obtained from a range of sources, including:

- The Bureau of Meteorology, which provided data from its consolidated collection of streamflow data from across Australia.
- Thiess Hydrographic Services, as custodians of water data in Victoria, provided data as required.
- The Pineena 9 DVD database was used to source data for sites in NSW.
- The Water Information Branch of the Department of Water provided data for Western Australian catchments.

Appropriate acknowledgement of this data provision and associated licence agreements are provided in Section 12.

6. Data Analysis at Case Study Locations

6.1. Streamflow data accuracy

When applying an automated process that partitions the baseflow component from a streamflow series, the accuracy of the estimate of baseflow is dependent upon the accuracy of the gauge recording the streamflow data. The measurement error associated with streamflow gauges is typically in the order of 5-10%, depending on the stability of the channel cross section. For concrete V-notch weirs during low flow conditions, errors in streamflow could be as low as 1%, whilst errors will increase at high flows. These relatively low errors at low flows indicate that streamflow data accuracy does not inhibit the accurate estimation of baseflow during periods of low flows, other than at streamflow gauging stations with highly variable geomorphic conditions. In contrast, streamflow gauges may not always be rated to perform accurately at water levels that occur during flood events. In such instances, the flow is estimated based on extrapolation of the available gauging records. This may be a significant source of uncertainty for streamflow records associated with large flood events. The quality code for streamflow records should be reviewed before data is analysed for baseflow.

6.2. Streamflow data preparation

Streamflow data often contains missing data due to hydrographic equipment failures or events occurring outside of the range for which the streamflow recording equipment has been rated. Equipment failures are to a large extent unavoidable and some missing data is likely to occur in most streamflow records. Typically, baseflow separation requires processing using a continuous data series. This may involve the use of an infilling process to eliminate periods of missing data.

In general, streamflow data infilling should be minimised because any baseflow signal identified in the infilled data will generally reflect the infilling technique and not the actual baseflow processes. An example of this is the use of regressions to infill streamflow data. If streamflow data is infilled from an adjacent streamflow gauge, then the baseflow properties of the infilled data will reflect those of the streamflow data used to infill the missing data, and may or may not reflect the behaviour in the catchment itself. Similarly, the use of a rainfall-runoff model will have a pre-defined baseflow recession constant, which may or may not reflect actual baseflow behaviour, depending on the suitability of the model calibration and the range of flows over which it is calibrated. If any infilling of data is undertaken, consideration should be given to the likely compatibility of baseflow properties between the raw data at the site of interest and the infilled data. There can be advantages in infilling streamflow data in baseflow studies if only short periods of data are missing. Having a complete record allows baseflow statistics to be prepared for different seasons using a comparable length of record. Neal et.al. (2004) adopted a maximum extent of infilled data of 5% of the record for use in regional baseflow assessment, which is a reasonable guide for local investigations as well.

For this study, periods of missing data were infilled using linear interpolation. This produced a continuous time series which was used for the separation of baseflow. These periods of missing data were subsequently removed from the data series for analysis purposes, so as to ensure that flood events extracted from the data did not include periods of missing and poor quality

data. Essentially, the infilling process was undertaken to ensure that the separated baseflow was not impacted upon by the boundary conditions associated with missing periods.

Data analysis in this study was undertaken following a thorough review of the quality codes associated with the hourly and daily records. Any data that was of questionable quality was eliminated from the analysis.

In instances where other hydrogeological factors mimic or interfere with the baseflow signal (as discussed in Section 2), baseflow separation should not be attempted without treatment of the data and even then with caution. This can be achieved by either accounting for those upstream influences in the streamflow data at the gauging station location, or by undertaking baseflow separation on inflows between streamflow gauging stations. In both cases, flow monitoring errors are likely to compound and hence there is much scope for variability and uncertainty in baseflow estimates. Baseflow should be relatively stable (or follow an exponential decay function in the absence of catchment rainfall) on successive days, so comparison of baseflow estimates on successive days will give an indication of the uncertainty in those estimates.
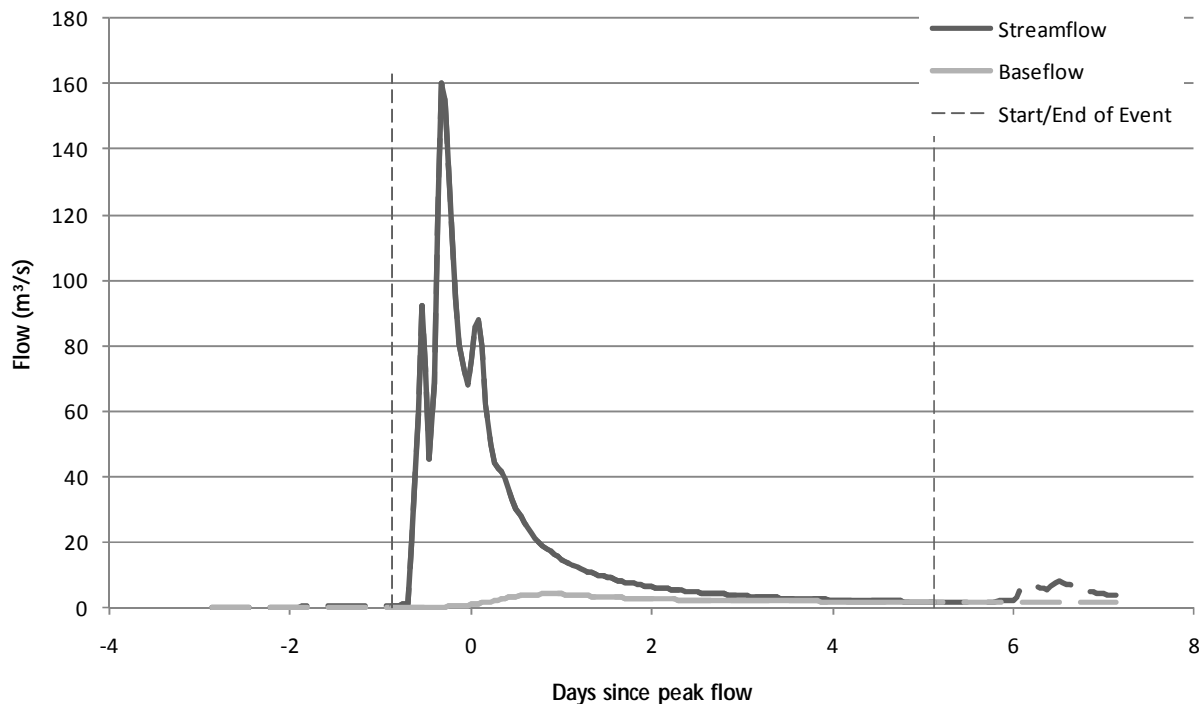
6.3. Identification of flood events

At each case study catchment location, analysis was undertaken to extract flood events using the peaks over threshold approach. In order to capture a full spectrum of flood event sizes, the number of events extracted was equal to four times the number of years of streamflow data available. Independence between events was defined based on a minimum interval of 7 days and a minimum difference in the magnitude of successive events of 75%.

This analysis produced the date and magnitude of the relevant flood events. The Generalised Pareto Distribution was fitted to these events by L-moments to identify the Average Recurrence Interval (ARI) associated with each flood event. The range in event sizes extracted depended on the availability of streamflow data at the particular location, however event ARIs typically ranged between less than 0.5 years to greater than 50 years.

To enable the calculation of statistics for each flood event, it was necessary to identify the start and end of the event. There is some difficulty and subjectivity associated with this, as there is conjecture around identifying the point at which quickflow is assumed to cease. Even the most sophisticated baseflow separation techniques are constrained by this uncertainty.

For the purposes of this study, the start and end of each event were defined via an automated approach, so as to minimise the subjectivity associated with the decision and to ensure a consistent approach was applied across all case study catchments and events. This automated process calculated the difference between the baseflow and streamflow series, and identified instances where this difference was minimised. A moving average with a duration of 23 hours was also applied to the difference between the baseflow and streamflow, and minimums in the moving average were identified. The start and end of each event was determined by the occurrence of both a local and moving average minimum within a consecutive 23 hour period. The moving average was incorporated into this process to prevent any small local minima from being misinterpreted as the start or end of the event. This approach ensured that instances of slight fluctuations in the streamflow or baseflow data did not trigger the start or end of the event.

Figure 13 demonstrates the outcomes of this approach for a multi-peaked event on the Bell River at Newrea (streamflow gauge site 421018) – each fluctuation in streamflow that occurs during the main component of the event takes place over such a short period of time that the variations in flow do not trigger the criteria for the start or end of the event.

Figure 13 Hydrograph demonstrating the automated approach to baseflow separation and identification of start and end of a multi-peaked runoff event on the Bell River at Newrea, NSW for January 1984

In contrast, fluctuations that occur over longer durations do tend to trigger the criteria for the start and end of events. For example, the automated approach considers the events in Figure 14 to be independent.
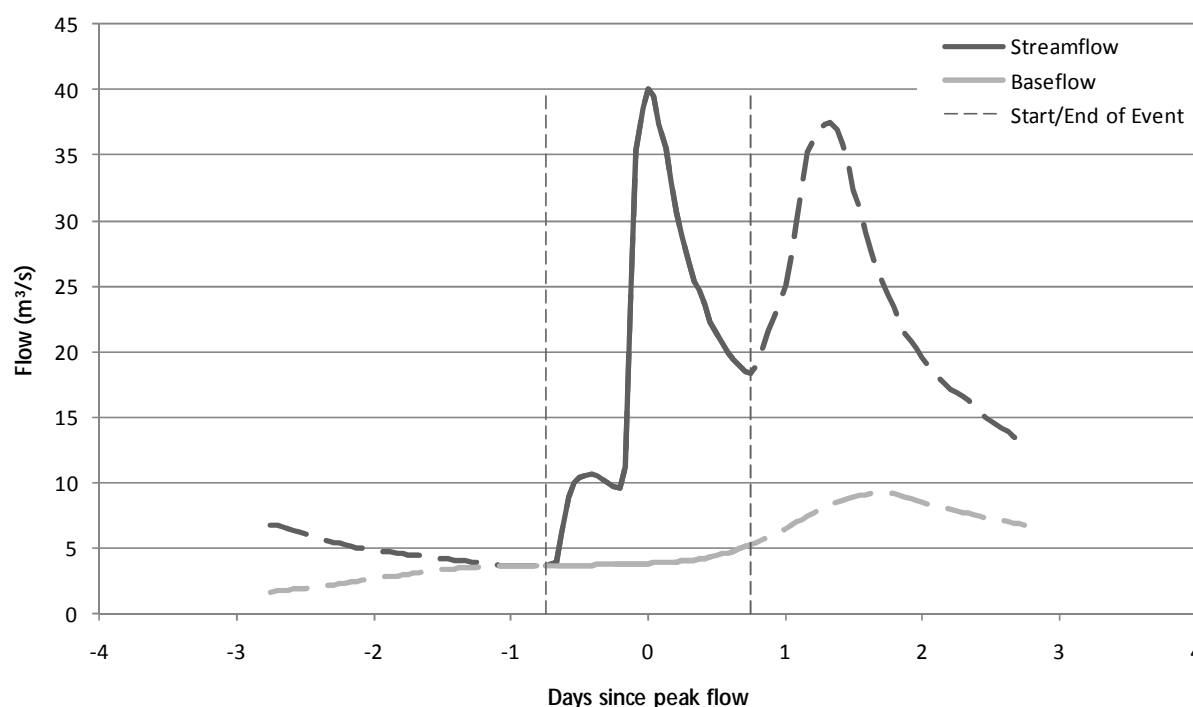
Figure 14 Hydrograph demonstrating the automated approach to baseflow separation and identification of start and end of a runoff event on the Bell River at Newrea, NSW for September 1986

Using this approach, each of the flood events identified through the flood frequency analysis was characterised.

This method was largely successful across the case study sites, and a manual review of the hydrograph for each event was undertaken to confirm the outcomes. In some instances, it is recognised that a more technically correct definition of the event could be achieved through manual manipulation of the start and/or end dates. Such instances were infrequent for the case study catchments presented in this report. Consequently, this approach was adopted as it was considered to robustly eliminate the subjectivity around the definition of event start and end. Furthermore, the method was considered reasonable, given the statistics of interest for analysis (refer to the following section) in this study.

However, it is recognised that further development of the method may be required to ensure the approach reasonably identifies all events at all locations. In particular, one of the eight case study catchments (stream gauge site 606001, Deep River at Teds Pool in Western Australia) was analysed using this approach, however the outcomes were less plausible than at the other case study locations. This location is situated in the south-west of Western Australia, where the local hydrogeological conditions result in a unique streamflow and baseflow response. Further details regarding this case study location are provided in Section 7.8.

Given this phase of the study is focussed around the development of the method and testing at a small number of case study sites, the analysis produced generally positive results. However, there may be a need for further refinement or regionalisation once the approach is applied to further catchments across Australia.

6.4.   Statistical analysis of baseflow characteristics

For each event identified at each of the case study locations, a range of baseflow related statistics have been calculated. These statistics have been selected to provide a means to assess baseflow contributions to streamflow events. Considering the example hydrograph presented in Figure 15, the statistics of interest include:

1)   The event baseflow index (BFI), which is given by the total baseflow volume for the duration of the event divided by the total streamflow volume. This is the ratio of the shaded areas in the example hydrograph.

2)   Ratio of the baseflow at the time of the streamflow peak (B) to the peak streamflow (A), given by B/A.

3)   Ratio of the peak baseflow (C) to the peak streamflow (A), given by C/A.

The timing associated with these key features is also collated for each event.
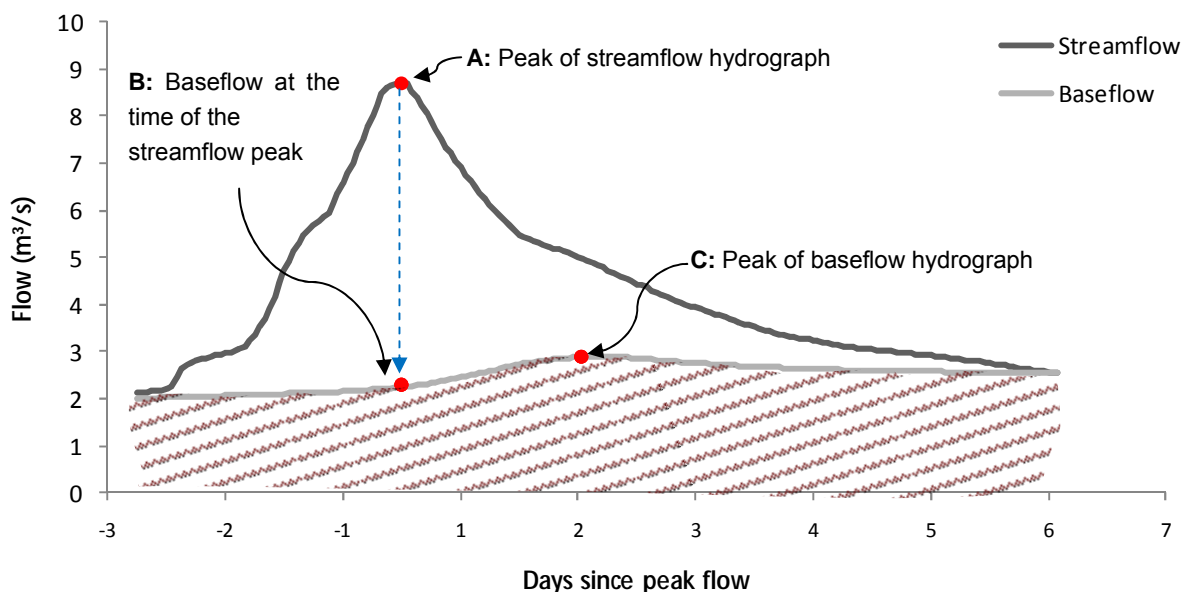
Figure 15 Flow hydrograph for an event at Victorian site 229214 (Little Yarra River at Yarra Junction) displaying key features

Each of the statistics above were extracted for each flow event, and the collection of these statistics at a particular site was presented as a scatter plot against the ARI of the total flow event (ie: runoff + baseflow).

The BFI represents the relative contribution of baseflow to total streamflow on a standardised basis for comparison between sites along a river with different upstream catchment areas and in different catchments. For a particular event, the BFI is given by the ratio of the lower shaded area to the total shaded area in the example hydrograph in Figure 15.

The baseflow index is generally regarded as an indicator of the hydrogeological conditions in a particular catchment. The Institute of Hydrology (1980) presents typical baseflow index ranges for particular rock types and regolith. Sinclair Knight Merz (2003) developed a prediction equation to estimate baseflow index in ungauged catchments in Victoria using catchment characteristics. These characteristics included vegetation cover and rainfall (indicators of input water into groundwater and surface water), stream frequency (an indicator of potential connectivity of groundwater to surface water drainage lines) and soil permeability rating (an

indicator of hydraulic conductivity and transmissivity). This enables baseflow properties to be estimated in catchments with no streamflow gauging information or with streamflow conditions not amenable to a baseflow separation.

Whilst long-term average baseflow index is generally regarded as an indicator of hydrogeologic conditions, it is important to remember that baseflow index is a measure relative to total streamflow. Over short time intervals, baseflow index will generally reflect fluctuations in quickflow rather than changes in baseflow. During extended dry periods the baseflow index will be equal to 1.0, whilst during flood events, the baseflow index will be close to zero. This is important to note for the purposes of this study, as different sized flood events will respond with different BFI ratios.

Research has shown that there is a clear gradient in baseflow index from the southern Murray-Darling Basin in Victoria to the northern Murray-Darling Basin in Queensland (Neal et al, 2004). This was attributed to the prevalence of either summer dominant or winter dominant rainfall regimes in these different parts of eastern Australia. The likely influence of the climate regime on baseflow index is supported by the statistical significance of rainfall in the regional prediction equation for baseflow index developed in Sinclair Knight Merz (2003). The outcomes of this study will provide information on the link between event BFI and the size of the flood event.

7. Case Study Catchments

A supporting report (SKM, in preparation) will be completed for delivery in conjunction with the data collation and catchment characteristics database. This additional report will outline the selection criteria to identify catchments for analysis in ARR Update Project 7, and will contain a complete list of sites selected. Of these, a section of case study catchments were chosen for analysis in this first phase of the project. These sites were identified based on spatial coverage, and to capture a range of climate, hydrological and hydrogeological conditions across Australia. These case studies provide a reasonable basis from which to develop the method that will ultimately be applied across the complete list of selected sites. Figure 16 indicates the location of these case study catchments across Australia, and Table 1 provides further details of the catchment locations. Additional catchment characteristics are summarised in Appendix B. Further details on the catchment characteristics and the data extraction process are contained in a supporting report and database.

Table 1 Case study catchments

Site number	Site name	Catchment area (km^2)	Period of record (years)
110003a	Barron River at Picnic Crossing (Queensland)	231	83
145018a	Burnett Creek upstream of Maroon Dam (Queensland)	81	38
204041	Orara River at Bawden Bridge (New South Wales)	1637	46
421018	Bell River at Newrea (New South Wales)	1248	33
223202	Tambo River at Swifts Creek (Victoria)	903	62
229214	Little Yarra River at Yarra Junction (Victoria)	154	45
803002s	Leonard River at Mt Herbert (Western Australia)	440	32
606001	Deep River at Teds Pool (Western Australia)	347	33

- Figure 13 - Map of case study catchment locations

● Gauges

SINCLAIR KNIGHT MERZ

L:\WES\Projects\VW04648\Technical\Spatial\ArcGIS\Gauge_Locations.mxd

7.1. Barron River at Picnic Crossing, Queensland (110003A)

7.1.1. Catchment Description

The Barron River is located in northern Queensland, within a tropical environment. The upper reaches of the river (upstream of Tinaroo Falls Dam) are unregulated. A high degree of agricultural activity occurs in the upper Barron River, with the original vegetation cleared from much of the catchment. The streamflow gauge at Picnic Crossing is situated immediately upstream of the Tinarroo Falls Dam, approximately 70 km south of Cairns. Appendix B provides details of the catchment characteristics at the site.

7.1.2. Flow Characteristics

The flow characteristics for Barron River at Picnic Crossing are presented in Table 2. The streamflow gauging station at this location (site 110003a) has been in operation since 1925, and recorded continuously over that time. The flow is highly seasonal, with significant events occurring primarily in autumn and summer months. Maximum hourly flows greater than 1000 m^3/s have been recorded, all occurring in autumn. No cease to flow events have been recorded at this location (Figure 17). Almost 400 gaugings have been recorded at this location, with the maximum gauging reflecting an ARI of 30 years. The Barron River is a naturally perennial stream, with baseflow thought to contribute to the flow of the local creeks, particularly in the upper catchment (SKM, 2007).

Table 2 Streamflow characteristics for Barron River at Picnic Crossing (110003a)

| Statistic	Value			
Start of record	November 1925			
End of record	July 2008			
Length of record (years)	83			
Percentage of missing data (%)	0			
Maximum recorded hourly flow (m^3/s)	1037			
Minimum recorded hourly flow (m^3/s)	0.11			
Proportion of time of cease to flow events (%)	0			
Maximum gauged flow (m^3/s)	484			
ARI of maximum gauged flow (years)	30			
Percentage of time hourly flow is greater than maximum gauged flow (%)	0.007			
	Dec-Feb	**Mar-May**	**June-Aug**	**Sep-Nov**
Proportion of events extracted (%)	51	46	3	0
Seasonal maximum flow event (m^3/s)	533	1088	23	10
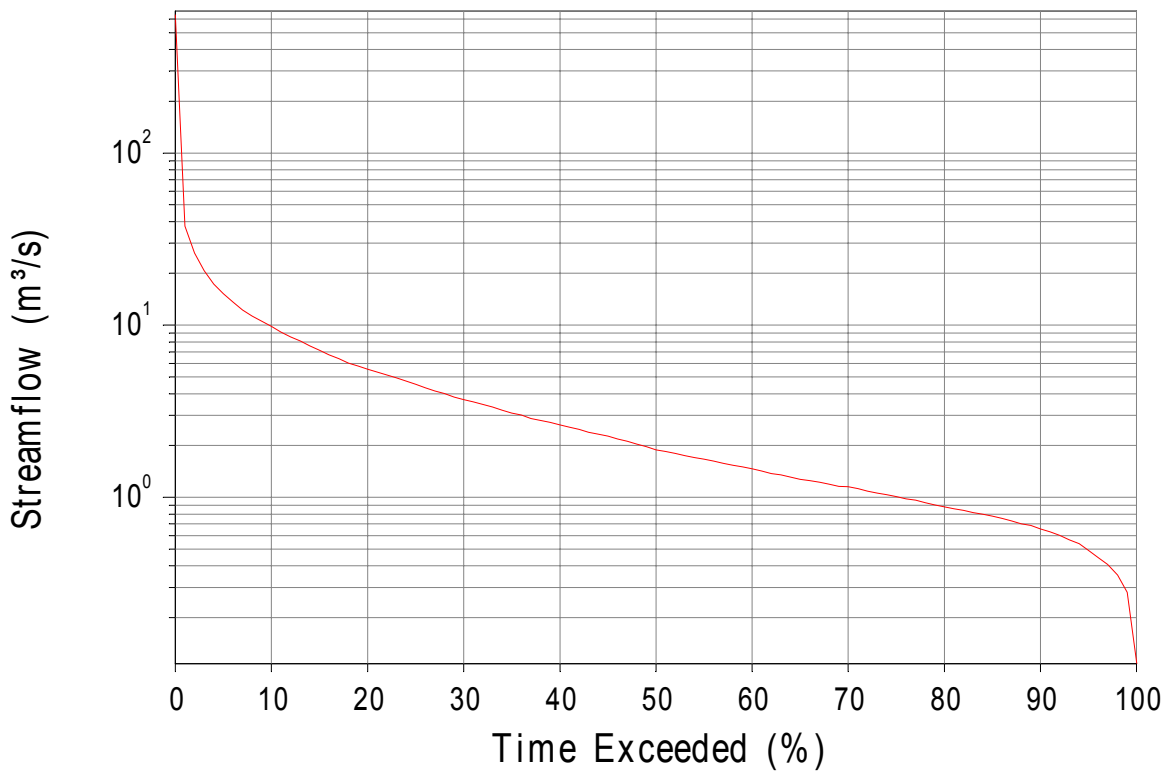
Figure 17 Flow duration curve for Barron River at Picnic Crossing (110003A)

More than 300 events over 83 years were extracted for the flood frequency analysis at the Barron River site (Figure 18). The majority of these events occurring from December to May, which includes the wet season in northern Australia. Figure 19 provides a summary of the range in event sizes that occur in each season. The average size of events is between 10 m^3/s and 63 m^3/s, however the biggest events are significantly larger.
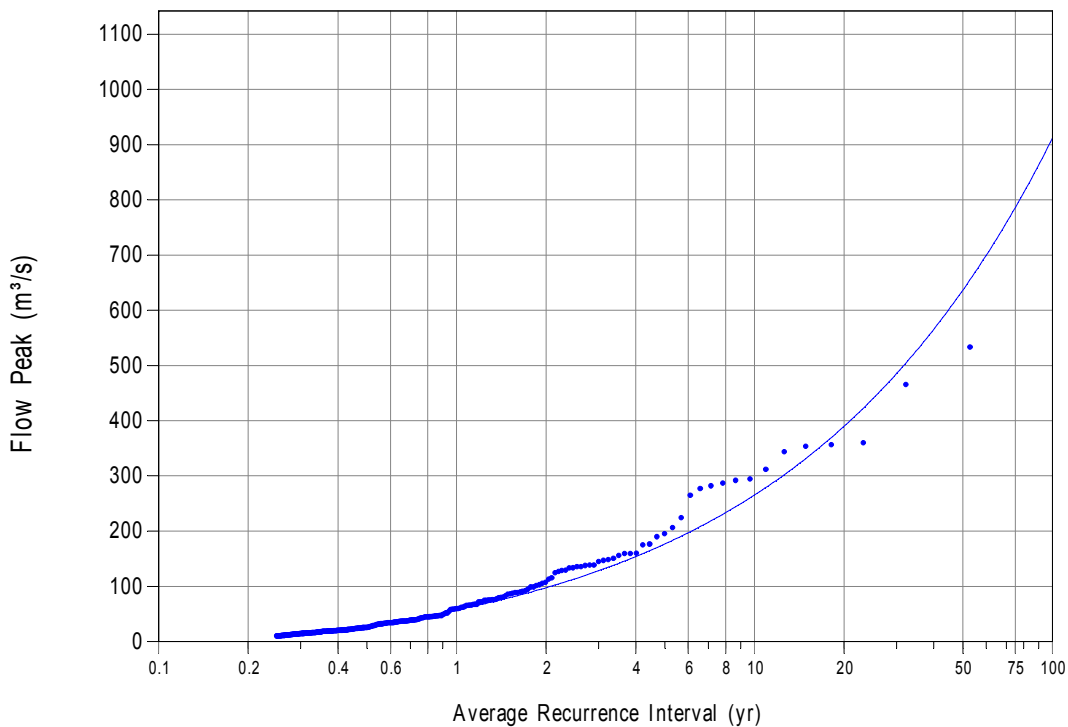
Figure 18 Flood frequency analysis, Barron River at Picnic Crossing (110003A)
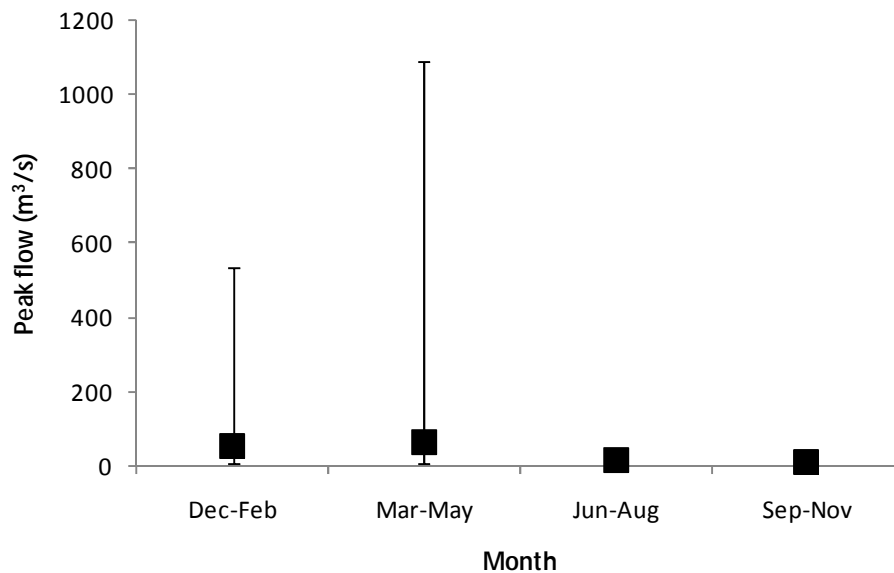
Figure 19 Seasonality of events, Barron River at Picnic Crossing (110003A). The box represents the magnitude of the mean flow event, and the whiskers represent the full range of events analysed for this study.

7.1.3. Baseflow Analysis

Nine passes of the Lyne and Hollick filter, with a parameter value of 0.925, were applied to extract the baseflow for each event at the Barron River site. Sample hydrographs are presented in Figure 20 and key statistics are summarised in Table 3. The variation in these statistics for different event sizes is presented in Figure 21. In general, the contribution of baseflow is greatest for smaller events and decreases with increasing ARI (Figure 21a and Figure 21b). The variability in these proportional statistics (indicated by the scatter in the data points) is greatest for smaller events, and decreases with ARI.

In contrast, the absolute magnitude of the baseflow tends to increase with ARI (Figure 21c). The degree of variability in this measure of baseflow is less than that observed in Figure 21a and Figure 21b, and tends to increase with increasing flood size. The high degree of scatter in Figure 21a-c is reflected in the low r^2 values, which are approximately 0.3 for each case.

Further plots are also presented in Appendix C, which demonstrates similar responses when the peak baseflow is considered.

Table 3 Baseflow statistics, Barron River at Picnic Crossing (110003a)

Statistic	BFI of event	Ratio of baseflow under streamflow peak : streamflow peak	Ratio of baseflow peak : streamflow peak
Average	0.54	0.31	0.42
Maximum	0.91	0.88	0.97
Minimum	0.04	0.01	0.06
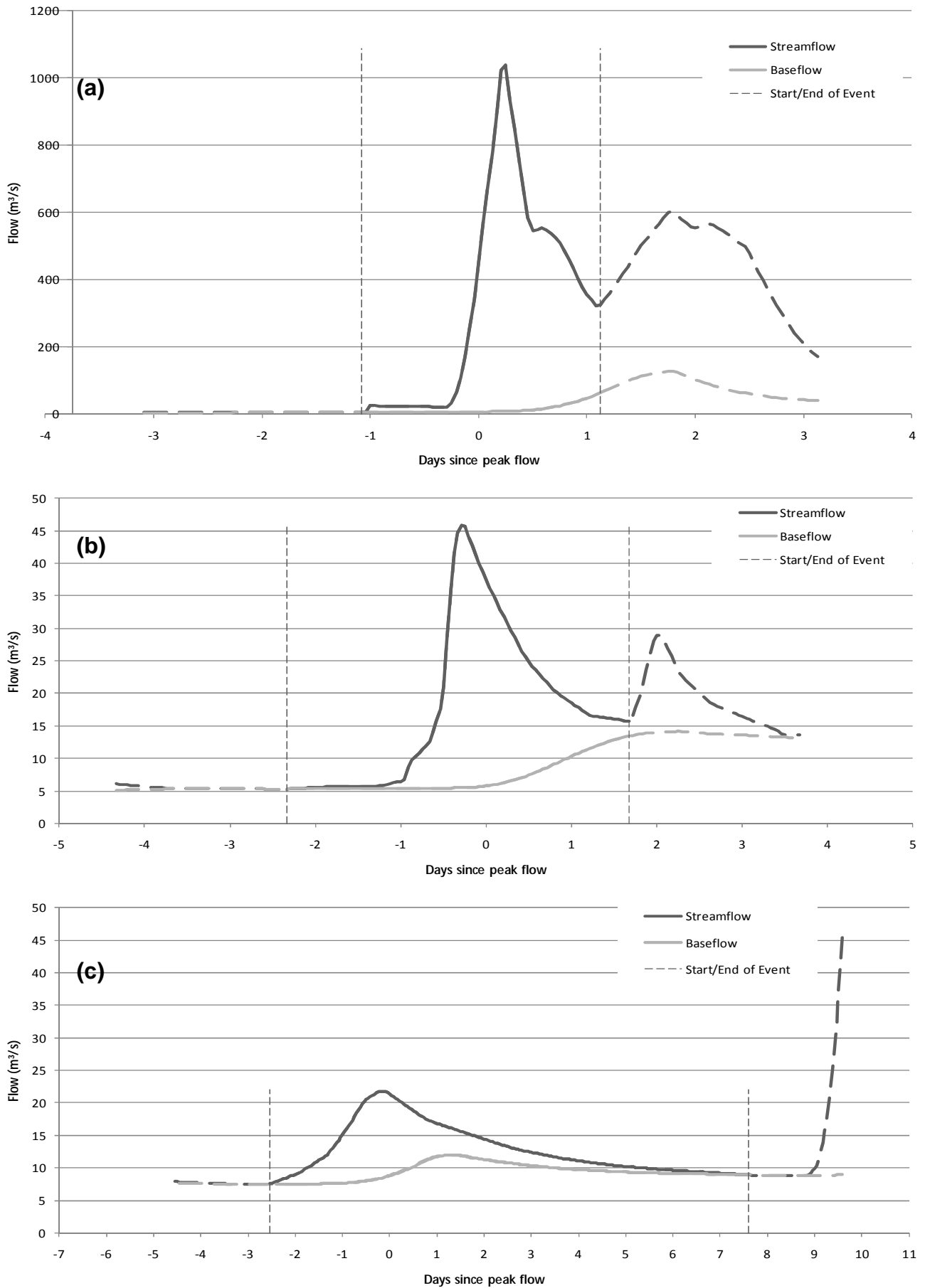
Figure 20 Sample hydrographs demonstrating the streamflow and baseflow characteristics for a range of events, Barron River at Picnic Crossing (110003A): (a) ARI of 138 years, (b) ARI of 0.87 years, (c) ARI of 0.44 years
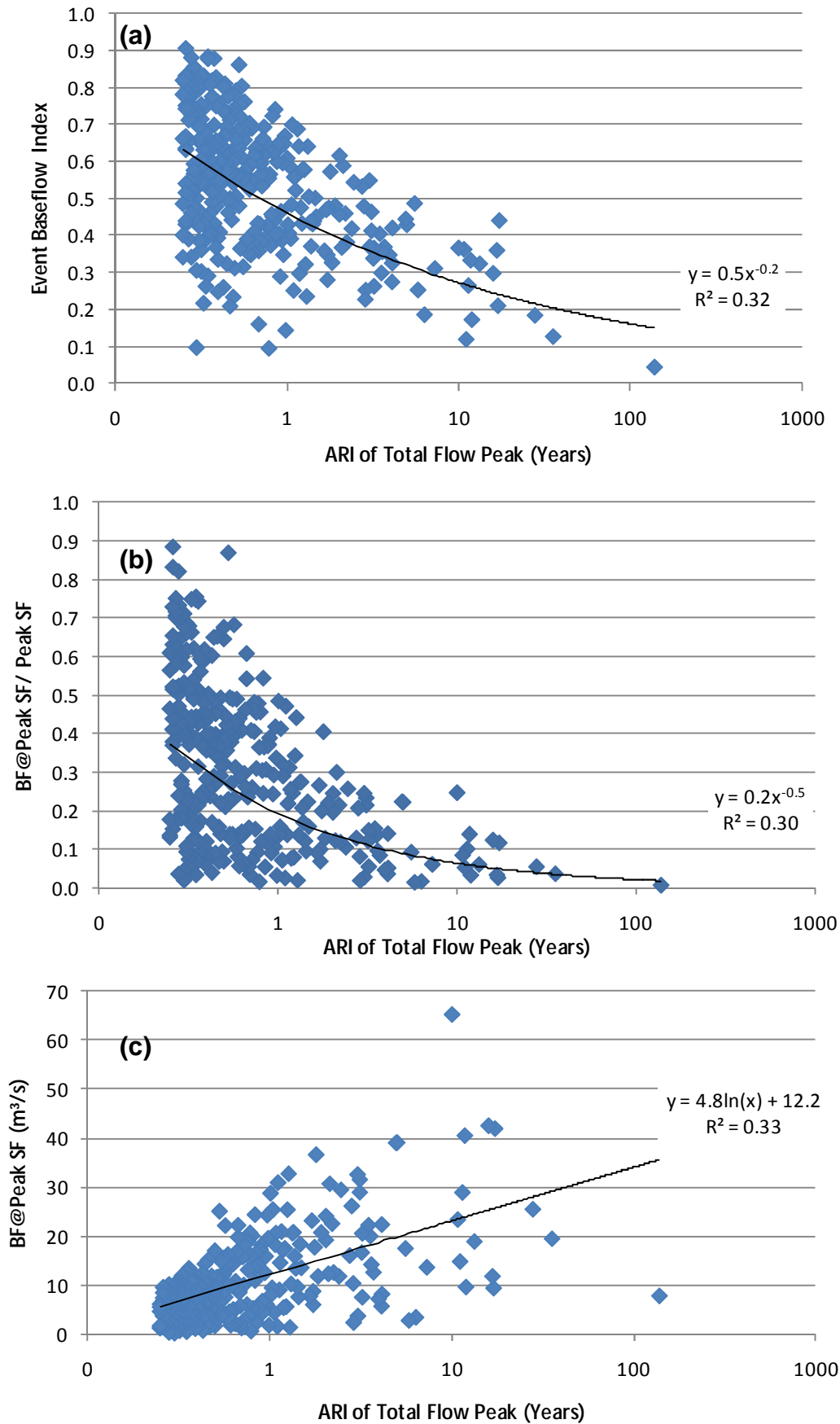
Figure 21 (a) Variation in event BFI with ARI of total flow peak, (b) Ratio of baseflow under streamflow peak to peak streamflow, (c) Absolute magnitude of baseflow under streamflow peak, Barron River at Picnic Crossing (110003a)

7.2.   Burnett Creek upstream of Maroon Dam, Queensland (145018a)

7.2.1. Catchment Description

The Burnett Creek is located in the upper reaches of the Logan River catchment, southern Queensland. The Burnett Creek gauging station of interest (upstream of Maroon Dam) is south of Brisbane. Appendix B summarises the key catchment characteristics at the site.

7.2.2. Flow Characteristics

The flow characteristics at the gauge location are presented in Table 4. This gauging location has been in operation since 1970, and has maintained regular records of flows over this time. Approximately 6% of the hourly flow record is missing or of poor quality. The maximum recorded flow is just over 375 m^3/s, while cease to flow events represent approximately 6% of the flow record (Figure 22). The maximum gauged measurement at the site was taken in 1971, and represents an event with ARI of 0.6 years. Approximately 0.23% of the flow record is above this gauged measurement. The largest flow events occur over the period December to February. The other seasons experience events of approximately half the magnitude of these peak flows.

Table 4 Streamflow characteristics for Burnett Creek upstream of Maroon Dam (145018a)

| Statistic	Value			
Start of record	May 1970			
End of record	October 2008			
Length of record (years)	38			
Percentage of missing data (%)	6			
Maximum recorded hourly flow (m^3/s)	376			
Minimum recorded hourly flow (m^3/s)	0			
Proportion of time of cease to flow events (%)	6			
Maximum gauged flow (m^3/s)	24			
ARI of maximum gauged flow	0.6			
Percentage of time hourly flow is greater than maximum gauged flow (%)	0.23			
	Dec-Feb	**Mar-May**	**June-Aug**	**Sep-Nov**
Proportion of events extracted (%)	46	25	10	18
Seasonal maximum flow event (m^3/s)	402	193	159	146
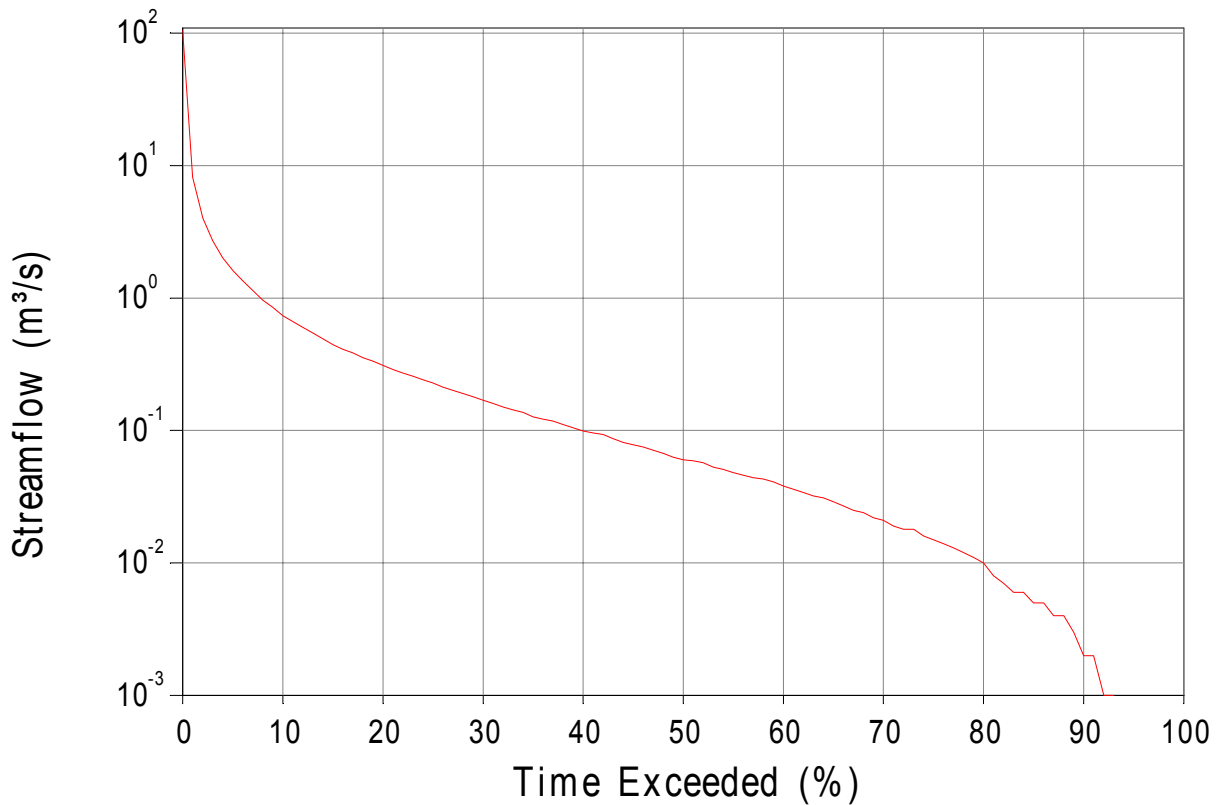
Figure 22 Flow duration curve, Burnett Creek upstream of Maroon Dam (145018a)

Figure 23 presents the flood frequency analysis for the Burnett Creek site. This analysis was undertaken using 154 events spanning 38 years. The largest of these events occur in the months of December, January and February. The range in event size is also greatest during these months (Figure 24).
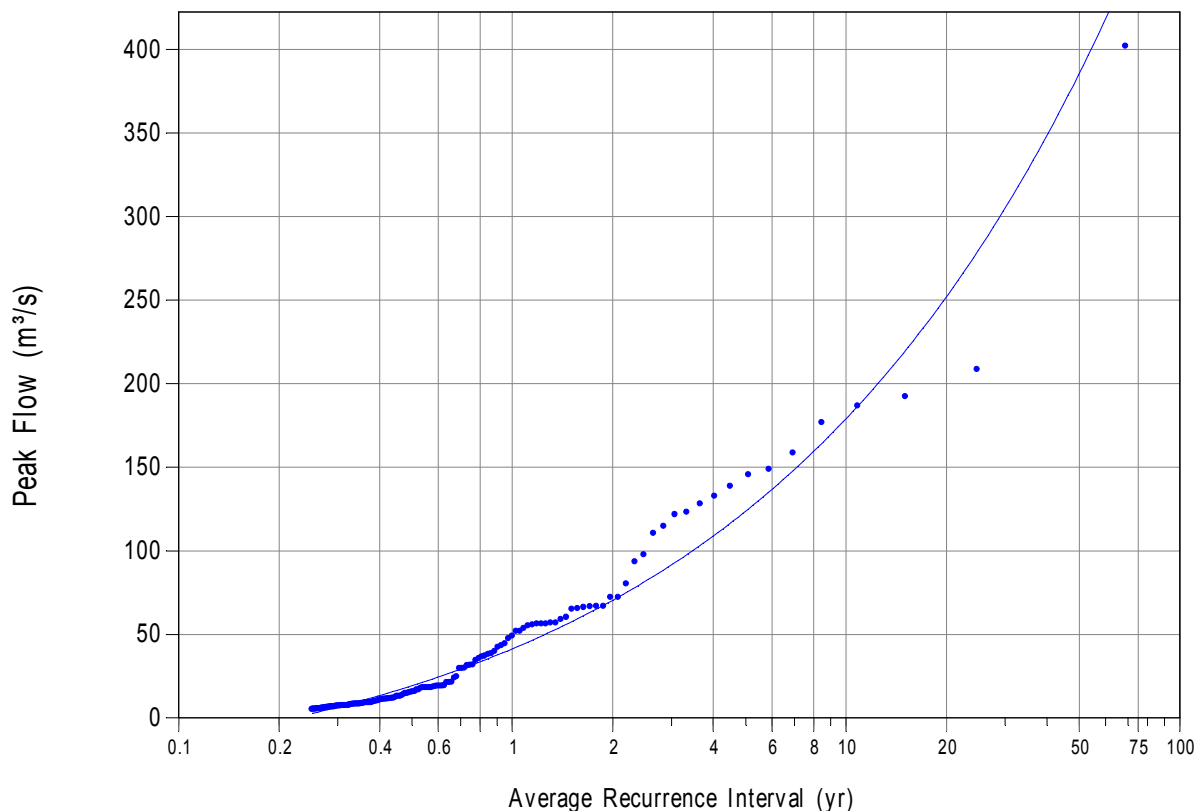
Figure 23 Flood frequency analysis, Burnett Creek upstream of Maroon Dam (145018a)
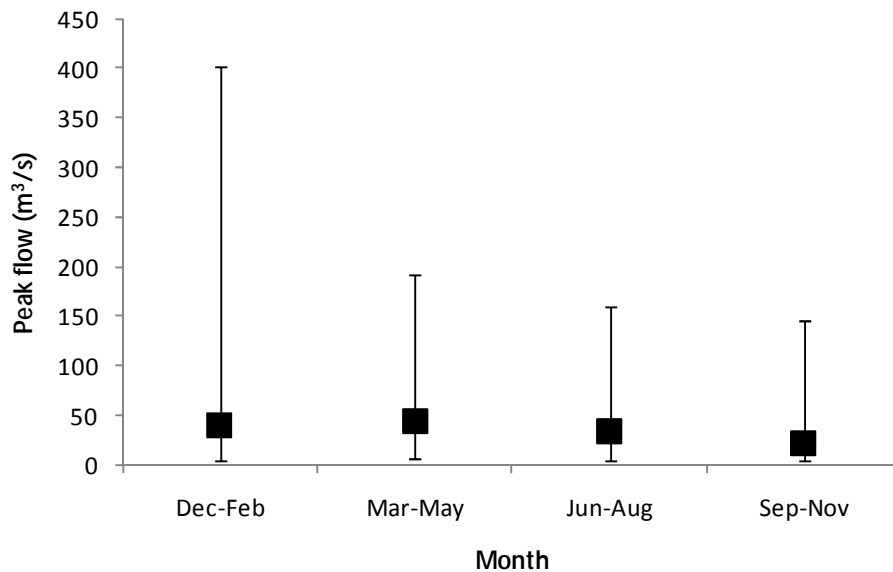
Figure 24 Seasonality of events, Burnett Creek upstream of Maroon Dam (145018a). The box represents the magnitude of the mean flow event, and the whiskers represent the full range of events analysed for this study.

7.2.3. Baseflow Analysis

Nine passes of the Lyne and Hollick filter, with a parameter value of 0.925, were applied to the hourly streamflow data at the site to extract the baseflow for each event. Sample hydrographs are presented in Figure 25 and key statistics are summarised in Table 5. The variation in these statistics is presented in Figure 26, with further details provided in Appendix B. The BFI and ratio of baseflow at the time of the streamflow peak to the peak streamflow tend to decrease with increasing event size. The degree of scatter associated with this response also tends to decrease as the event size increases.

In contrast, the magnitude of the baseflow at the time of the streamflow peak increases as the ARI of the total flow increases. Greater scatter and variability in the data is evident for larger event sizes.

The significant scatter in the data in Figure 26a-c results in low r^2 values for the fitted trendlines. The best fit is observed for Figure 26a, with a fit of approximately 0.3. The other lines have an r^2 value of 0.03.

Table 5 Baseflow statistics, Burnett Creek upstream of Maroon Dam (145018a)

Statistic	BFI of event	Ratio of baseflow under streamflow peak : streamflow peak	Ratio of baseflow peak : streamflow peak
Average	0.22	0.03	0.06
Maximum	0.61	0.22	0.39
Minimum	0.001	0.0003	0.001
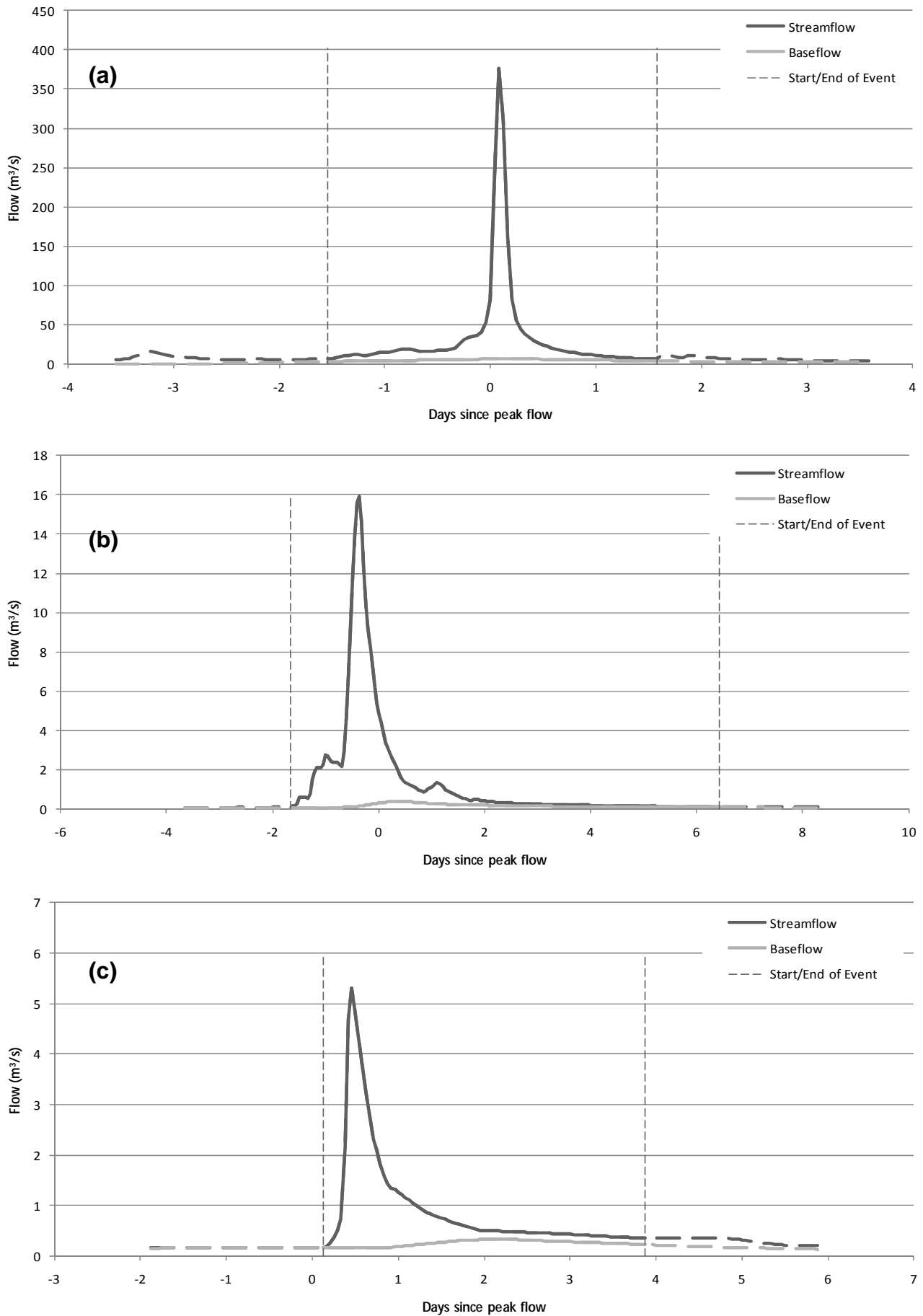
Figure 25 Sample hydrographs demonstrating the streamflow and baseflow characteristics for a range of events, Burnett Creek upstream of Maroon Dam (145018a): (a) ARI of 55 years, (b) ARI of 0.51 years, (c) ARI of 0.25 years
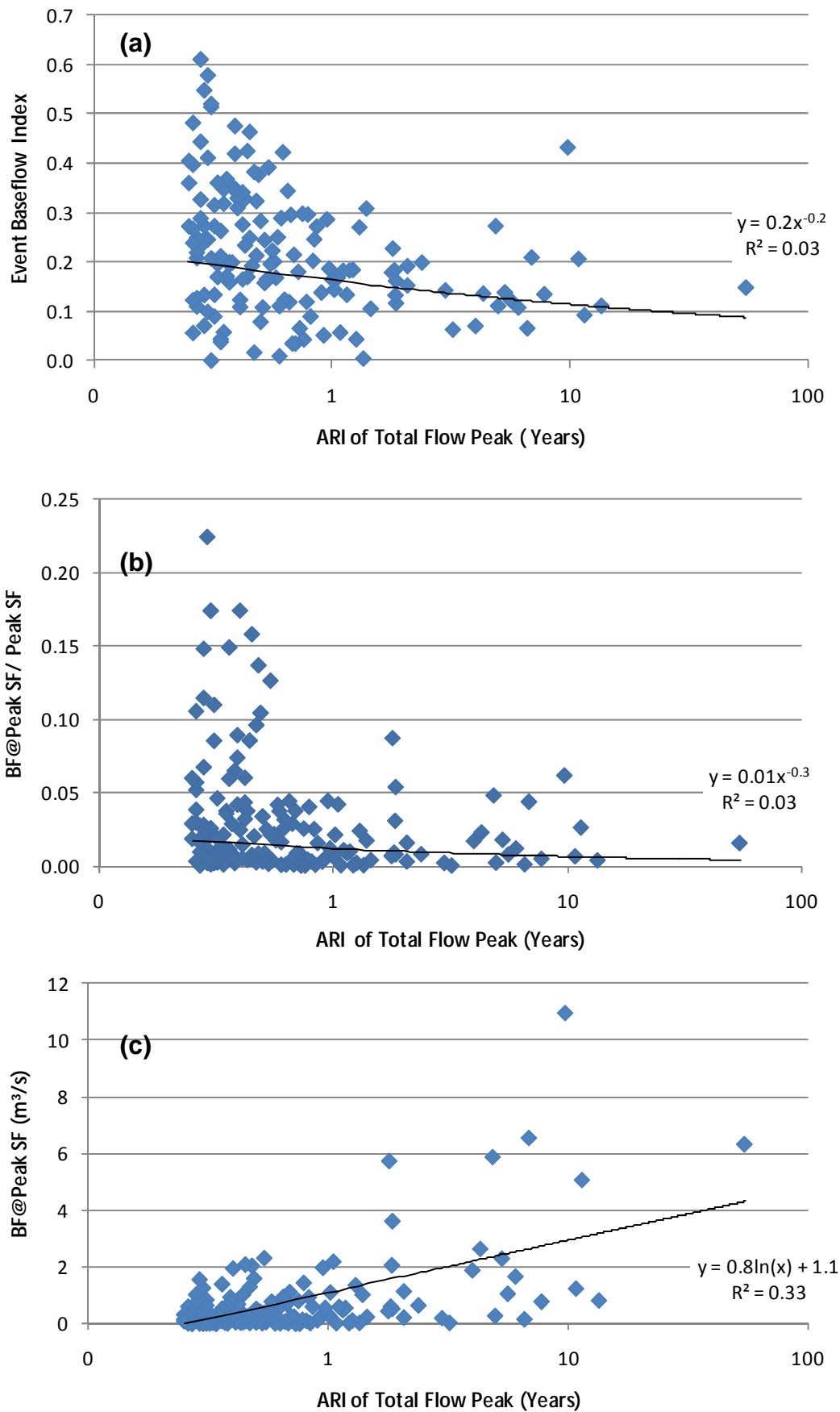
Figure 26 (a) Variation in BFI with ARI of total flow peak, (b) Ratio of baseflow under streamflow peak to peak streamflow, Burnett Creek (c) Absolute magnitude of baseflow under streamflow peak, Burnett Creek upstream of Maroon Dam (145018a)

7.3. Orara River at Bawden Bridge, New South Wales (204041)

7.3.1. Catchment Description

The Orara River is located in northern New South Wales, commencing in the mountainous region of the Great Dividing Range near to Coffs Harbour. Appendix B summarises the key characteristics for the catchment.

7.3.2. Flow Characteristics

The flow characteristics at the gauge location are presented in Table 6. The streamflow gauge at Bawden Bridge commenced operation in 1960, and data for 46 years was available for this study. Over this period, approximately 7.5% of hourly data records were missing or of poor quality. Cease to flow events occur over approximately 0.2% of the record (Figure 27). The maximum gauged measurement at the site was recorded during a largest flood event on record. The greatest floods occur from March to May, and the smallest events occur in June, July and August.

Table 6 Streamflow characteristics for Orara River at Bawden Bridge (204041)

| Statistic	Value			
Start of record	June 1960			
End of record	Feb 2006			
Length of record (years)	46			
Percentage of missing data (%)	7.5			
Maximum recorded hourly flow (m^3/s)	2365			
Minimum recorded hourly flow (m^3/s)	0			
Proportion of time of cease to flow events (%)	0.2			
Maximum gauged flow (m^3/s)	2832			
ARI of maximum gauged flow	46			
Percentage of time hourly flow is greater than maximum gauged flow (%)	0			
	Dec-Feb	**Mar-May**	**June-Aug**	**Sep-Nov**
Proportion of events (%)	37	40	15	15
Seasonal maximum flow (m^3/s)	1251	2366	873	1451
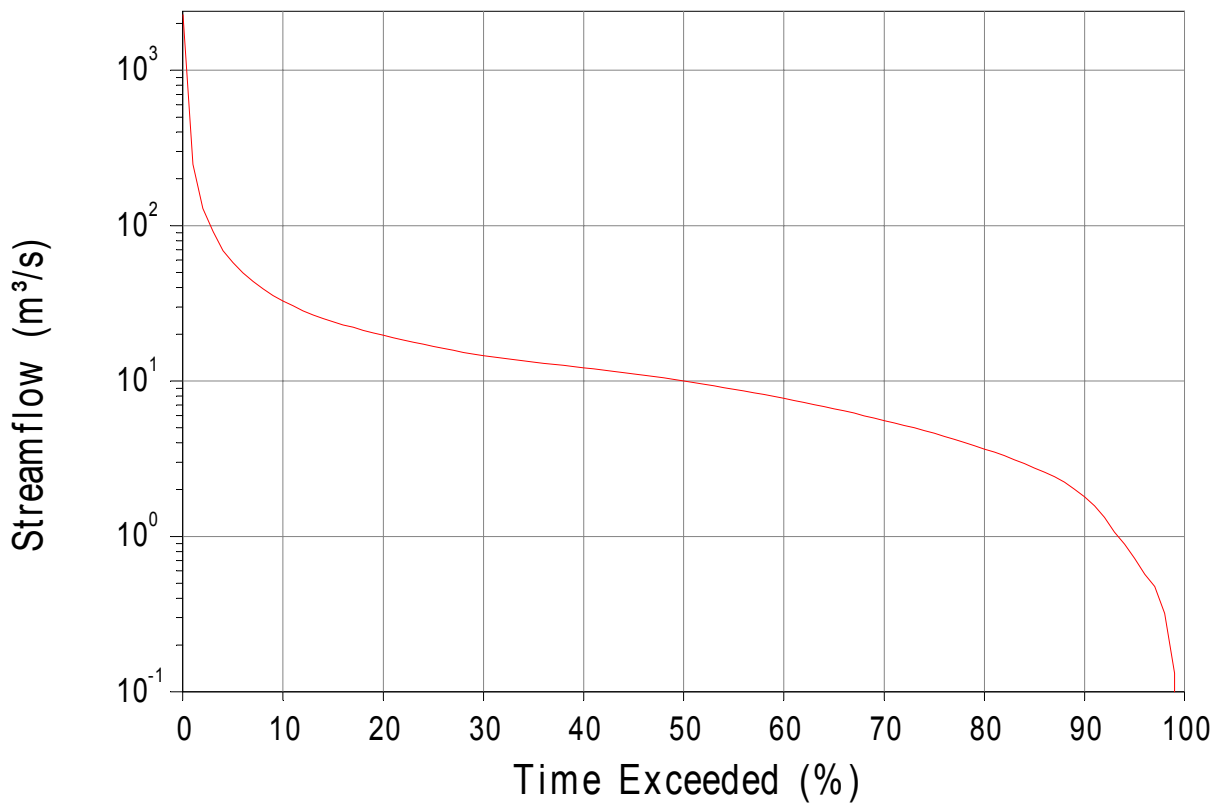
Figure 27 Flow duration curve, Orara River at Bawden Bridge (204041)

Figure 28 presents the flood frequency analysis for the site. Over 180 events were analysed for the catchment, extracted from over 45 years of streamflow data. The majority of these flow events occur from December to May, with the largest range in event size occurring in March, April and May (Figure 29). Despite fewer events occurring from September to November, the events during this season can be reasonably large.
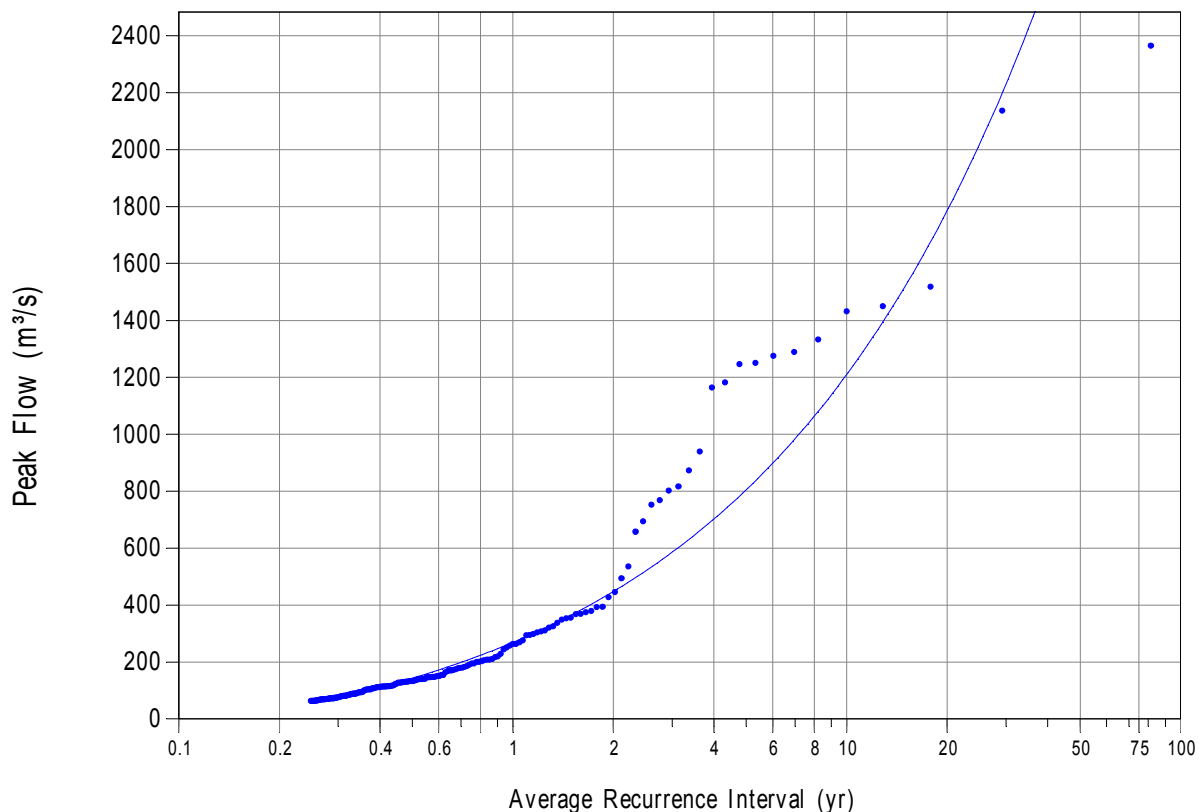
Figure 28 Flood frequency analysis, Orara River at Bawden Bridge (204041)
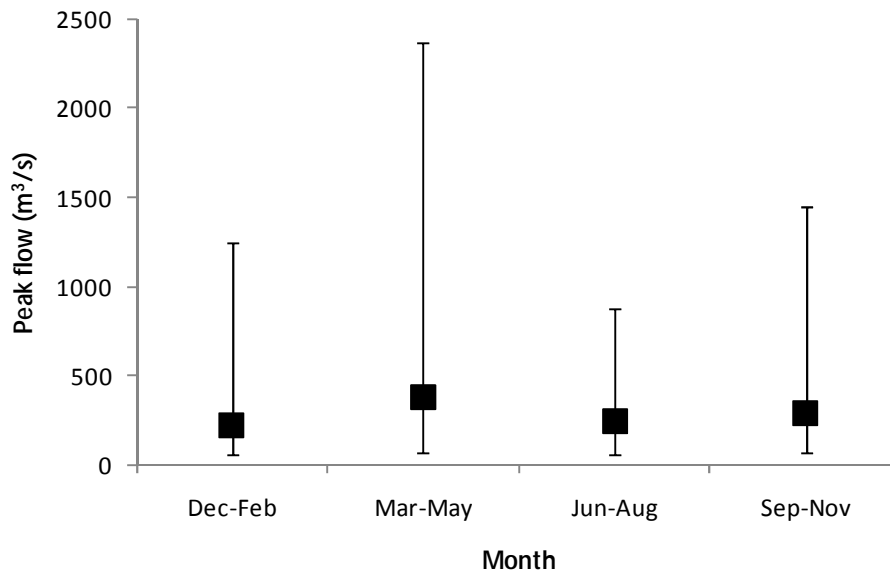
Figure 29 Seasonality of events, Orara River at Bawden Bridge (204041). The box represents the magnitude of the mean flow event, and the whiskers represent the full range of events analysed for this study.

7.3.3. Baseflow Analysis

Nine passes of the Lyne and Hollick filter, with a parameter value of 0.925, were applied to extract the baseflow for each event. Sample hydrographs are presented in Figure 30 and key statistics are summarised in Table 7. Figure 31a displays the variation in BFI with ARI. In general, as the event size increases, the BFI decreases. Figure 31b displays a similar trend for the ratio of the baseflow at the time of the streamflow peak to the peak streamflow. In both these figures, a large amount of scatter is evident for small events. The variability in the relationship generally reduces with ARI.

In contrast, the absolute magnitude of the baseflow at the time of the streamflow peak tends to increase as the ARI increases (Figure 31c). Variability in this measure tends to increase with event size. The goodness of fit measure (r^2) for all components of Figure 31 is low, indicating the poor correlation of these models.

Additional plots are presented in Appendix C, which display similar trends for the baseflow peak.

Table 7 Baseflow statistics, Orara River at Bawden Bridge (204041)

Statistic	BFI of event	Ratio of baseflow under streamflow peak : streamflow peak	Ratio of baseflow peak : streamflow peak
Average	0.44	0.25	0.34
Maximum	0.77	0.65	0.67
Minimum	0.08	0.01	0.05
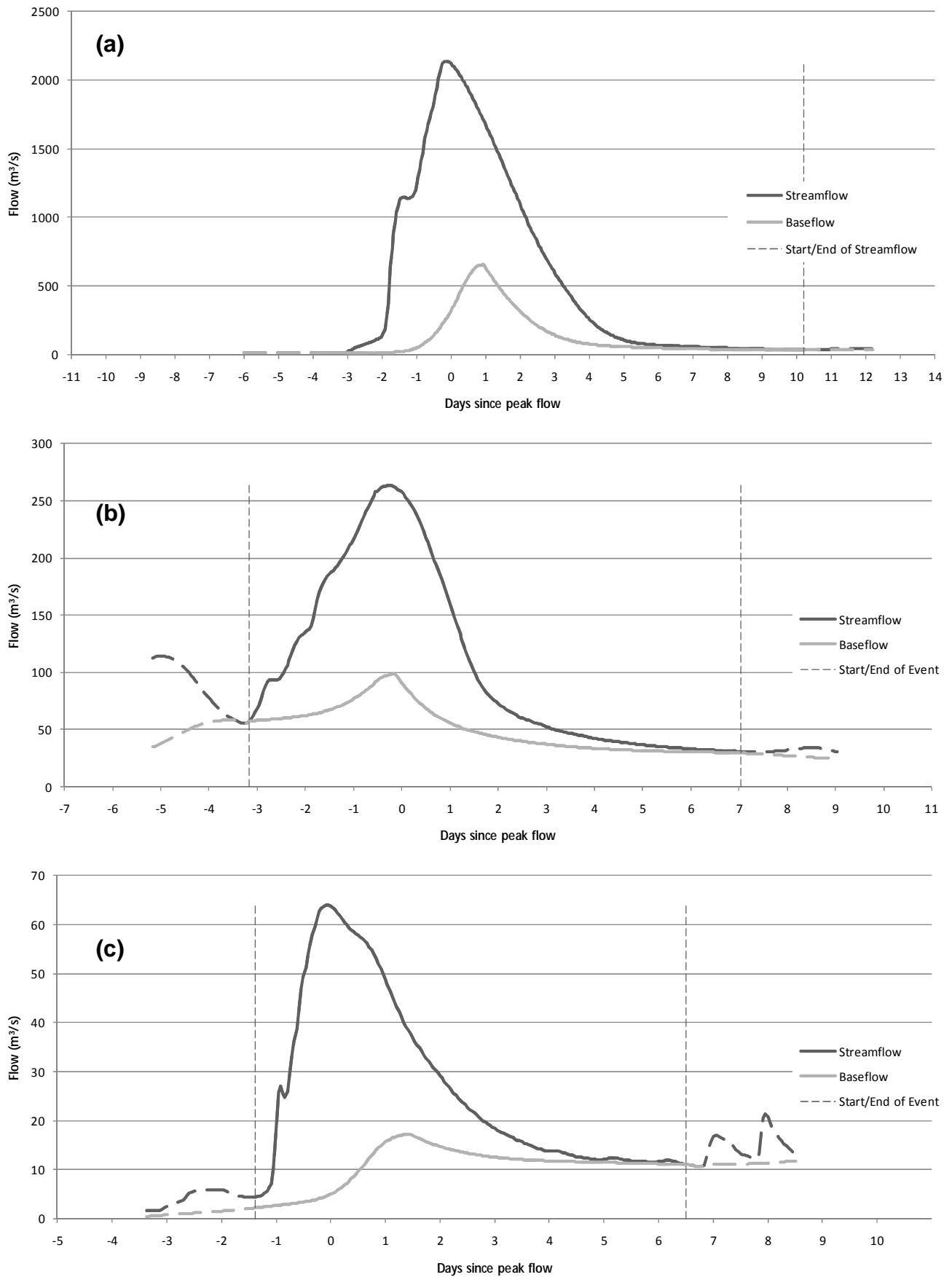
Figure 30 Sample hydrographs demonstrating the streamflow and baseflow characteristics for a range of events Orara River at Bawden Bridge (204041): (a) ARI of 28 years, (b) ARI of 1 year, (c) ARI of 0.25 years
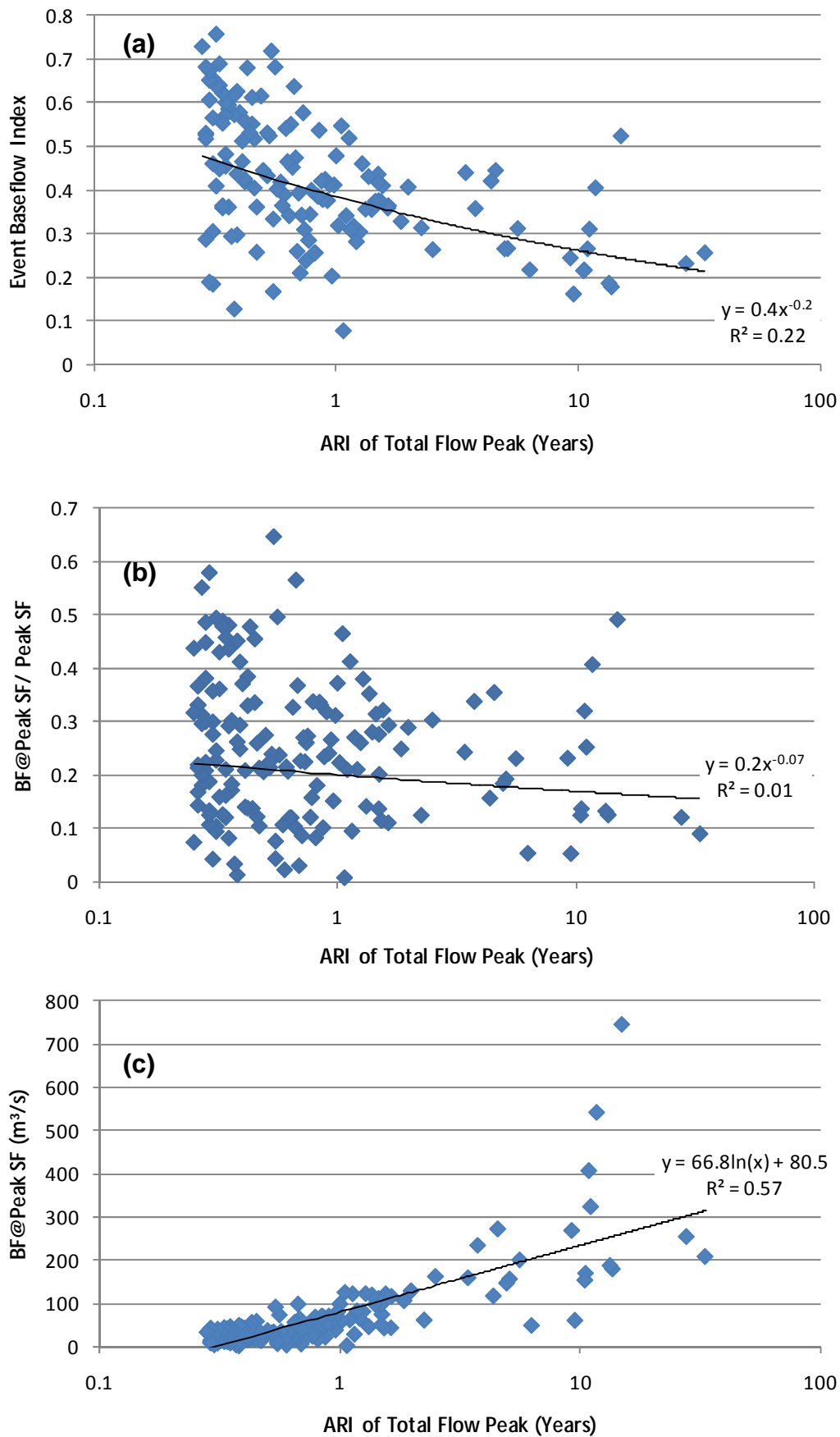
Figure 31 (a) Variation in event BFI with ARI of total flow peak, (b) Ratio of baseflow under streamflow peak to peak streamflow, (c) Absolute magnitude of baseflow under streamflow peak, Orara River at Bawden Bridge (204041)

7.4. Bell River at Newrea, New South Wales (421018)

7.4.1. Catchment Description

The Bell River is located in central New South Wales, in the Macquarie River Basin. The catchment has an area of 1248 km². Further details of the catchment characteristics are provided in Appendix B.

7.4.2. Flow Characteristics

The flow characteristics at the gauge location are presented in Table 8. The streamflow gauge at this site commenced operation in 1973 and has been operating continuously since that time. The maximum flow recorded at the site is greater than 1000 m^3/s, whilst cease to flow periods account for over 1% of the record (Figure 32). Almost 400 gaugings have been measured at the site, with all high flow events captured within the extent of these gauging records. The maximum gauged flow was measured at the time of the largest flood event, and captured the peak of the event. The maximum recorded hourly flow in Table 8 reflects the average hourly conditions, which is slightly lower than the instantaneous flood peak captured in the gauging measurements.

Table 8 Streamflow characteristics for Bell River at Newrea (421018)

| Statistic	Value			
Start of record	May-1973			
End of record	Jan-2006			
Length of record (years)	33			
Percentage of missing data (%)	0%			
Maximum recorded hourly flow (m^3/s)	1189			
Minimum recorded hourly flow (m^3/s)	0.00			
Proportion of time of cease to flow events (%)	1.3%			
Maximum gauged flow (m^3/s)	1238			
ARI of maximum gauged flow	35			
Percentage of time hourly flow is greater than maximum gauged flow (%)	0			
	Dec-Feb	**Mar-May**	**June-Aug**	**Sep-Nov**
Proportion of events extracted (%)	19	10	35	36
Seasonal maximum flow event (m^3/s)	883	942	941	587
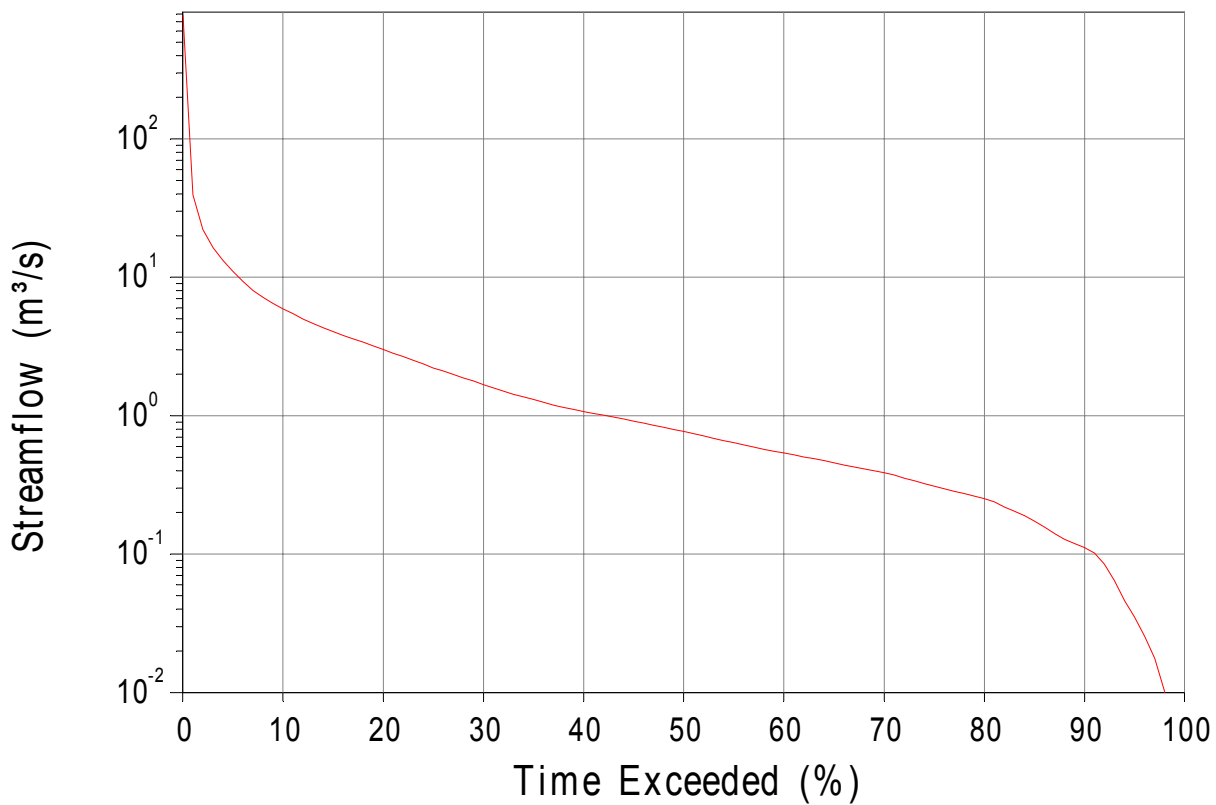
Figure 32 Flow duration curve, Bell River at Newrea (421018)

Figure 33 presents the flood frequency analysis for Bell River at Newrea, which was undertaken using 120 events from the time series. The seasonality of these events is presented in Figure 34. The average event size (shown by the solid box) is reasonably consistent across the seasons. The largest events tend to occur from March to August, although events occurring from December to February are also reasonably large. Most events occur over the period from June to November.
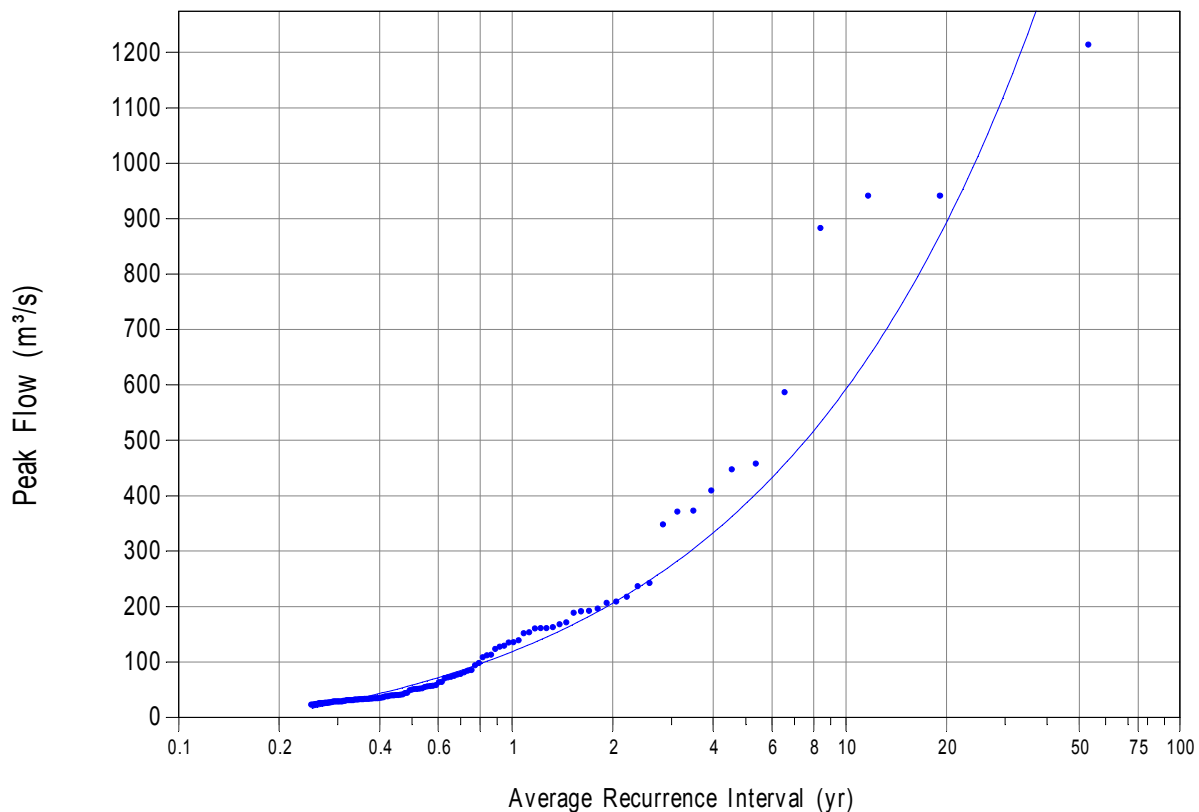
Figure 33 Flood frequency analysis, Bell River at Newrea (421018)
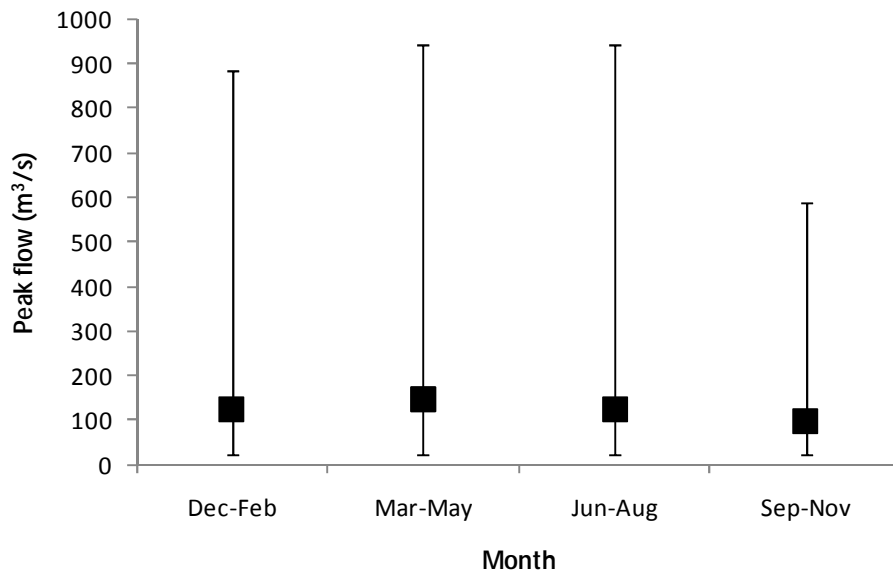
Figure 34 Seasonality of events, Bell River at Newrea (421018). The box represents the magnitude of the mean flow event, and the whiskers represent the full range of events analysed for this study.

7.4.3. Baseflow Analysis

Nine passes of the Lyne and Hollick filter, with a parameter value of 0.925, were applied to extract the baseflow for each event at the Bell River site. Sample hydrographs are presented in Figure 35 and key statistics are summarised in Table 3. The variation in these statistics for different event sizes is presented in Figure 36a and Figure 36b. In general, a downwards trend is observed, demonstrating that the ratio of baseflow tends to reduce as the magnitude of the total flow event increases. Additionally, the variability associated with these trends also reduces as ARI increase.

In contrast, Figure 36c displays the absolute magnitude of the absolute baseflow under the stremflow peak, which increases as the flood magnitude increases. The scatter associated with this relationship tends to increase with increasing flood event size. The trendlines fitted in Figure 36a-c indicate a poor correlation in the data, with r^2 values less than 0.25.

Additional plots are presented in Appendix C, which display similar trends for the baseflow peak.

Table 9 Baseflow statistics, Bell River at Newrea (421018)

Statistic	BFI of event	Ratio of baseflow under streamflow peak : streamflow peak	Ratio of baseflow peak : streamflow peak
Average	0.34	0.09	0.14
Maximum	0.73	0.51	0.65
Minimum	0.01	0.00	0.00
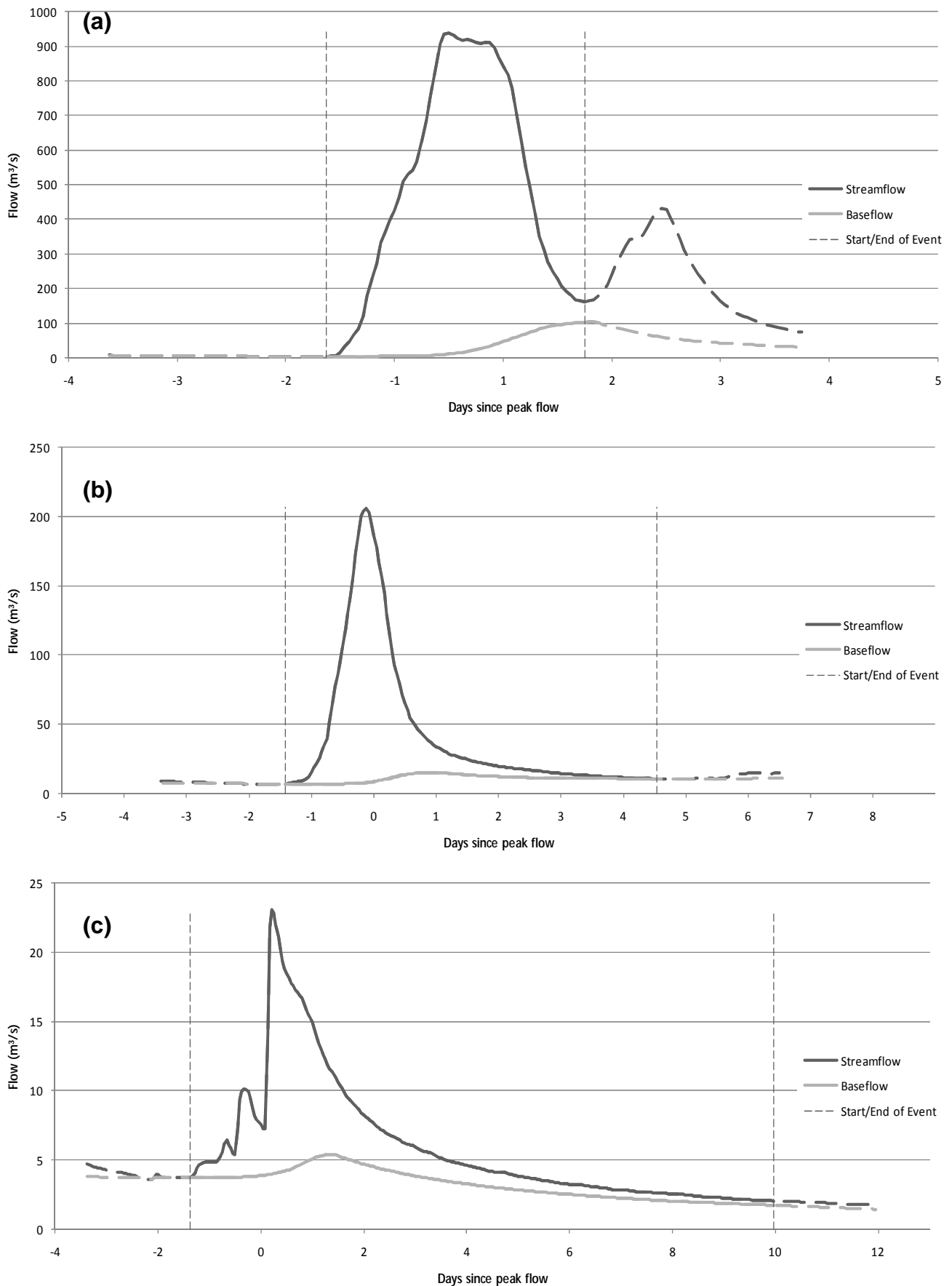
Figure 35 Sample hydrographs demonstrating the streamflow and baseflow characteristics for a range of events Bell River at Newrea (421018): (a) ARI of 22 years (b) ARI of 2 years (c) ARI of 0.26 years
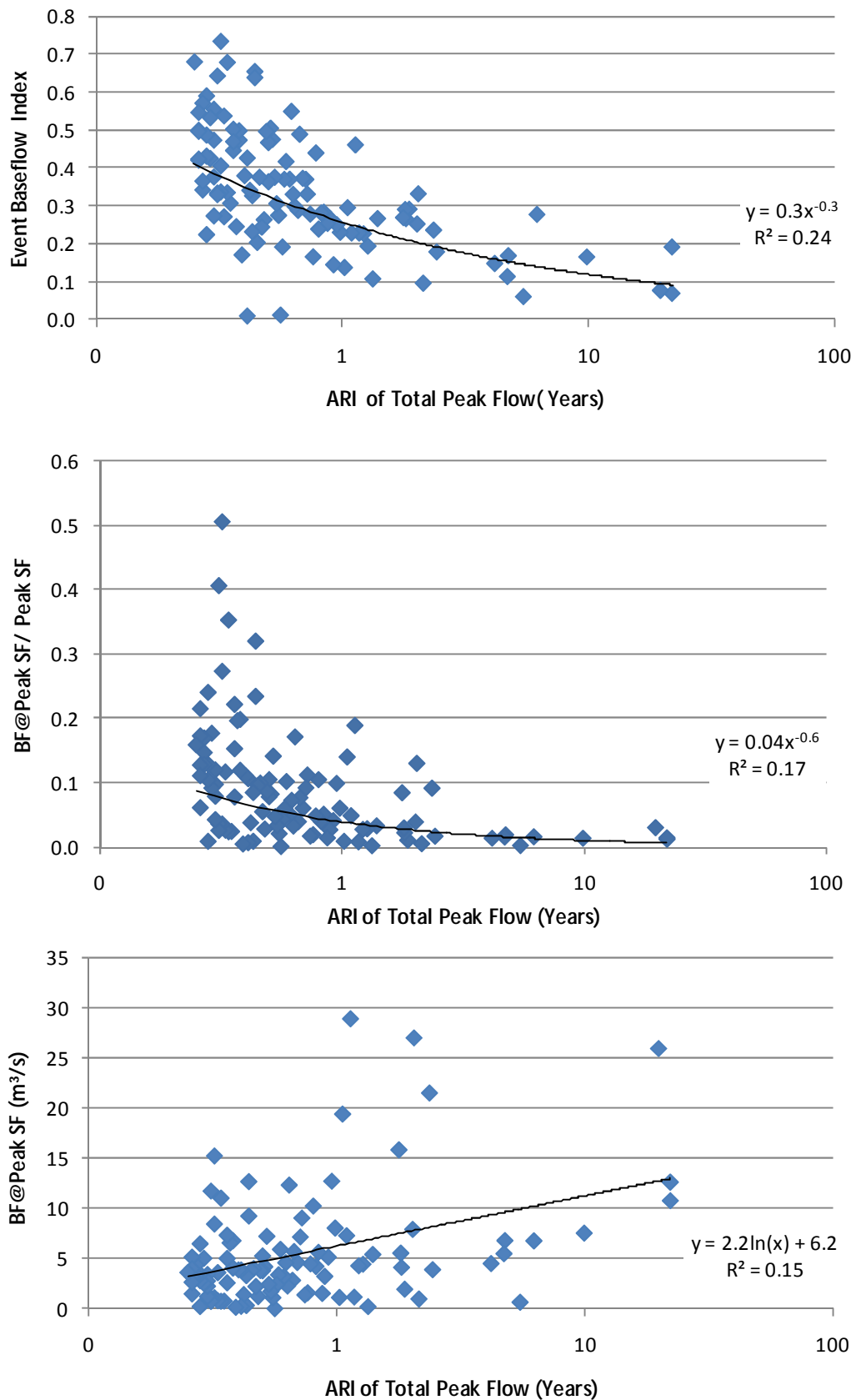
Figure 36 (a) Variation in event BFI with ARI of total flow peak, (b) Ratio of baseflow under streamflow peak to peak streamflow, (c) Absolute magnitude of baseflow under streamflow peak, Bell River at Newrea (421018)

7.5.   Tambo River at Swifts Creek, Victoria (223202)

7.5.1. Catchment Description

Tambo River is located in eastern Victoria, commencing in the alpine region of Victoria and flowing south to the Gippsland Lakes at the coast. The Swifts Creek gauging location has a catchment area of approximately 900km^2. Further catchment details are provided in Appendix B.

7.5.2. Flow Characteristics

The streamflow gauge at Swifts Creek has been in operation since 1947. Since that time, the gauge has moved slightly twice, however these changes are not considered significant in terms of data continuity. The data analysed for this study consists of a continuous record of data captured at the three locations (223202a, 223202b and 223202c). The flow characteristics at the gauge location are presented in Table 10. A small proportion of the cease to flow events occur at the site (Figure 37).

Table 10 Streamflow characteristics for Tambo River at Swifts Creek (223202)

| Statistic	Value			
Start of record	June 1947			
End of record	June 2009			
Length of record (years)	62			
Percentage of missing data (%)	0			
Maximum recorded hourly flow (m^3/s)	417			
Minimum recorded hourly flow (m^3/s)	0.00			
Proportion of time of cease to flow events (%)	0.1			
Maximum gauged flow (m^3/s)	126			
ARI of maximum gauged flow	8			
Percentage of time hourly flow is greater than maximum gauged flow (%)	0.026			
	Dec-Feb	**Mar-May**	**June-Aug**	**Sep-Nov**
Proportion of events extracted (%)	17	12	31	41
Seasonal maximum flow (m^3/s)	420	130	405	176
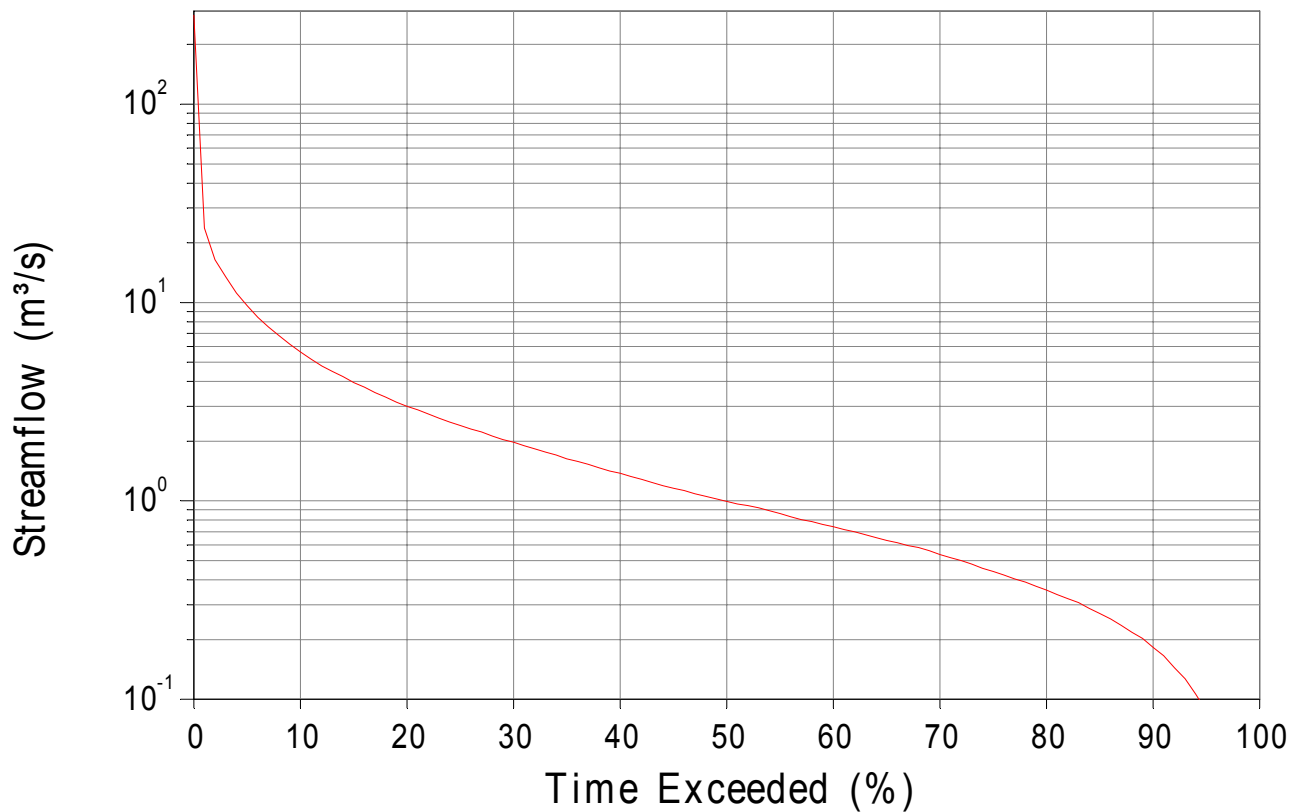
Figure 37 Flow duration curve, Tambo River at Swifts Creek (223202)

Figure 38 presents the flood frequency analysis for the Tambo River site. Almost 250 events spanning over 60 years were analysed for this location. The majority of flood events occur in September to November, however these events tend to be smaller than the events that occur from December to February and June to August (Figure 39).
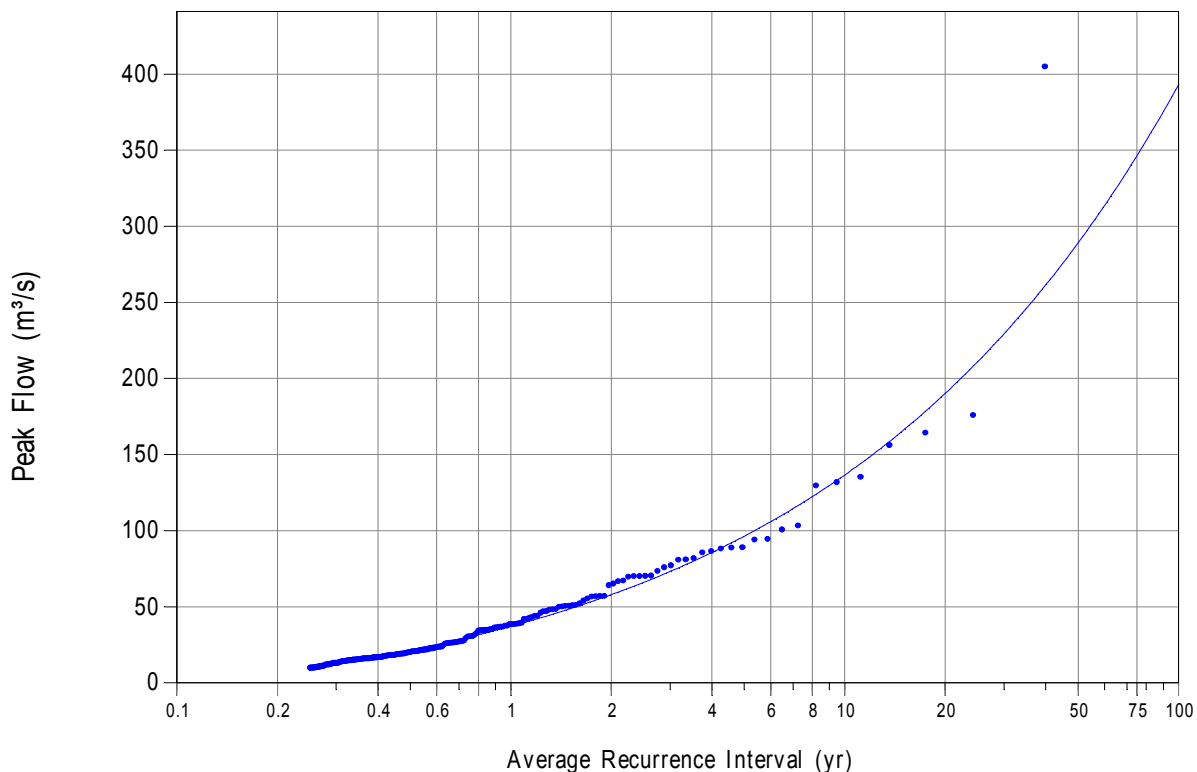
Figure 38 Flood frequency analysis, Tambo River at Swifts Creek (223202)
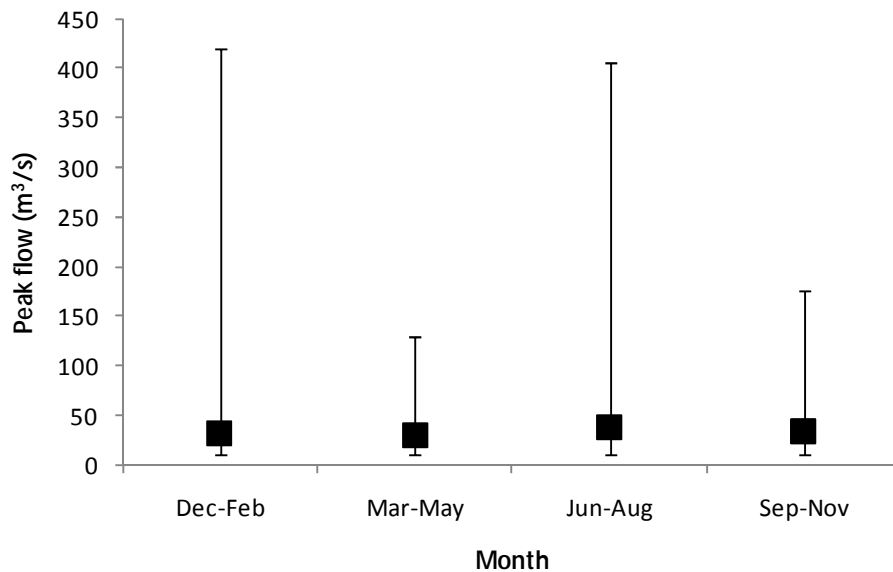
Figure 39 Seasonality of events, Tambo River at Swifts Creek (223202). The box represents the magnitude of the mean flow event, and the whiskers represent the full range of events analysed for this study.

7.5.3. Baseflow Analysis

Nine passes of the Lyne and Hollick filter, with a parameter value of 0.925, were applied to extract the baseflow for each event. Sample hydrographs are presented in Figure 40 and key statistics are summarised in Table 11. Variation in the BFI with the ARI of the total flow event is presented in Figure 41a. A large degree of scatter is evident, particularly for smaller events. However, the general trend demonstrates that BFI decreases as the event size increases. Figure 41b displays a similar result for the ratio of the baseflow under the streamflow peak to the peak streamflow.

In contrast, the absolute magnitude of the baseflow under the streamflow peak and the degree of scatter in this statistic tend to increase for larger events (Figure 41c). The trendlines in Figure 41 demonstrate a poor correlation, with low r^2 values. Additional scatter plots for other statistics are presented in Appendix B.
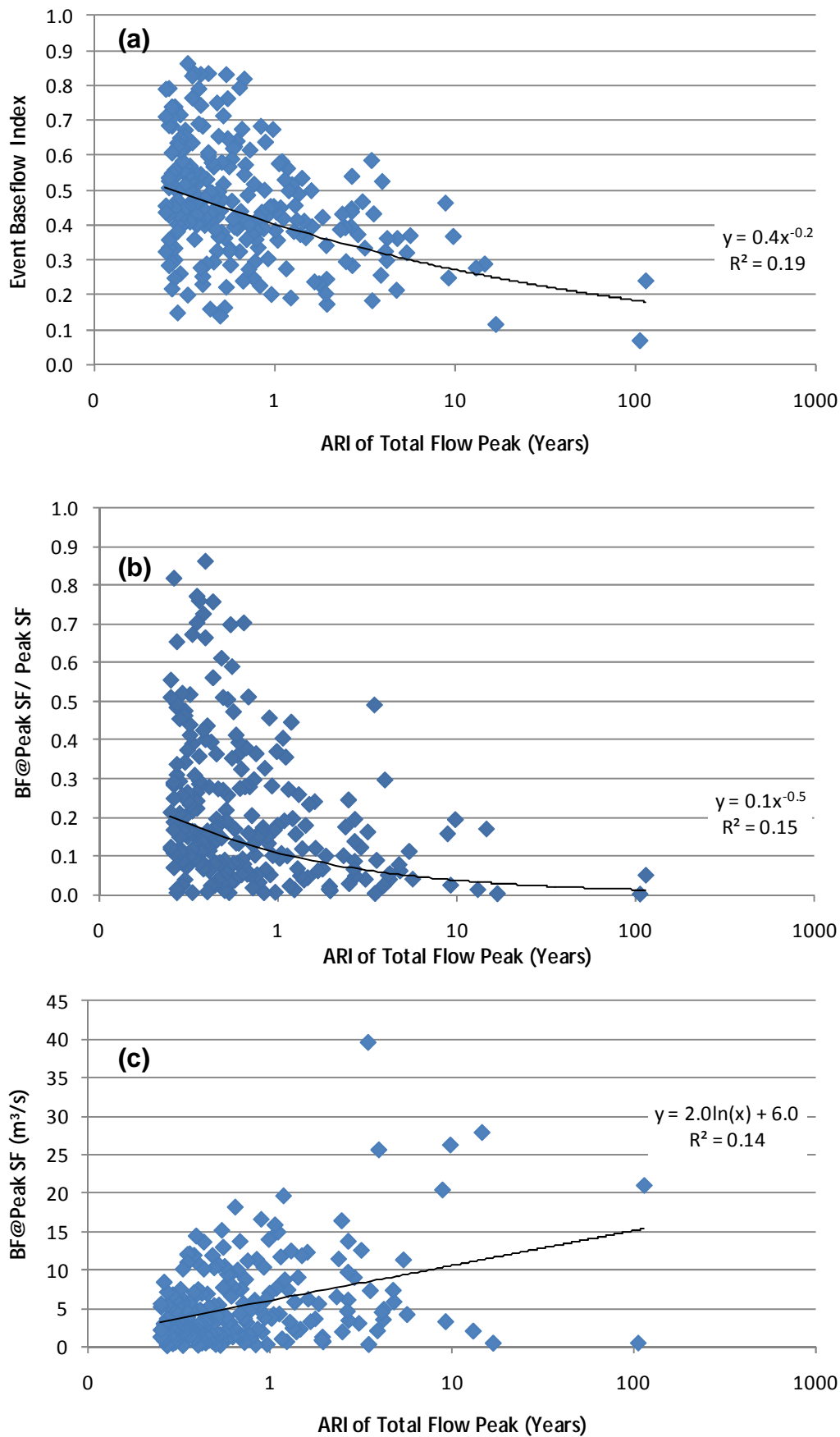
Table 11 Baseflow statistics, Tambo River at Swifts Creek (223202)

Statistic	BFI of event	Ratio of baseflow under streamflow peak : streamflow peak	Ratio of baseflow peak : streamflow peak
Average	0.46	0.21	0.33
Maximum	0.86	0.86	0.91
Minimum	0.07	0.001	0.01
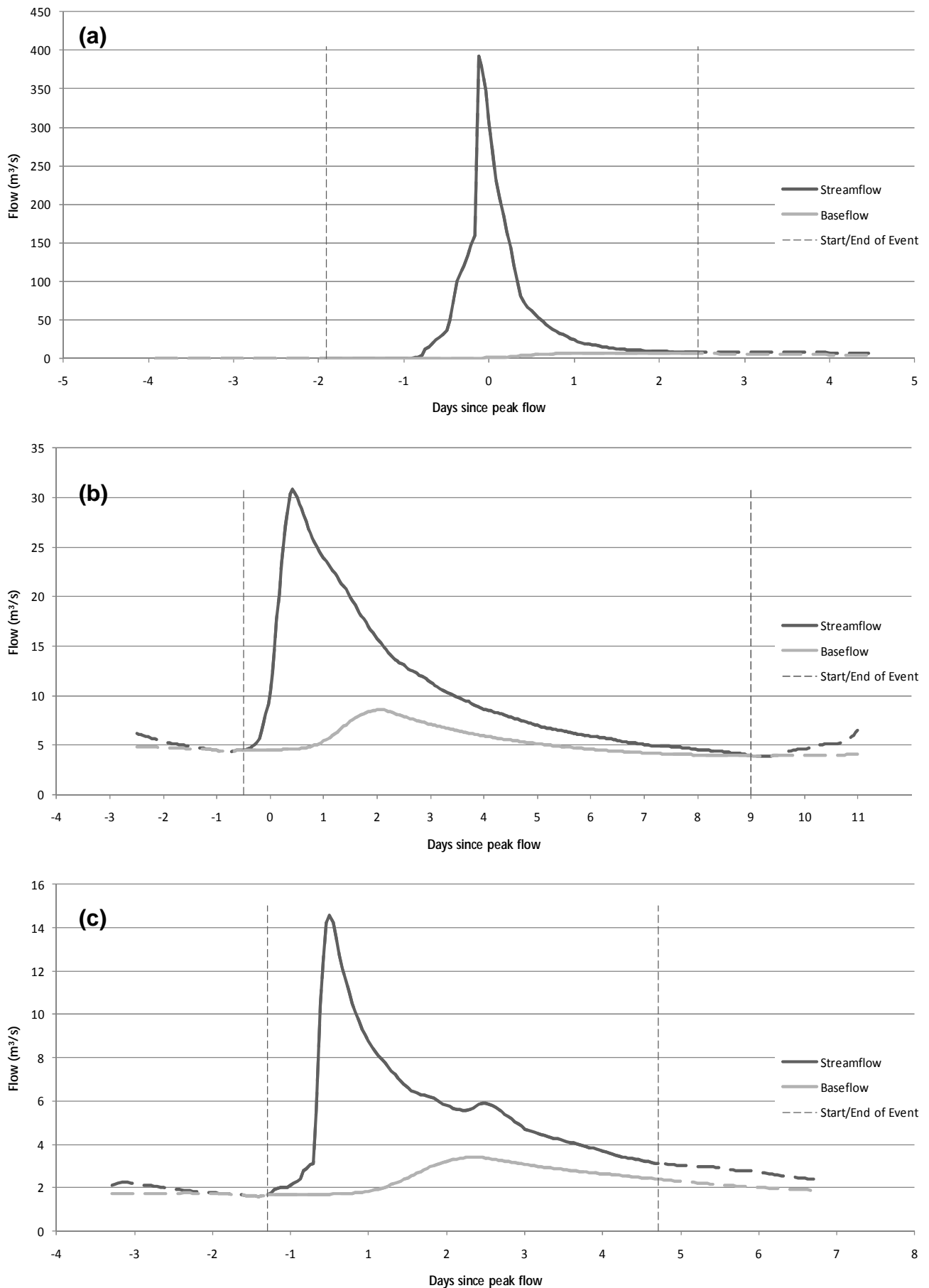
Figure 40 Sample hydrographs demonstrating the streamflow and baseflow characteristics for a range of events, Tambo River at Swifts Creek (223202): (a) ARI of 106 years, (b) ARI of 0.77 years, (c) ARI of 0.33 years

Figure 41 (a) Variation in event BFI with ARI of total flow peak, (b) Ratio of baseflow under streamflow peak to peak streamflow, (c) Absolute magnitude of baseflow under streamflow peak, Tambo River at Swifts Creek (223202)

7.6. Little Yarra River at Yarra Junction, Victoria (229214)

7.6.1. Catchment Description

The Little Yarra River is located in Victoria, commencing in the Yarra Ranges to the east of Melbourne. The upper reaches of the catchment are heavily forested, with logging occurring in some areas. Appendix B summarises the catchment characteristics at the site.

7.6.2. Flow Characteristics

The flow characteristics at the gauge location are displayed in Table 12. The streamflow gauge at this site commenced operation in 1963, and has recorded continuously since that time. The average daily flow ranges between 0.11 m^3/s and 21.6 m^3/s, whereas maximum hourly flows of over 60 m^3/s have been recorded. No cease to flow events are recorded at this location, as displayed in the flow duration curve (Figure 42). Over 300 gaugings have been measured at this site since it opened, with the maximum gauging representing an event with ARI of approximately 39 years.

Table 12 Streamflow characteristics for Little Yarra River at Yarra Junction (site 229214)

| Statistic	Value			
Start of record	April 1963			
End of record	January 2009			
Length of record (years)	45			
Percentage of missing data (%)	1			
Maximum recorded hourly flow (m^3/s)	60			
Minimum recorded hourly flow (m^3/s)	0.10			
Proportion of time of cease to flow events (%)	0			
Maximum gauged flow (m^3/s)	27			
ARI of maximum gauged flow	39			
Percentage of time hourly flow is greater than maximum gauged flow (%)	0.004%			
	Dec-Feb	Mar-May	June-Aug	Sep-Nov
Proportion of events extracted (%)	12	14	34	39
Seasonal maximum flow event (m^3/s)	23	14	29	31
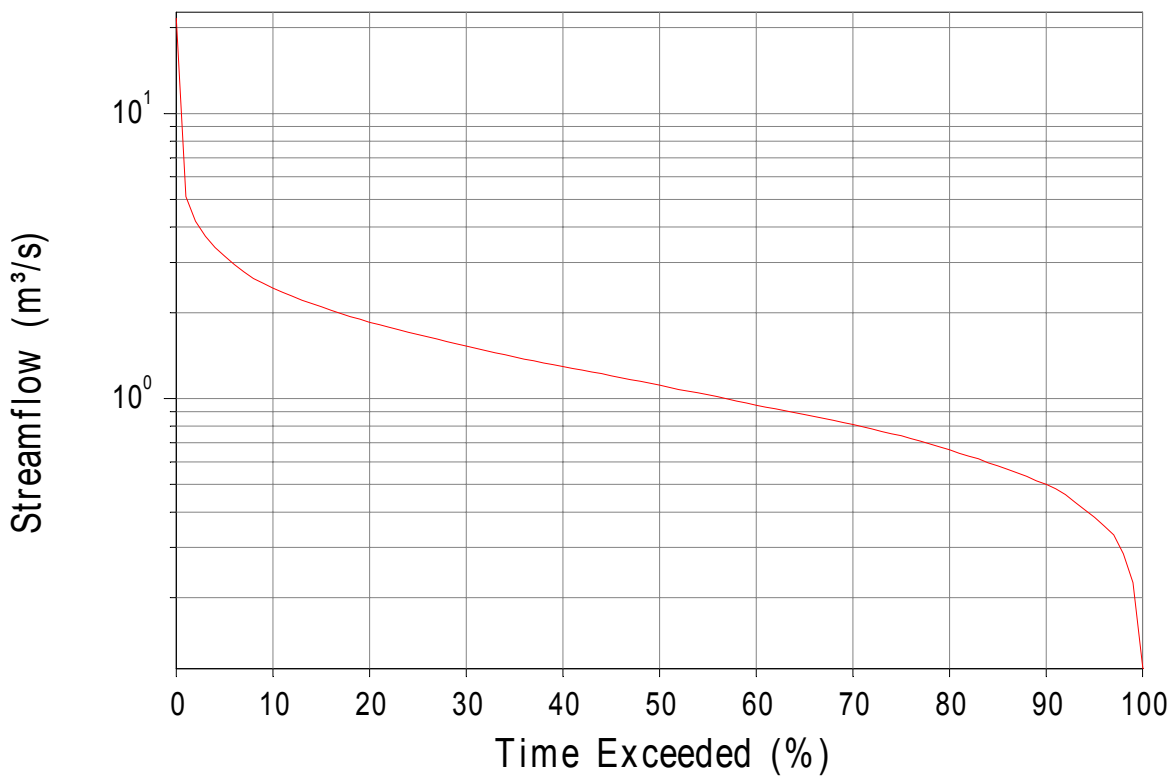
Figure 42 Flow duration curve, Little Yarra River at Yarra Junction (site 229214)

Figure 43 displays the flood frequency analysis for the site, undertaken using information on 180 events over 45 years of data. The bulk of these events occur in winter and spring. Figure 44 provides a summary of the range in event sizes that occur in each season, with the solid box representing the average event size and the bars extending to the maximum and minimum event sizes. The average event size is reasonably consistent regardless of the season. The largest events tend to occur from June to November (maximum ARI of 80 years), whereas the largest event to occur in the period between March to May has an ARI of 5 years.
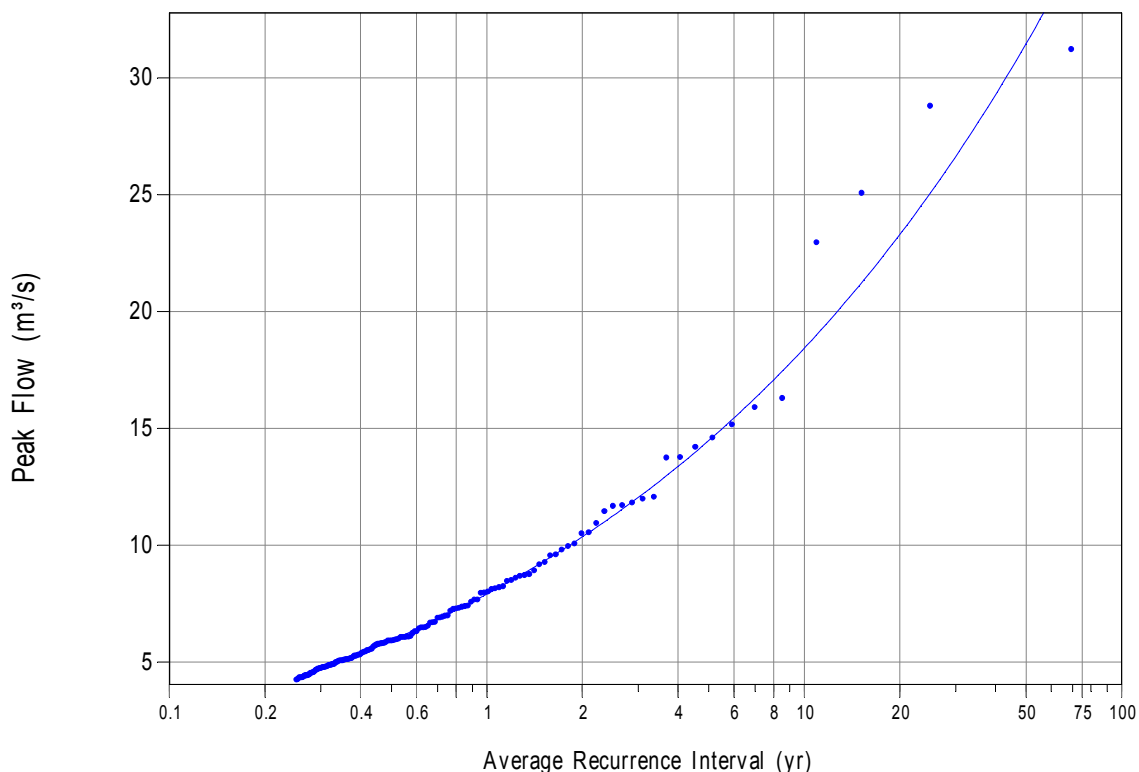
Figure 43 Flood frequency analysis, Little Yarra River at Yarra Junction (site 229214)
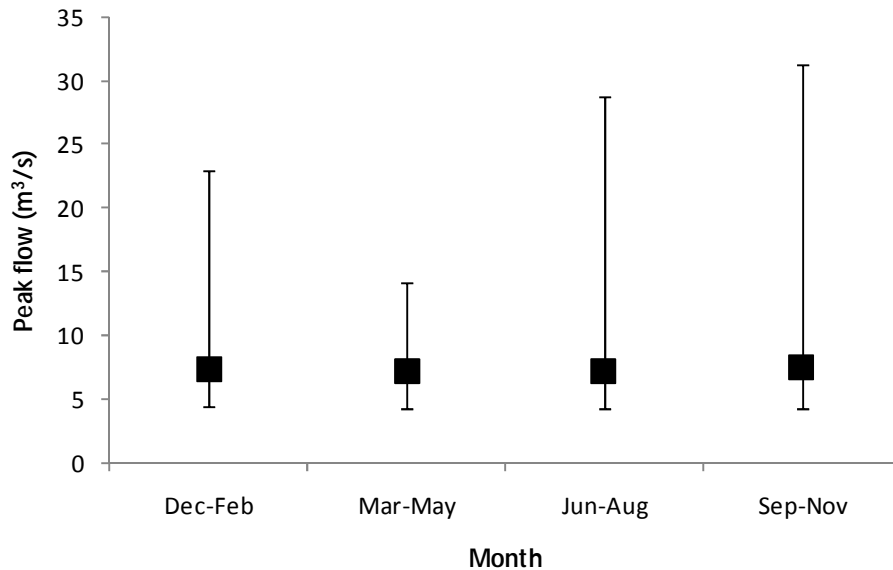
Figure 44 Seasonality of events, Little Yarra River at Yarra Junction (site 229214). The box represents the magnitude of the mean flow event, and the whiskers represent the full range of events analysed for this study.

7.6.3. Baseflow analysis

Baseflow separation of the hourly streamflow data was undertaken using 9 passes of the Lyne and Hollick filter (each pass represents filtering in a single direction), with a parameter value of 0.925 (refer to Figure 45 for sample hydrographs). The statistics described in Section 6.4 were calculated for each flood event at the site. Table 13 summarises these statistics for all flood events analysed. The variation in these statistics for different event sizes is presented in Figure 46a and Figure 46b. A slight downwards trend in all statistics are observed as event ARI increases. The ratio of the baseflow under the streamflow peak to the peak streamflow produces the strongest relationship, although both statistics display a high degree of variability for small event sizes. The absolute magnitude of the baseflow under the streamflow peak is presented in Figure 46c, and displays an upward trend with baseflow increasing as ARI of the total flow increases. Additional scatter plots for other statistics are presented in Appendix B. The relationships in Figure 46 all have a poor fit, with low r^2 values.

Table 13 Baseflow statistics, Little Yarra River at Yarra Junction (site 229214)

Statistic	BFI of event	Ratio of baseflow under streamflow peak : streamflow peak	Ratio of baseflow peak : streamflow peak
Average	0.58	0.32	0.39
Maximum	0.87	0.71	0.72
Minimum	0.22	0.03	0.07
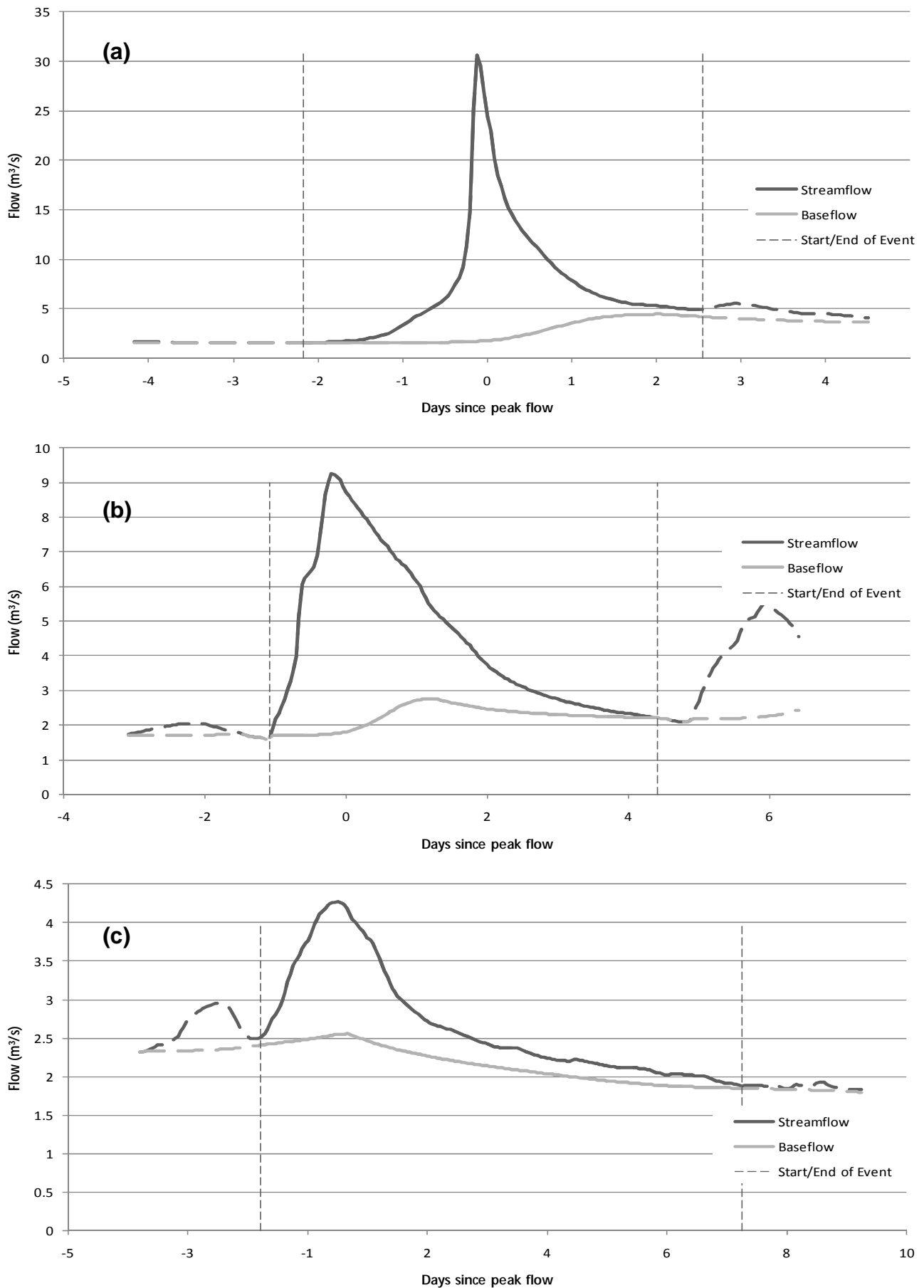
Figure 45 Sample hydrographs demonstrating the streamflow and baseflow characteristics for a range of events, Little Yarra River at Yarra Junction (229214): (a) ARI of 49 years, (b) ARI of 1.5 years, (c) ARI of 0.5 years
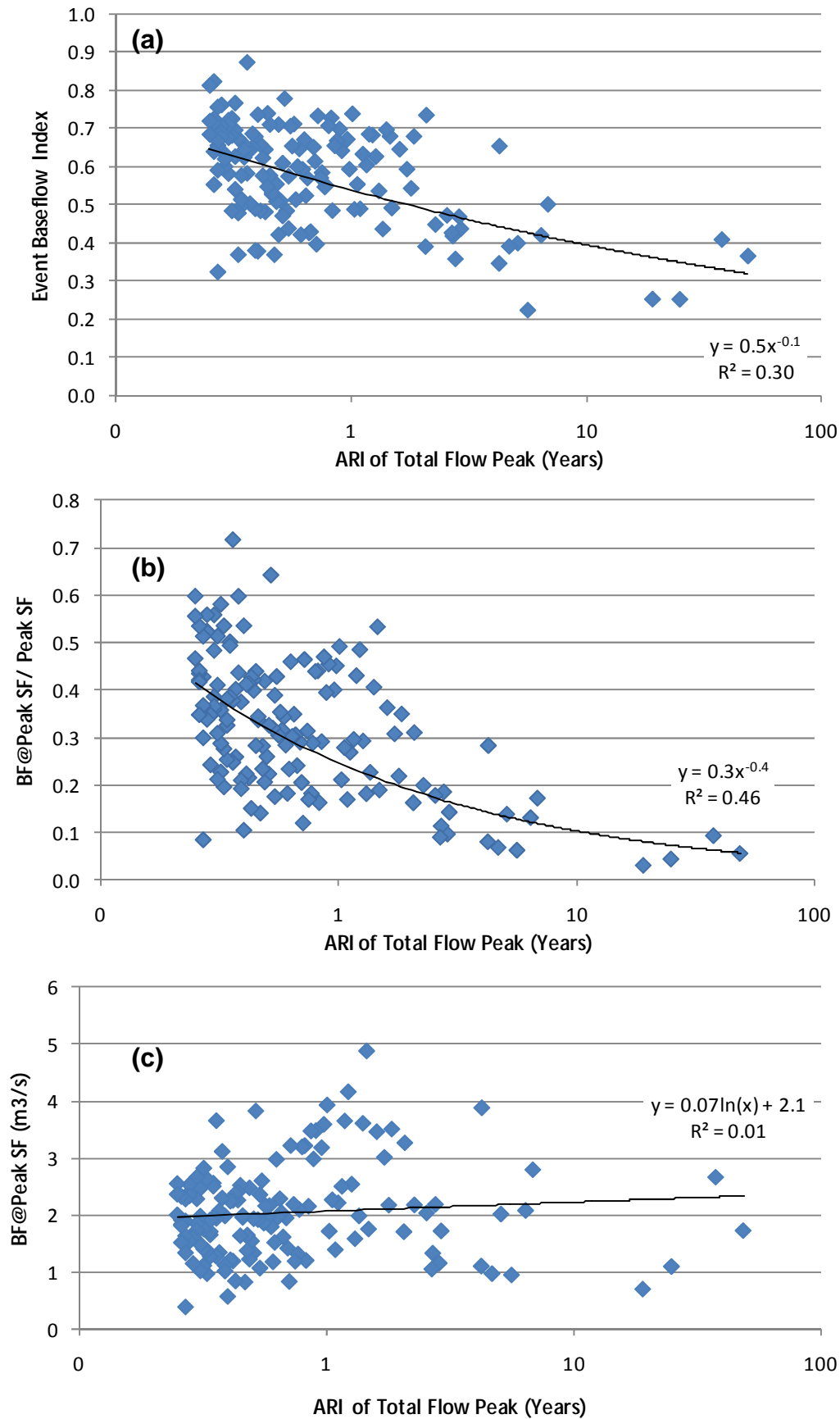
Figure 46 (a) Variation in event BFI with ARI of total flow peak, (b) Ratio of baseflow under streamflow peak to peak streamflow, (c) Absolute magnitude of baseflow under streamflow peak, Little Yarra River at Yarra Junction (229214)

7.7. Lennard River at Mt Herbert, Western Australia (803002S)

7.7.1. Catchment Description

The Lennard River is situated in northern Western Australia, in the Kimberley region, inland from Derby. The site at Mt Herbert has a catchment area of 440km^2. Further catchment specific information is provided in Appendix B.

7.7.2. Flow Characteristics

The flow characteristics at the gauge location are presented in Table 14. The streamflow gauge at this site commenced operation in 1967 and closed in 1999. Over this time, 31 years of data was collated, with approximately 4% missing. The flow is ephemeral, with extended periods of cease to flow (Figure 47).

Table 14 Streamflow characteristics for Lennard River at Mount Herbert (803002s)

Statistic	Value			
Start of record	October 1967			
End of record	August 1999			
Length of record (years)	31			
Percentage of missing data (%)	4			
Maximum recorded hourly flow (m^3/s)	1375			
Minimum recorded hourly flow (m^3/s)	0.00			
Proportion of time of cease to flow events (%)	42.4			
Maximum gauged flow (m^3/s)	71			
ARI of maximum gauged flow	0.3			
Percentage of time hourly flow is greater than maximum gauged flow (%)	0.9			
	Dec-Feb	**Mar-May**	**June-Aug**	**Sep-Nov**
Proportion of events extracted (%)	63	32	2	3
Seasonal maximum flow event (m^3/s)	1399	892	230	179
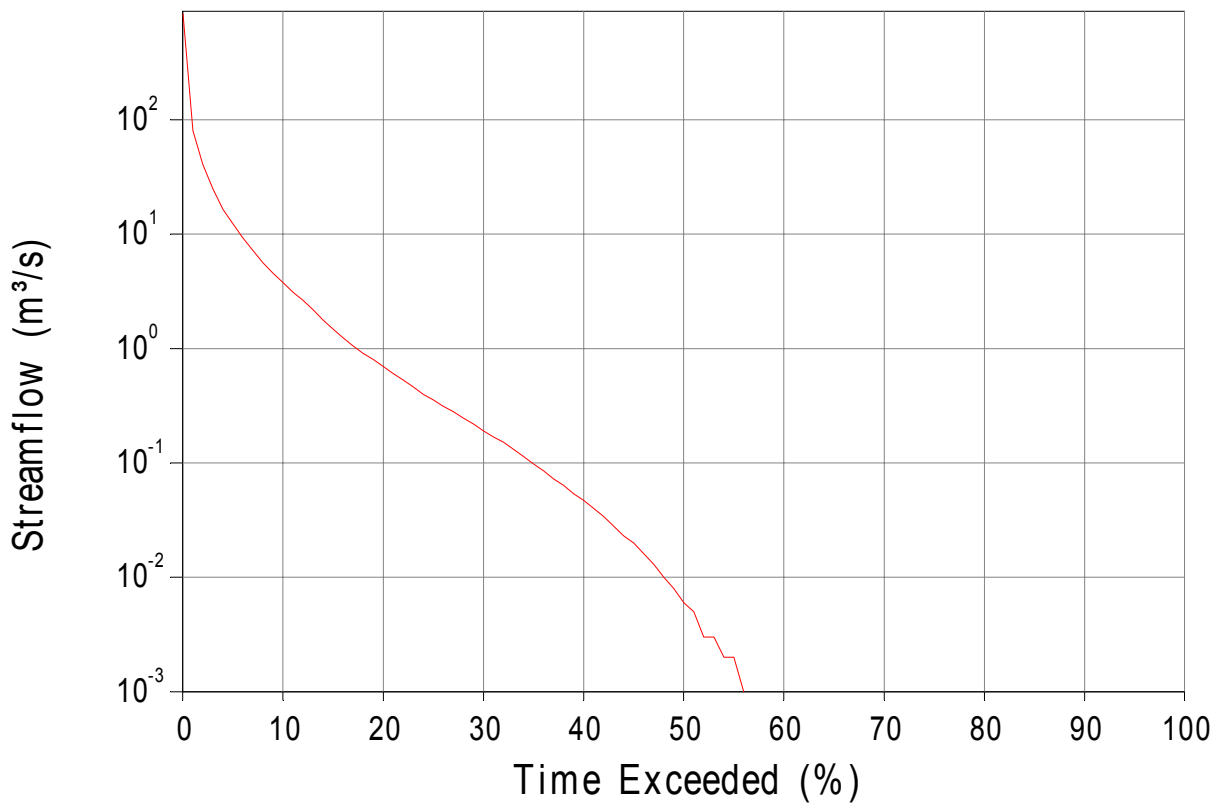
Figure 47 Flow duration curve, Lennard River at Mount Herbert (803002s)

Figure 48 presents the flood frequency analysis for the Lennard River site. Over 120 events were analysed for this assessment, spanning over 30 years. The majority of flow events, including the largest flood, occur between December and February. The average event size in other months is similar (Figure 49).
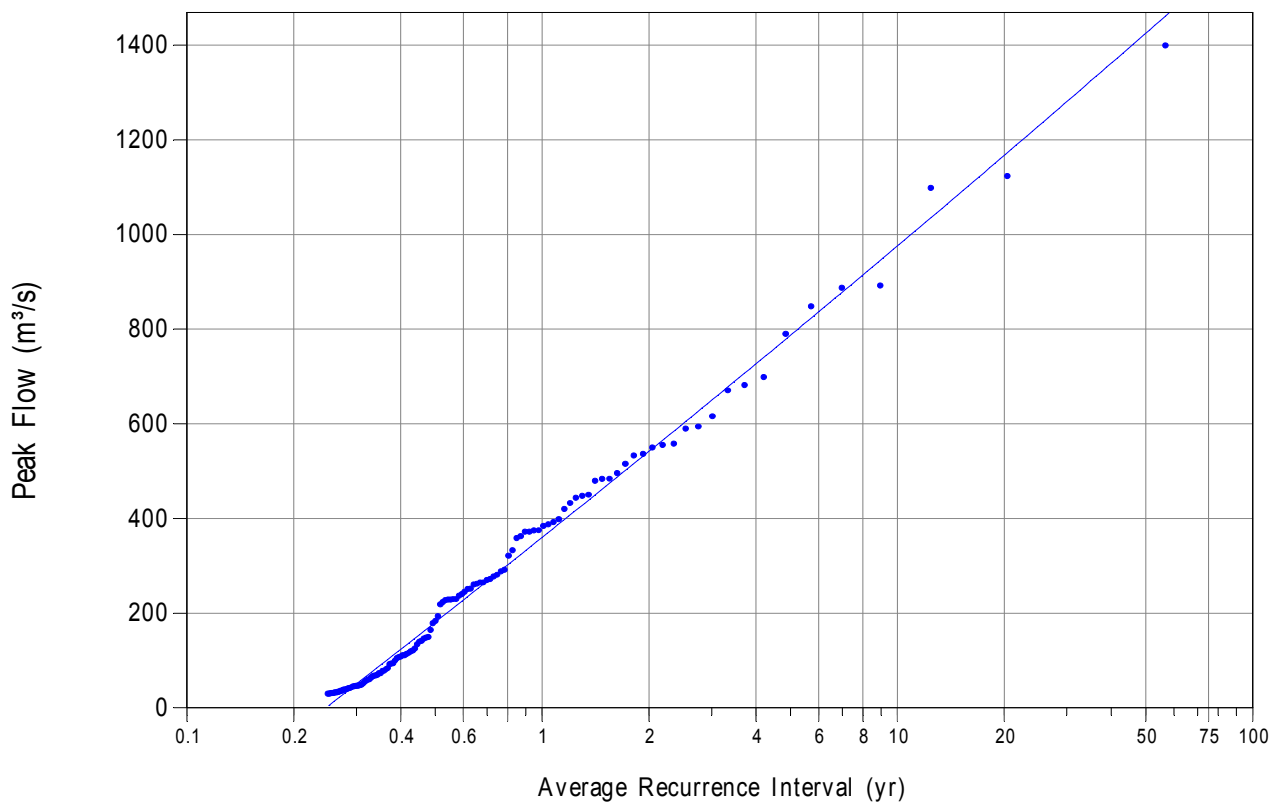
Figure 48 Flood frequency analysis, Lennard River at Mount Herbert (803002s)
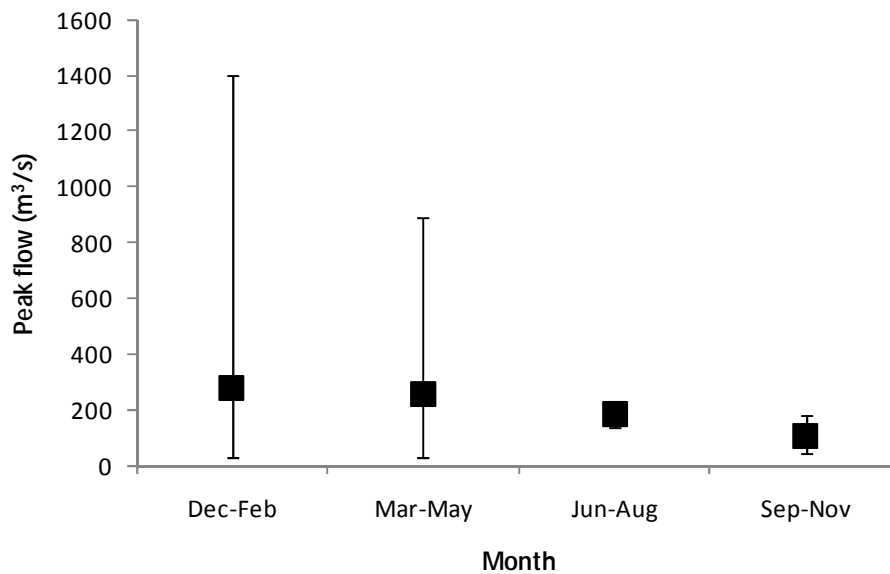
Figure 49 Seasonality of events, Lennard River at Mount Herbert (803002s). The box represents the magnitude of the mean flow event, and the whiskers represent the full range of events analysed for this study.

7.7.3. Baseflow Analysis

Nine passes of the Lyne and Hollick filter, with a parameter value of 0.925, were applied to extract the baseflow for each event. Sample hydrographs are presented in Figure 50 and key statistics are summarised in Table 15. Variation in BFI with ARI of the total flow event is presented in Figure 51a. A high degree of scatter is evident in the data particularly for small event sizes, however a general downward trend highlights that BFI decreases as ARI increases. The fitted trendline through the data representing the ratio of the baseflow under the streamflow peak to the peak streamflow indicates an increase in the ratio as ARI increases (Figure 51b). However, this response is considered to be an artefact of the model fit. This response indicates the need for further regionalisation analysis in northern Australia. Again, a large amount of scatter is evident for small ARI.

The absolute magnitude of the baseflow under the streamflow peak also increases with increasing event size (Figure 51c). In this instance, variability in the data increases with ARI. A poor fit is observed for the relationships in Figure 51, with low r^2 values.

Table 15 Baseflow statistics, Lennard River at Mount Herbert (803002s)

Statistic	BFI of event	Ratio of baseflow under streamflow peak : streamflow peak	Ratio of baseflow peak : streamflow peak
Average	0.16	0.03	0.05
Maximum	0.68	0.26	0.31
Minimum	0.0033	0.0000	0.0005
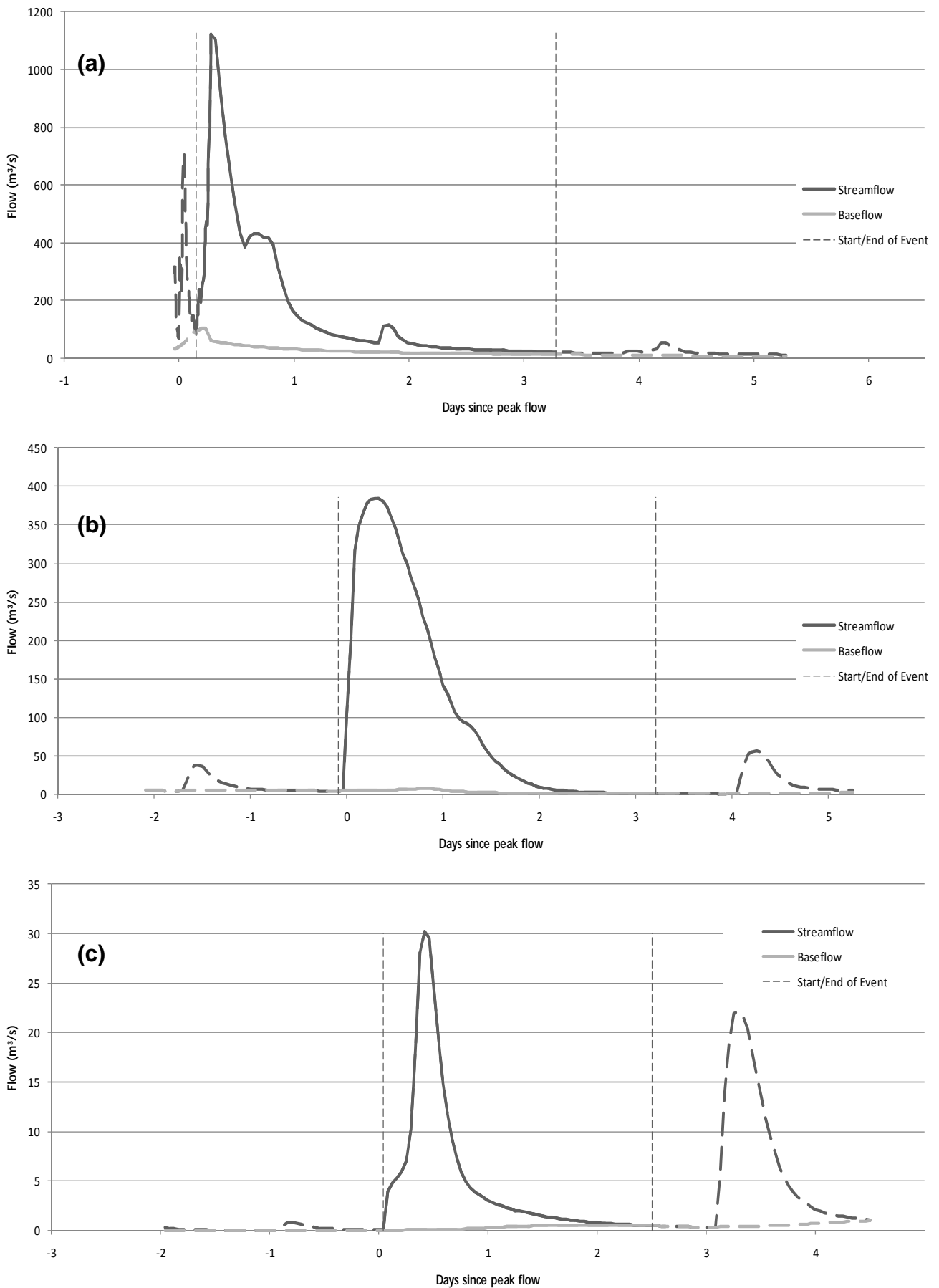
Figure 50 Sample hydrographs demonstrating the streamflow and baseflow characteristics for a range of events, Lennard River at Mount Herbert (803002s): (a) ARI of 17 years, (b) ARI of 1 year, (c) ARI of 0.25 years
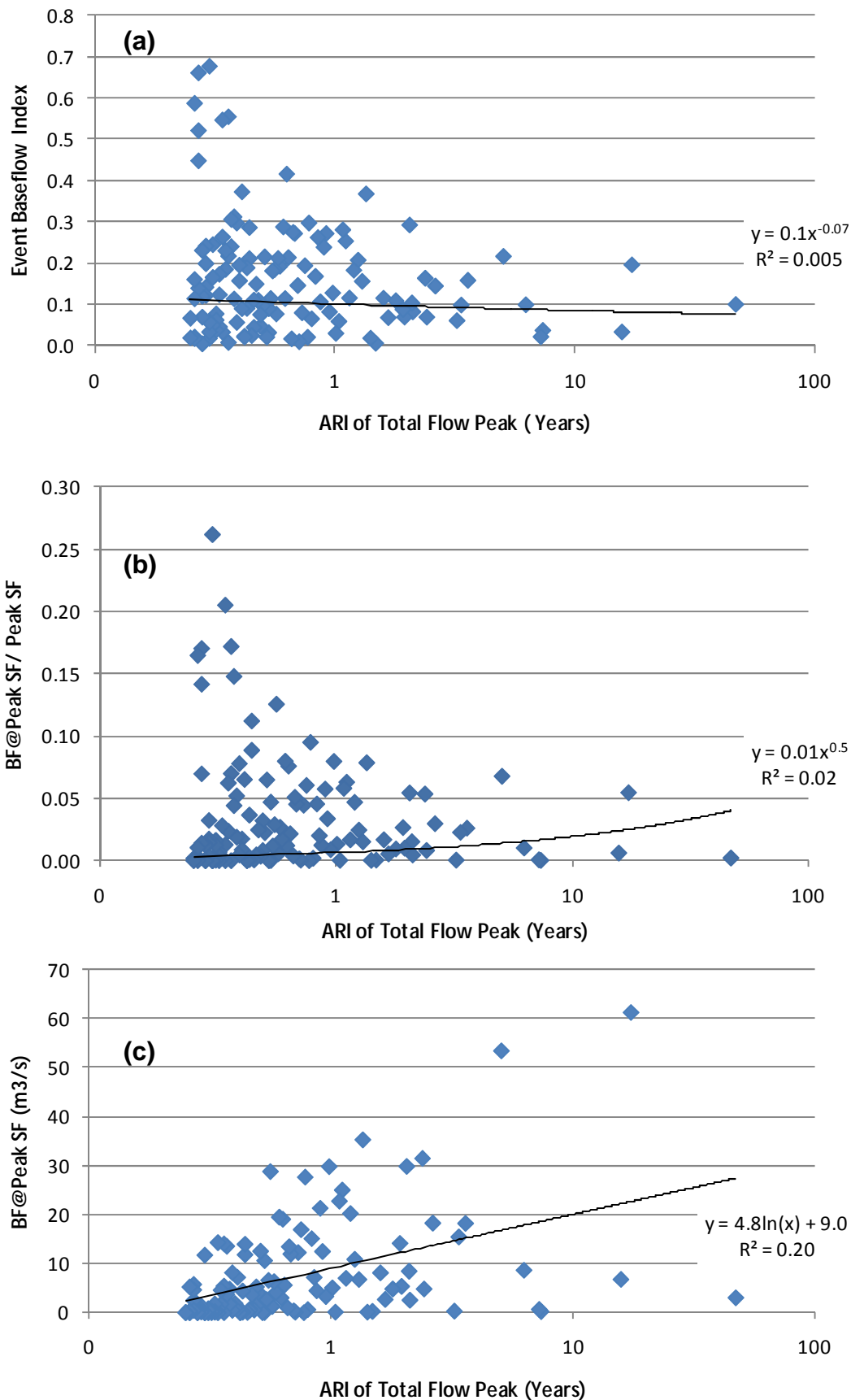
Figure 51 (a) Variation in event BFI with ARI of the total flow peak, (b) Ratio of baseflow under streamflow peak to peak streamflow, (c) Absolute magnitude of baseflow under streamflow peak, Lennard River at Mount Herbert (803002s)

7.8. Deep River at Teds Pool, Western Australia (606001)

7.8.1. Catchment Description

Deep River is situated in the south west corner of Western Australia, flowing south towards Warpole on the southern coast. Appendix B presents key catchment characteristics for the site.

7.8.2. Flow Characteristics

Streamflow records at Teds Pool commenced in 1975, and have captured over 30 years of data. Approximately 24% of the record is made up of cease to flow events, which primarily occur during summer and autumn (Figure 52). Only a small proportion of the flow record is above the maximum gauged flow. The flow characteristics at the gauge location are presented in Table 14.

Table 16 Streamflow characteristics for Deep River at Teds Pool (site 606001)

Statistic	Value			
Start of record	May, 1975			
End of record	January, 2009			
Length of record (years)	33			
Percentage of missing data (%)	0.01			
Maximum recorded hourly flow (m^3/s)	42			
Minimum recorded hourly flow (m^3/s)	0.00			
Proportion of time of cease to flow events (%)	24			
Maximum gauged flow (m^3/s)	40			
ARI of maximum gauged flow	73			
Percentage of time hourly flow is greater than maximum gauged flow (%)	0.004			
	Dec-Feb	**Mar-May**	**June-Aug**	**Sep-Nov**
Proportion of events extracted (%)	0	1	59	40
Seasonal maximum flow event (m^3/s)	N/A	4	42	23
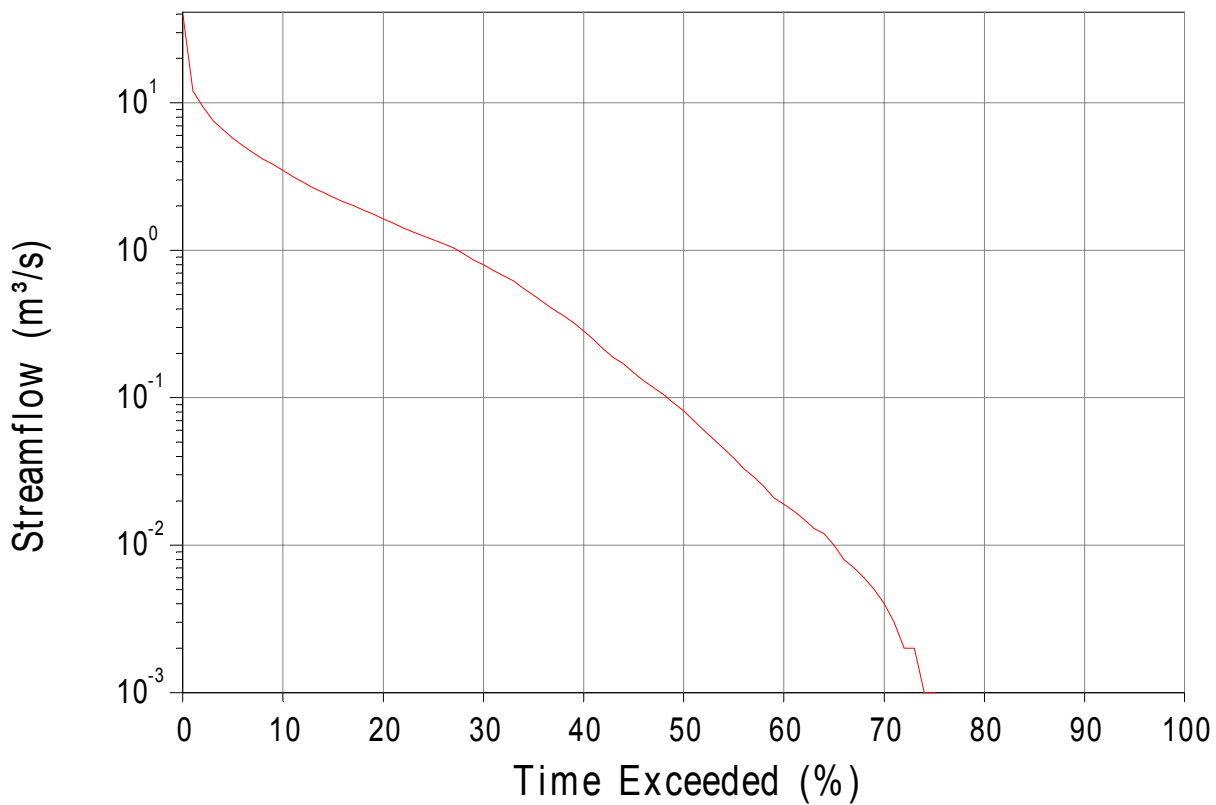
Figure 52 Flow duration curve, Deep River at Teds Pool (site 606001)

Figure 48 presents the flood frequency analysis for Deep River at Teds Pool. Over 130 events were analysed at this site, extracted from more than 30 years of records. The average magnitude of flood events from June to November is reasonably consistent (Figure 54), however the largest flow events at the site occur during the months of June, July and August. No events occur during the months of December to February at this site.
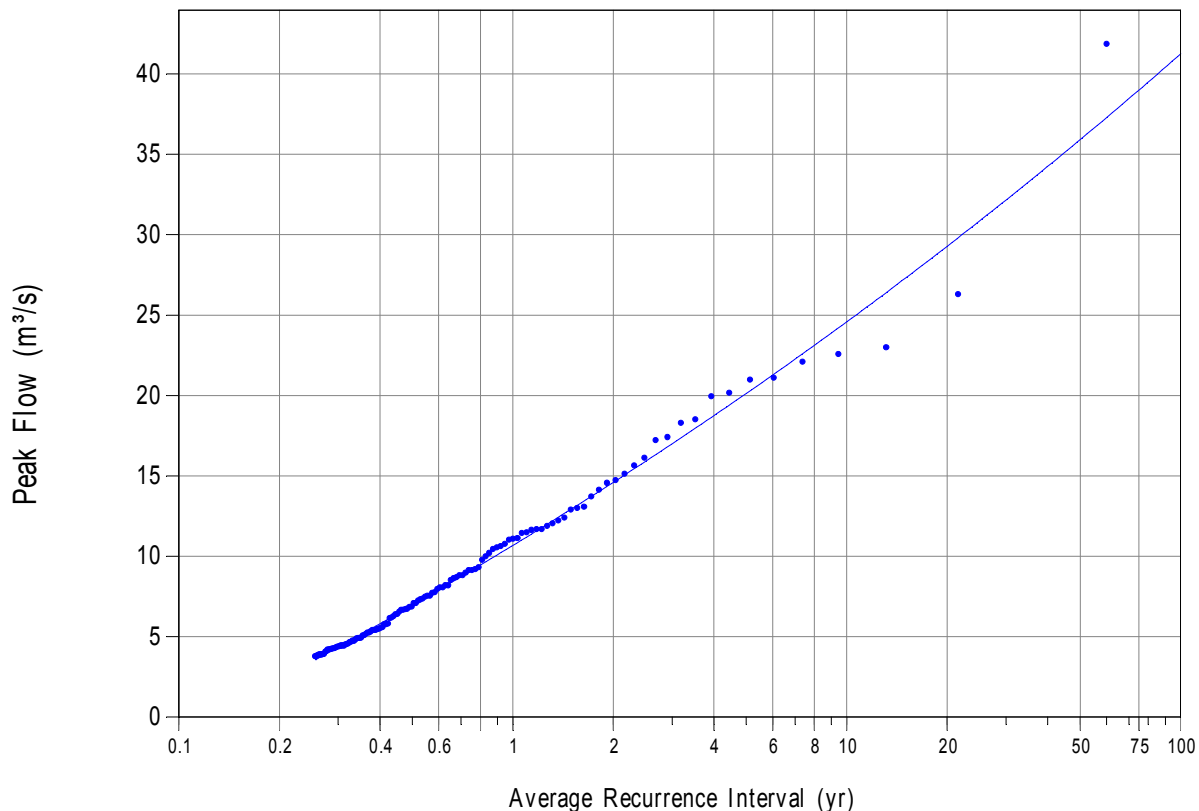
Figure 53 Flood frequency analysis, Deep River at Teds Pool (site 606001)
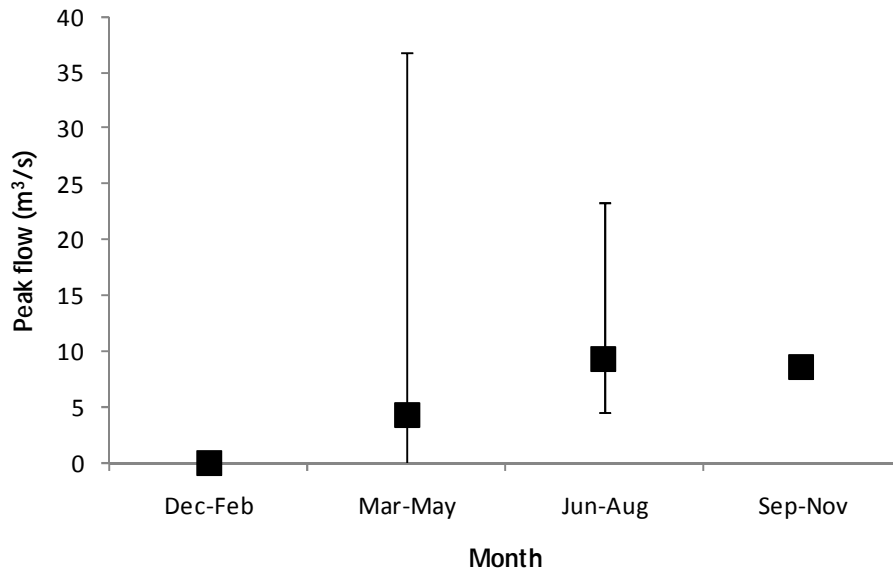
Figure 54 Seasonality of events, Deep River at Teds Pool (site 606001). The box represents the magnitude of the mean flow event, and the whiskers represent the full range of events analysed for this study.

7.8.3. Baseflow Analysis

Analysis of the streamflow data at the Deep River site identified a unique challenge in terms of application of the method. The streamflow events extracted displayed characteristics quite unlike those observed at the other case study locations. In particular, the events tended to be very drawn out, with gradual increases in flow and slow recessions. At this location, the modified Lyne and Hollick filter was not considered to reasonably replicate the understood physically processes of baseflow, and the estimated baseflow series was deemed less plausible than those generated at other locations.

Figure 55 presents an example flood hydrograph and the estimated baseflow when the method described in Section 4 is applied. As can be seen, the baseflow peak is unrealistically high for the main flood event presented. This issue was observed to occur across a number of events, ranging through the full spectrum of ARI magnitudes.
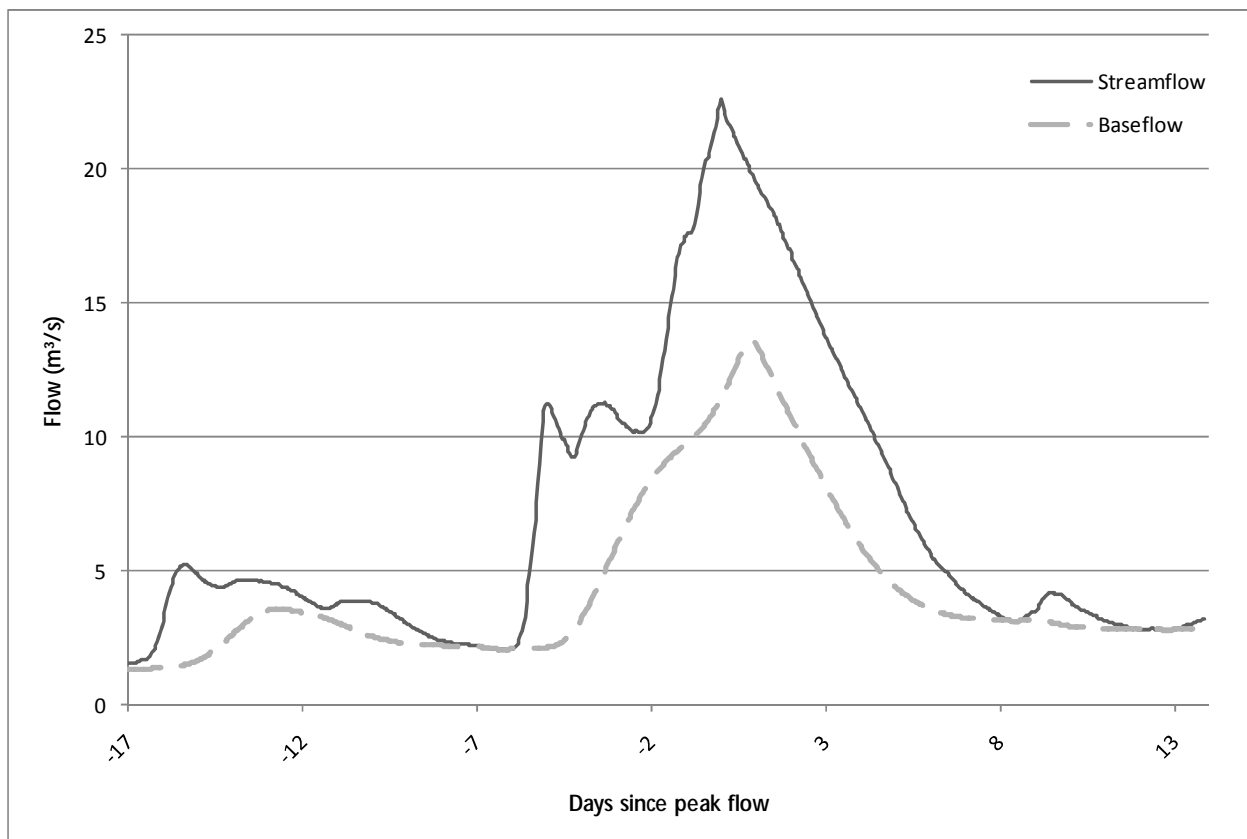
Figure 55 Example flood hydrograph, Deep River at Teds Pool (606001) illustrating problems in estimated baseflow using adopted method

Furthermore, the automated approach to identifying the start and end of flood events was also less successful at this location. A reasonably high proportion of the events analysed at this location are considered to require manual manipulation to correct the automatically defined start and end of the event.

These issues were assumed to be a result of the unique hydrogeological conditions that are found in the south-west of Western Australia. Further analysis of the catchment characteristics in Phase 2 of the study will help to clarify these assumptions.

This catchment case study is presented to display the challenges faced in developing a method that is uniformly applicable to all catchments. The results of the analysis for this location indicate that the method may require further manipulation to better estimate baseflow in areas with unique hydrogeological conditions. In order to overcome these challenges, it is intended that further evaluation of the approach be undertaken at this and other unique locations. Options to improve the methods may include:

- Further manipulation of the Lyne and Hollick filter through modification to the filter parameter or number of passes applied;
- Further investigation of alternative approaches that have been successfully applied to unique catchments;
- Regionalisation of the method, such that particular locations or catchment characteristics trigger the application of an alternative approach; or
- Some combination of the above.

Finalisation of the method across the full selection of catchments is to be completed in Phase 2 of this study. As such, the next stages of the project present an opportunity to further refine the process for widespread application. The issues identified at this Western Australian case study catchment, plus any other challenges identified at other catchment locations, will be resolved in the regionalisation tasks that follow.

Given the difficulties discussed above, the results for this site have been excluded from the comparison between sites presented in the next section of this report.

8. Comparison between catchments

Analysis undertaken at each catchment identified a number of characteristics that can be compared across the case study catchments. The discussion presented below provides some initial comparison between sites, however full comparison is not possible until a more complete set of catchments has been analysed, and regional trends can be identified.

For each of the statistics calculated in the previous sections, a scatter plot was presented to demonstrate the scatter in the data. A line of best fit was applied to the data to understand the general trend in each statistic for different event sizes. The ARI being considered represents the ARI of the total flow event, and includes the quickflow and baseflow components of the flow. The line of best fit for each statistic can then be compared across the case study catchments. The trendlines presented in this section reflect the line of best fit through data with a significant degree of scatter, and as noted in the analysis for each catchment, the r^2 values observed for each of these lines of best fit were quite low.

The variation in BFI with ARI of the total flow peak is presented in Figure 56 for each case study catchment. In all catchments, the BFI decreases as the magnitude of the flood event increases. Whilst there is some similarity in the slope of the lines for different catchments, without further sites for comparison it is difficult to confirm the significance of these similarities. However, these similarities may be used to initiate regionalisation options in the next phase of the project. In general, comparison between the catchments demonstrates that variability in the event BFI decreases as the magnitude of the flood event increases. Similar observations are noted in Figure 57 and Figure 58. Also notable in these figures are the relatively flat slope in the line for catchment 204041 and the slight upwards slope for high ARI for catchment 803002s. The importance of these trends will be further investigated in Stage 2 of the study, and may be used in the regionalisation of catchments.

Variation in the absolute magnitude of baseflow is presented in Figure 59 and Figure 60. These plots present the flow scaled relative to catchment area (ie: magnitude expressed in m^3/s per km^2). For all catchments, the magnitude of baseflow occurring at the time of peak streamflow increases as the ARI of the total flood event also increases. Similarly, the magnitude of the peak baseflow for the event also increases with ARI. In general, the variation of baseflow magnitude between catchments tends to increase as the size of the total flow event increases. The gradient of these trend lines may reflect local or regional conditions. Further catchment analysis in Phase 2 of this study will provide additional sites from which regionalisation conclusions can be drawn.
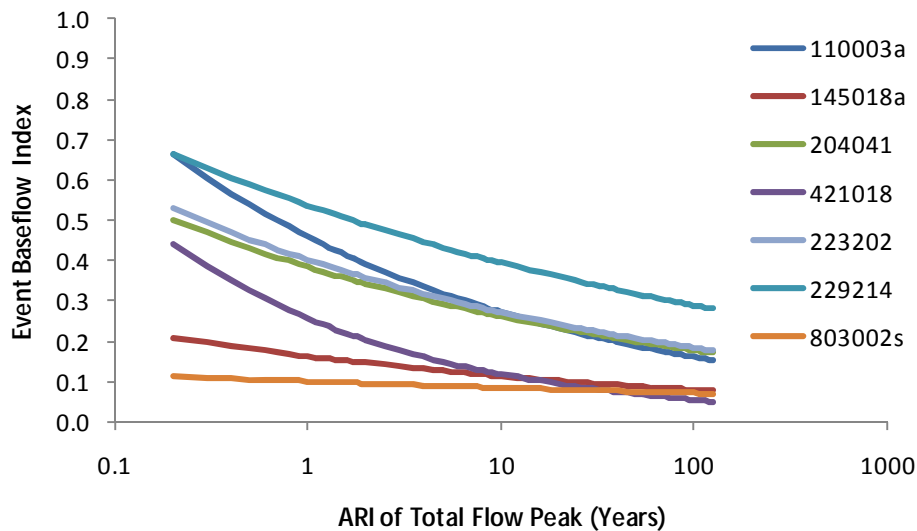
Figure 56 Variation in BFI with ARI of the total flow peak
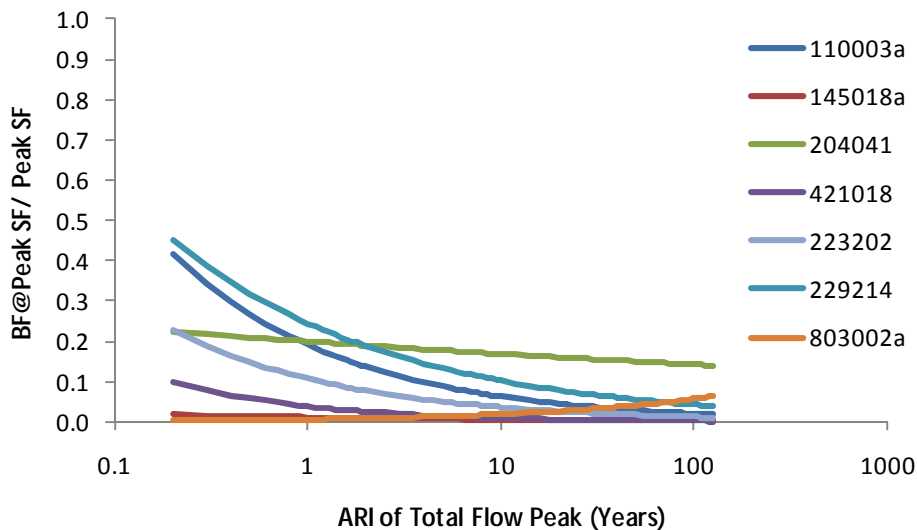
Figure 57 Variation in the ratio of the baseflow under the streamflow peak to peak streamflow with ARI of the total flow peak
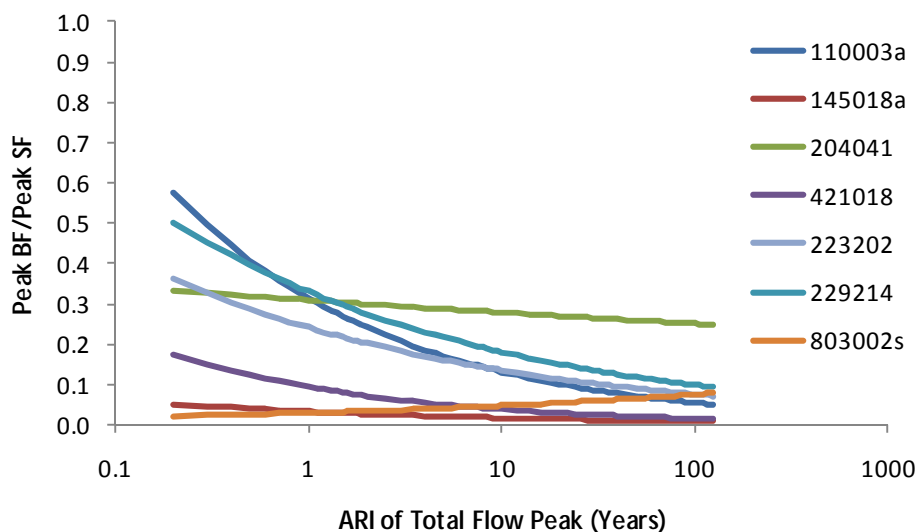
Figure 58 Variation in the ratio of peak baseflow to peak streamflow with ARI of the total flow peak
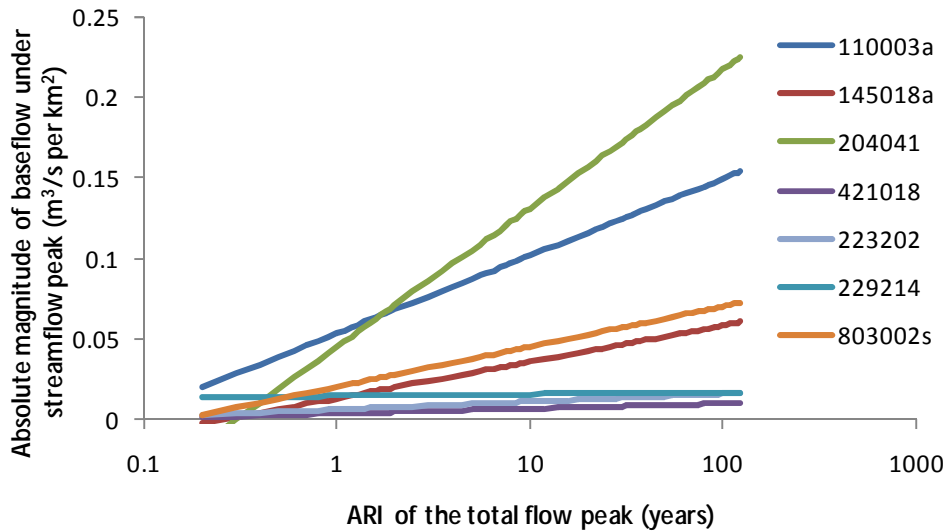
Figure 59 Variation in the absolute magnitude of the baseflow under the streamflow peak with ARI of the total flow peak
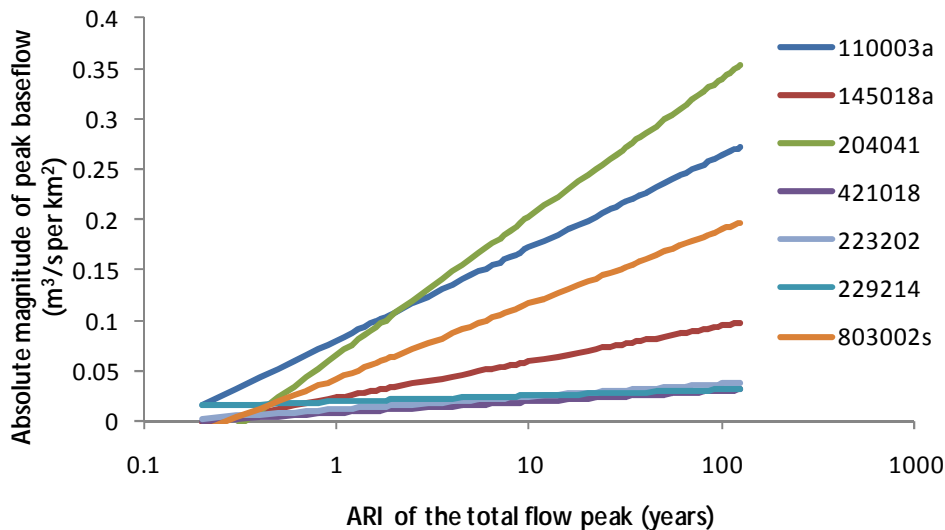
Figure 60 Variation in the absolute magnitude of the peak baseflow with ARI of the total flow peak

The following figures provide an alternative approach to presenting the results and display frequency distribution plots for the various statistics extracted. Figure 59 shows the frequency distribution fitted to the BFI of each event for the case study catchments. In this figure, the x-axis reflects the ARI of the event BFI and the y-axis presents the event BFI. In general, all catchments display a similar trend, with the BFI ratio increasing logarithmically to some maximum value. The rate of increase of the BFI with increasing ARI and the resulting maximum BFI value may be representative of regional conditions.
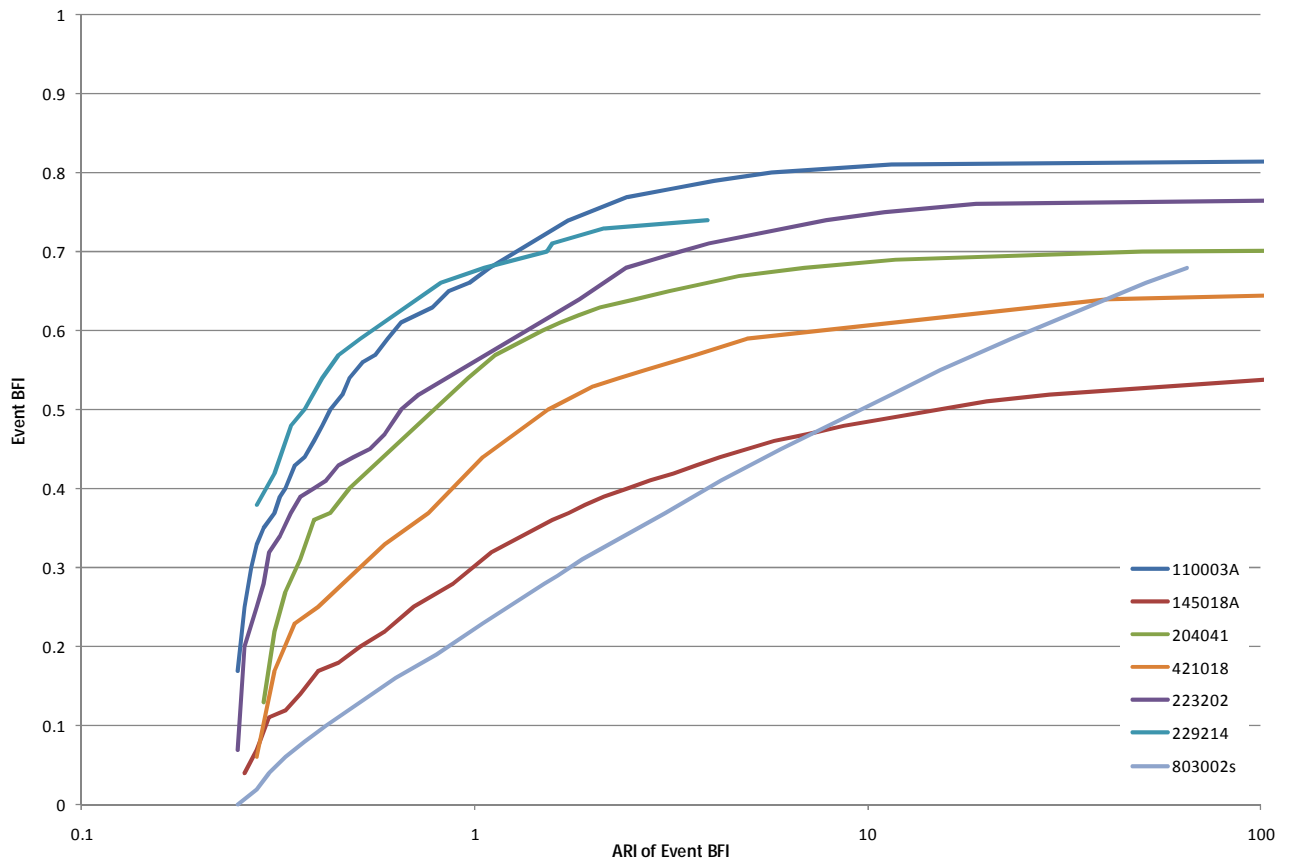
Figure 61 Distribution of event BFI (independent of return period of total flow)

Figure 62 presents a similar concept, displaying the fitted ARI distribution for the event based ratio of the baseflow under the streamflow peak to the peak streamflow for each catchment. The shape of this trend is not consistent for all catchments. Logarithmic responses are observed for some catchments, while others display exponential behaviour. The variation in this ratio as ARI increases may also be reflective of the regional characteristics, and indicates the need for further consideration in the next phase of the study.

Figure 63 displays the frequency distribution fitted to the ratio of peak event baseflow to peak streamflow.
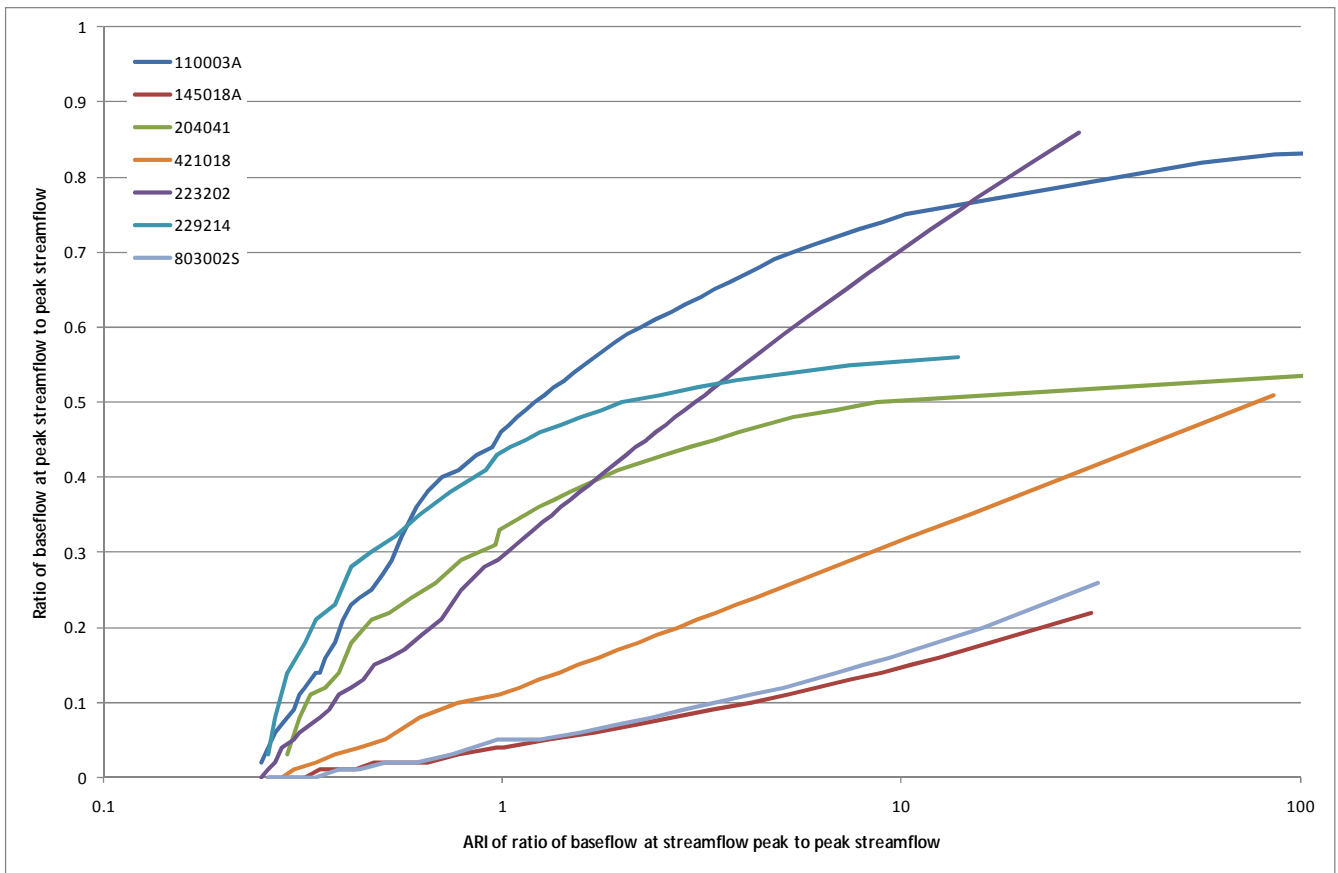
Figure 62 Distribution of event calculated ratios of the baseflow under the streamflow peak to peak streamflow (independent of return period of total flow)
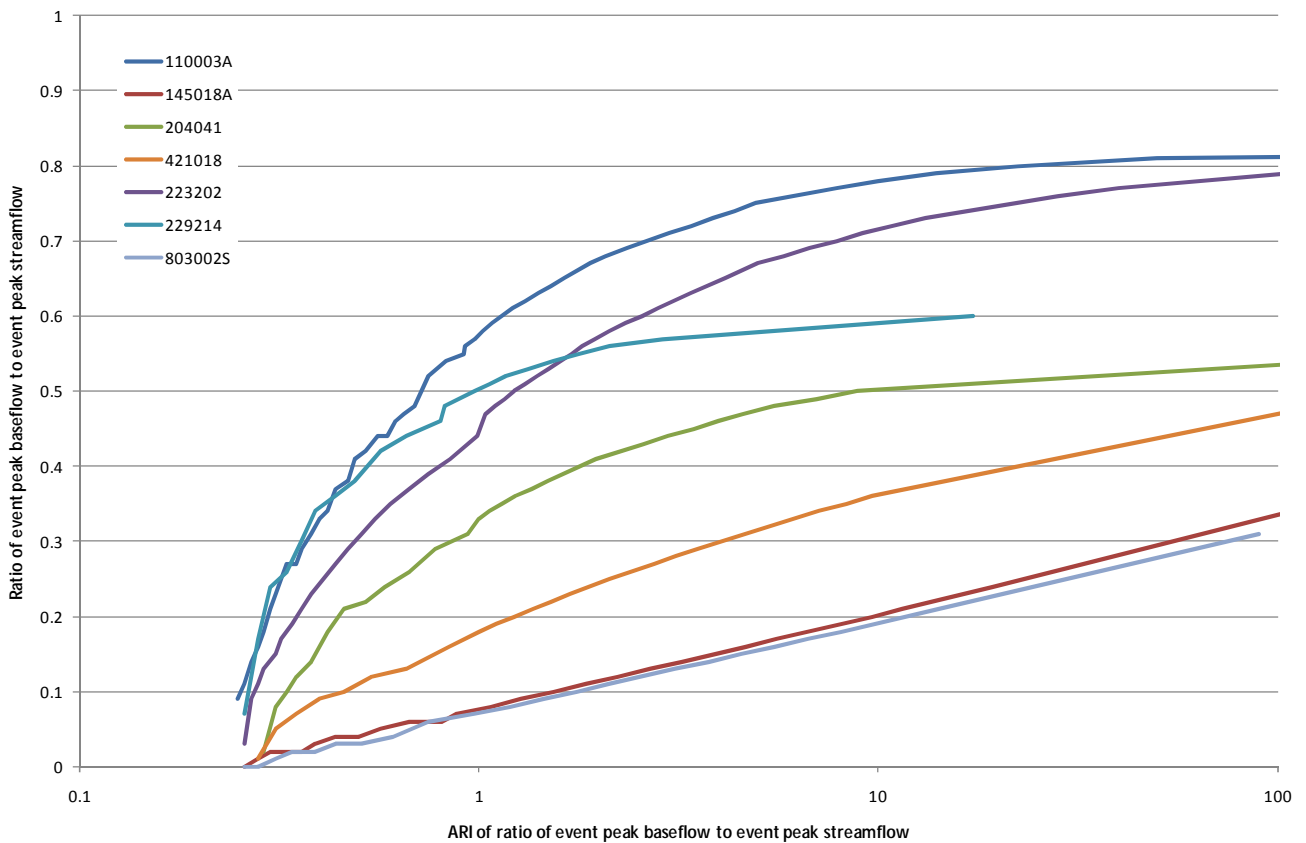
Figure 63 Distribution of event calculated ratios of peak event baseflow to peak event streamflow (independent of return period of total flow)

9. Next steps for the study

Phase 1 of this study focussed on the collation of data and the demonstration of the baseflow separation method. This report documents these components of the study. Further work in Phase 1 is still to be completed, specifically the extraction of catchment characteristics for the full set of study catchments. This process will result in a database of catchment characteristics for all selected catchments across Australia. Over 250 catchments have been identified as suitable for analysis in later stages of this project. For each catchment, approximately 80 different characteristics will be provided, including climatic, hydrologic and catchment based features. These characteristics will be consolidated into a database with a separate report summarising the catchment selection process and the characteristics of interest.

The next phase of the study (Phase 2) involves a number of key aspects, including:

- **Further evaluation of the method across the wider selection of catchments**. The method developed in Phase 1 of the study will be applied across other catchments to ensure the approach is uniformly applicable in all locations. Any issues identified at specific locations will be considered in detail and modifications to the approach may be made at this stage. For instance, options to resolve the issues identified at the south-west Western Australian site will be considered, including regionalisation of the technique based on local conditions, further manipulation of the filter parameter or number of passes, or further testing of alternative approaches. Any other issues will be identified and rectified in a similar manner.

- **Extraction of baseflow characteristics for full set of study catchments**. Approximately 280 catchments have been identified for analysis in Stage 2 of the project. In general, over 30 years of data is available at each location. Using the method described in this report, $4n$ events will be extracted for each catchment, where n is the number of years of record. This equates to the analysis of over 30,000 events across Australia. Existing automated procedures will be refined to handle the large volume of data to be processed.

- **Development of the regional prediction equations**. This may require identification of smaller homogenous catchment groupings prior to undertaking the regression analysis, which will serve to maximise the ability to predict baseflow contribution to flood peaks in a range of areas with fundamentally different underlying drivers of baseflow. The prediction equations will be tested through a cross-validation approach, which will be undertaken by partitioning the case study data sets. Goodness of fit statistics will be reported on.

- **Application of the regional prediction equations.** Once a suitable set of prediction equations has been developed, these will be applied to catchments throughout Australia to create a GIS layer of estimated baseflow contribution to flood peaks of given ARIs across the country. The exact nature of this GIS layer (grid, contour map, or regression equations which enable a user to calculate values for their own location) will be formulated based on the nature of the outcomes of the previous prediction equation task. The range of catchment characteristics over which each equation was developed and applied will be compared to note any uncertainties in application of the equations.

- **Development of guideline procedures.** The application of the regional prediction equations will be documented for inclusion in Australian Rainfall and Runoff. The nature of the information to be included in the guidelines will depend on the outcome of the analysis.

- **Testing of guideline procedures.** The documented procedures will be tested to assess the ability of experienced practitioners to successfully apply the new procedure. Feedback will be sought from those practitioners to assess the ease with which the guidelines could be applied, as well as the ability of the practitioner to reproduce an identical output to that intended in the sample problem provided to them.

10.   Conclusions

In most cases, baseflow is a minor component of extreme floods but can potentially be a significant component of smaller flood events. Larger contributions of baseflow occur where the catchment geology naturally produces high yielding aquifers with large baseflows. The current version of Australian Rainfall and Runoff provides guidance for estimating surface runoff, but there is little advice on the incorporation of baseflow into design flood events.

ARR Update Project 7 aims to develop a method for estimating baseflow contribution to different sized events across Australia. This report summarises the work undertaken as a part of Phase 1 of the overall project, and focuses on the physical processes of groundwater-surface water interaction, theoretical approaches to baseflow separation, and the testing of these methods to various case study catchments across Australia in order to develop a suitable approach for more widescale application.

Most previous studies have concentrated on the application of automated baseflow separation approaches to daily data. For the purposes of this study, it was necessary to identify an automated baseflow separation technique that can consistently provide a plausible baseflow time series from hourly streamflow data at a large number of catchments across Australia. A number of different methods were tested at case study catchments, with the most plausible baseflow hydrographs produced when a modified version of the Lyne and Hollick filter was applied.

The selected method utilised existing theory in the form of the Lyne and Hollick filter. Modifications to the application of this filter were made to enable the method to be applied to hourly data. The Lyne and Hollick filter is applied 9 times across the hourly data with a filter parameter value of 0.925. Based on analysis at case study catchments, this method produces plausible baseflow hydrographs for a range of event sizes at eight of the nine case study catchments. The results obtained at one case study site in Western Australia were considered less plausible, and require further analysis. Regionalisation of the method may help to establish an approach that is more suitable across all catchment conditions.

The outcomes from the case study analysis demonstrate that the baseflow contribution to the total flood peak varies depending on event size and location. The proportional contribution of baseflow to the event peak tends to decrease as the magnitude of the total flood event increases. This trend was observed for three different measures of baseflow calculated in this study:

- Event BFI (the ratio of the event baseflow volume to the event streamflow volume);
- Ratio of the baseflow under the streamflow peak to the peak streamflow; and
- Ratio of the peak baseflow to the peak streamflow.

The variability associated with these estimates of baseflow relative to the total streamflow generally decreased with increasing ARI both at individual sites and between sites. Further investigations in Phase 2 of the project may help to explain the reasons for the variability in baseflow contribution to flood peak at low ARI.

The absolute magnitude of baseflow generally increased as the size of the total flood event increased. This trend was observed when considering the magnitude of the baseflow at the time of the streamflow peak and also the peak baseflow. The magnitude of the baseflow was often easier to

predict than other measures of baseflow, with less variability than the results for the proportional contribution to floods.

Phase 2 of the study will further refine the recommended baseflow separation approach to ensure that the method is applicable in all locations across Australia. The finalised technique will be applied to events extracted from hourly data at more than 250 catchments. An existing automated approach will be refined to better handle the large volume of data to be processed.

Catchment characteristics will be extracted for each catchment and summarised in a report and database. These characteristics will be utilised to establish regional prediction equations that will enable the user to estimate baseflow contribution to a design flood event of any size in any region of Australia. Guidelines will be prepared to describe the relevant procedures for this application.

11. References

Arnold, J.G, Allen, P.M. and Bernhardt, G. (1993). A compresive surface groundwater flow model. Journal of Hydrology 142:47-68.

Arnold, J.G., Allen, P.M. (1999) Automated methods for estimating baseflow and groundwater recharge from streamflow records. Journal of the American Water Resources Association. Vol 35, Number 2, pp 411-424.

Arnold, J.G., Allen, P.M. Muttiah, R. And Bernhardt, G. (1995). Automated baseflow separation and recession analysis techniques. Groundwater 33: 1010-1018.

Boughton, W. (1988). Partitioning streamflow by computer. Institution of Engineers, Civil Engineering Transactions. CE30(5), 285-291.

Boughton, W.C. (1993) A Hydrograph-Based Model for Estimating the Water Yield of Ungauged Catchments. Hydrology and Water Resources Symposium, Newcastle, June 30 – June 2.

Brodie, R.S. and Hostetler, S. (2005) A review of techniques for analysing baseflow from stream hydrographs. Proceedings of the NZHS-IAH-NZSSS 2005 conference, 28 November – 2 December 2005, Auckland, New Zealand.

Chapman, T. (1999). A comparison of algorithms for stream flow recession and baseflow separation. Hydrological Processes, 13 p701-714.

Chapman, T.G. (1991) Comment on "Evaluation of Automated Techniques for Base Flow and Recession Analyses" by R.J. Nathan and T.A. McMahon. Water Resources Research Vol 27, Number 7, pp 1783-1784.

Chapman, T.G. and Maxwell, A.I. (1996). Baseflow separation – Comparison of numerical methods with tracer experiments. Proceedings of the 23rd Hydrology and Water Resources Symposium, Hobart Australia, 21-24 May 1996.

Chen, X., Chen, D.Y., and Chen, X. (2006) Simulation of baseflow accounting for the effect of bank storage and its implication in baseflow separation. Journal of Hydrology 327, 539-549.

Cordery, I. (1998) The unit hydrograph method of flood estimation. Section 2 of Book V, Estimation of design flood hydrographs. Australian Rainfall and Runoff – A guide to flood estimation. The Institution of Engineers, Australia.

Daamen, C., McAuley, C. And Durkin, P. (2006) Effects of urban development on groundwater baseflow in streams. Proceedings of Enviro06 Conference, 9-11 May 2006, Melbourne, Australia.

Eckhardt, K. (2005). How to construct recursive digital filters for baseflow separation. Hydrological Processes. 19, 507-515.

Evans, R. and Neal, B. (2005) Baseflow analysis as a tool for groundwater – surface water interaction assessment. Proceedings of the International Water Conference, New Zealand Hydrological Society, New Zealand Society of Soil Science, and the International Association of Hydrogeologists (Australian Chapter). Auckland, New Zealand, 28 November to 2 December 2005.

Freeze, R. A. and J. A. Cherry. 1979. Groundwater. Prentice Hall, Inc.

Frohlich K, Frolich W and Wittenberg H (1994) Determination of groundwater recharge by baseflow separation: regional analysis in northeast China. FRIEND: Flow Regimes from International Experimental and Network Data, Proceedings of Braunschweig Conference, October 1993. IAHS Publ. No 221.

Furey, P.R. and Gupta, V.K. (2001) A physically based filter for separating base flow from streamflow time series. Water Resources Research 37(11): 2709-2722.

Furey, P.R. and Gupta, V.K. (2003) Tests of two physically based filters for base flow separation. Water Resources Research. 39(10), 1297.

Gustard, A., Roald, L.A., Demuth, S., Lamadjeng, H.S., and Gross, R., (1989). Flow Regimes from Experimental and Network Data (FrEND), 2 Volumes: I Hydrological Studies, II Hydrological Data. Institute of Hydrology, Wallingford, UK, 344pp.

Institution of Engineers, Australia (1987) Australian Rainfall and Runoff. (Ed: Pilgrim, D.H.) Institution of Engineers, Australia.

Institute of Hydrology (1980) Low flow studies. Research Report 1. Institute of Hydrology, Wallingford UK.

Jakeman, A.J and Hornberger, G.M. (1993) How much complexity is warranted in a rainfall-runoff model? Water Resources Research 29, pp2637-2649.

Jones, J.P., Sudicky, A.E., Brookfield, A.E. and Park, Y.J. (2006). An assessment of the tracer based approach to quantifying groundwater contributions to streamflow. Water Resources Research 42(2).

Langbein, W.B. (1938). Some channel storage studies and their application to the determination of infiltration. Eos Trans, American Geophysical Union, 19, pp 435-447.

Lim, K.J., Engerl, B.A., Tang, Z., Choi, J., Kim, K., Muthukrishnan, S. And Tripathy, D. (2005) Automated Web GIS Based Hydrograph Analysis Tool, WHAT. Journal of the American Water Resources Association, 41(6):1407-1416.

Lin, K., Gui, S., Zhang, Q. and Liu, P. (2007) A new baseflow separation method based on analytical solutions of the Horton infiltration capacity curve. Hydrological Processes, 21, 1719-1736.

Linsley Jr, R.J., Kohler, M.A. and Paulhus, J.L.H. (1982) Hydrology for Engineers. 3rd Edition. McGraw-Hill.

Linsley, R.K., Kohler, M.A., Paulhus, J.L.H., Wallace, J.S. (1958) Hydrology for Engineers. McGraw Hill, New York.

Lyne, V. And Hollick, M. (1979) Stochastic time-variable rainfall-runoff modelling. Institute of Engineers Australia National Conference. Publ. 79/10, 89-93

Mandeville, A.N. (2004) The reservoir inflow sequence (RIS) method of hydrograph analysis applied to a set of 25 flood events observed on a catchment located in Western United Kingdom. Hydrology: Science and Practice for the 21st Century 1:171-179.

Mau D.P. and Winter T.C. (1997) Estimating Ground-Water Recharge from Streamflow Hydrographs for a Small Mountain Watershed in a Temperate Humid Climate, New Hampshire, USA. Ground Water 35(2):291-304

Murphy, RE, Neal, B, Nathan, RJ, Evans, R and Helm, L (2006) Non-climatic temporal trend in baseflow in areas of high groundwater use. Proceedings of 30th Hydrology and Water Resources Symposium, 4-7 December 2006, Launceston, Tasmania.

Mugo, J.M. and Sharma, T.C. (1999) Application of a conceptual method for separating runoff components in daily hydrographs in Kimakia Forest Catchments, Kenya. Hydrological Processes 13, pp 2931-2939.

Nathan, R.J, and McMahon, T.A. (1990) Evaluation of Automated Techniques for Base Flow and Recession Analyses. Water Resources Research, Vol 26, Number 7, pp1465-1473.

Nathan, R.J. and Weinmann, P.E. (1993) Low flow atlas for Victorian streams. Prepared for the Department of Conservation and Natural Resources – Victoria.

Neal, B.P., Nathan, R.J. and Evans, R. (2004) Survey of baseflows in unregulated streams of the Murray-Darling Basin. 9th Murray-Darling Basin Groundwater Workshop, 17-19 February 2004. Bendigo, Victoria.

Newbury, R.W., Cherry, J.A. and Cox, R.A. (1969) Groundwater-streamflow systems in Wilson Creek Experimental Watershed, Manitoba. Canadian Journal of Earth Sciences, 6:613-623.

Peel, M.C., Chiew, F.H.S, Western, A.W, and McMahon, T.A. (2000) Extension of unimpaired monthly streamflow data and regionalisation of parameter values to estimate streamflow in ungauged catchments. Report prepared for the National Land and Water Resources Audit. Theme 1 – Water Availability. July 2000.

Pilgrim, D.H., D.D. Huff, T.D. Steele (1979) Use of specific conductance and contact time relations for separating flow components in storm runoff. Water Resources Research 15: 329-339.

Rice, K.C. and Hornberger, G.M. (1998) Comparison of hydrochemical tracers to estimate source contributions to peak flow in a small forested headwater catchment. Water Resources Research 34:1755-1766.

Rutledge, A.T (1993) Computer programs for describing the recession of groundwater discharge and for estimating mean groundwater recharge and discharge from streamflow records. US Geological Survey Water Resources Investigations Report, 93-4121.

Rutledge, AT. And Daniel, C.C. (1994) Testing and automated method to estimate groundwater recharge from streamflow records. Groundwater 32(2):180-189.

Schwartz, S.S. (2007) Automated algorithms for heuristic baseflow separation. Journal of the Americal Water Resources Association. Vol 43, No 6. pp1583-1594.

Sklash, M.G. and Farvolden, R.N. (1979) The role of Groundwater in Storm Runoff. Journal of Hydrology. 43:45-65.

SKM (2003) Sustainable Diversion Limit Project: Estimation of Sustainable Diversion Limit parameters over winterfill periods in Victorian catchments. Prepared for the Department of Sustainability and

Environment.

SKM (2007) Using baseflow for monitoring stream condition and groundwater and surface water resource condition change – Task 2 Milestone Report. Final, June 2007.

SKM (in preparation) Baseflow for catchment simulation – Data collation and catchment characteristics. Report being prepared for Australian Rainfall and Runoff Update Project 7.

Sloto RA and Crouse MY, 1996. HYSEP: A computer program for streamflow hydrograph separation and analysis. US Geological Survey, Water Resources Investigations Report 96-4040

Smakhtin, V.U. (2001) Low-flow hydrology: a review. Journal of Hydrology. v240. 147-186.

Snyder, F.F. (1939) A concept of runoff-phenomena. Eos Trans, American Geophysical Union, 20, pp 725-738.

Spongberg M.E. (2000) Spectral Analysis of base flow separation with digital filters. Water Resources Research. 36(3):745-752.

Szilagyi, J. (1999) On the use of semi-logarithmic plots for baseflow separation. Groundwater, Volume 37 Number 5, pp 660-662.

Szilagyi, J. And Parlange, M.B. (1998). Baseflow separation based on analytical solutions of the Boussinesq equation. Journal of Hydrology, 204: 251-260.

Tan, S.B.K., Lo, E.Y., Shuy, E.B., Chua, L.H.C., and Lim, W.H. (2009a) Generation of total runoff hydrographs using a method derived from a digital filter algorithm. Journal of Hydrologic Engineering, Volume 14, Number 1. January 1, 2009. pp 10-106.

Tan, S.B.K., Lo, E.Y., Shuy, E.B., Chua, L.H.C., and Lim, W.H. (2009b) Hydrograph separation and development of empirical relationships using single parameter digital filters. Journal of Hydrologic Engineering, Volume 14, Number 3. March 1, 2009. pp 271-279.

Tularam, G.A, and Ilahee, M. (2007) Base Flow Separation Using Exponential Smoothing and its Impact on Continuous Loss Estimates. In Oxley, L. and Kulasiri, D. (eds) MODSIM 2007 International Congress on Modelling and Simulation. Modelling and Simulation Society of Australia and New Zealand, December 2007. pp1679-1776. ISBN: 978-0-9758400-4-7.

Tularam, G.A, and Ilahee, M. (2008) Exponential Smoothing Method of Base Flow Separation and Its Impact on Continuous Loss Estimates. American Journal of Environmental Sciences 4 (2):136-144.

Wittenberg H. (1999) Baseflow recession and recharge as nonlinear storage processes. Hydrological Processes, 13:715-726

Wittenberg H. And Sivapalan M. (1999) Watershed groundwater balance estimation using streamflow recession analysis and baseflow separation. Journal of Hydrology 219:20-33

Ye, W (1996) Climate impacts on streamflow in Australian catchments. PhD Thesis, Australian National University, Canberra.

Zhang, W., Guo, S., and Lin, K. (2005) A proposed method for baseflow hydrograph separation – formula derivation. Chinese Journal of Hydrology 25(5):11-15.

12. Acknowledgements

Where available, the Bureau of Meteorology provided data from their consolidated collection of streamflow data from across Australia.

Data from NSW were sourced from version 9 of the Pinneena database (2006). This data is provided by the NSW Department of Water and Energy, Dumaresq-Barwon Border Rivers Commission, Many Hydraulics Laboratory, Murray-Darling Basin Authority and State Water.

Thiess Hydrographic Services, as custodians of water data in Victoria, provided data for some Victorian sites.

Some of the Western Australian streamflow data used in this report were obtained from the Water Information System (WIN) and Hydstra database, managed by the Department of Water, Water Information Provision Section, Perth, Western Australia. Information supplied by the Department of Water is protected by the Copyright Act 1968. That copyright belongs to the State of Western Australia. Apart from any fair dealing for the purpose of private study, research, criticism or review, as permitted under the Copyright Act 1968, no part may be reproduced or reused for any purpose without the written permission of the Department of Water.

Appendix A   **Comparison of baseflow separation techniques**

The determination of an appropriate baseflow separation technique for use across a large number of varied catchments involved the application of many of them to test catchments. This was done to examine the general features of the baseflow series calculated, determine the ease with which the methods could be applied and make some comparisons about the usefulness of each to this application. The techniques ranged from simple graphical methods to more complex algorithms and physically-based models which utilised data besides streamflow or more developed models based on groundwater interactions.

The results of each of the applied methods are presented and discussed in the following section.

Local Minimum Technique

The duration of quickflow (N, in days) is calculated using on the relationship N=A0.2, based on Linsley et al (1975). This relationship estimates the number of days of quickflow based on the catchment area (A, in square miles). The interval used in baseflow separations is taken as the value 2N rounded to the nearest odd integer (simply referred to as 2N in the following description).

The local minimum technique is incorporated into the HYSEP computer algorithm, and inspects the streamflow data on each day to identify whether it is the minimum value over the period of one half the quickflow duration minus one day (i.e. 0.5*(2N-1) days) before and after the day being considered (Sloto and Crouse, 1996). The baseflow component is determined using linear interpolation between the local minimum points.

The method was originally developed for application to daily data. Application to daily data does not provide a 'classical' baseflow shape for the flood events, as the baseflow component is calculated simply by linearly interpolating between minimum flow occurrences. Application to hourly data produces a similar baseflow estimate (Figure 4).

Smoothed Minima Technique

The baseflow separation procedure used in the FREND analysis (Gustard et al, 1989) was developed over a large number of catchments across Europe. The method, applied on a daily timestep, involves finding minima in groups of 5 consecutive, non-overlapping data points, and then finding subsequent minima in the created series of minima. These points are then joined to form the baseflow series. Gustard et al used this method on daily data, and it was applied here on both daily and hourly timesteps.

Applying the method on an hourly timescale amplified the issues with this approach. The change in streamflow at each timestep on an hourly scale is not as large as the difference on a daily time scale. Using a group of five data points, the minima selected was often not a true local minima, or differed by only a very small amount from the values around it. This resulted in significant periods of time where the calculated baseflow was either greater than the streamflow and was constrained to the value of the streamflow, or was very close to the streamflow value. Therefore, only periods that had a rapid change in streamflow had a distinct baseflow series, as in Figure 4.

This method bears similarities to the local minima technique, since the baseflow is assumed to be defined by the minima in the streamflow data. Although easily automated, the smoothed minima technique does not extract many of the features generally considered characteristic of baseflow, such as a delayed baseflow peak, and includes significant quickflow in the estimated baseflow.

Fixed Interval Technique

The fixed interval technique separates the streamflow hydrograph into discrete periods of fixed duration, as calculated using the quickflow duration (2N rounded to the nearest odd integer, simply referred to as 2N in the following description) based on the relationship N=A0.2 (Linsley et al, 1975).

The baseflow component in each discrete interval of duration 2N is estimated as the minimum streamflow within that period, producing a step shaped response with constant baseflow within each discrete time period.

Regardless of the timestep of the streamflow data, the resulting baseflow does not include ideal baseflow characteristics (Figure 4).

Sliding Interval Technique

The sliding interval approach estimates the baseflow within a particular time period as the minimum streamflow within that period. The duration of each time period is given by the quickflow duration (2N rounded to the nearest odd integer) based on the relationship N=A0.2 (Linsley et al, 1975).

This method is similar to the fixed interval approach, although the duration of interest is moved through each timestep of the streamflow time series data, producing a smoothed baseflow response. Despite this, the resulting baseflow series is not physically plausible (Figure 4).

One parameter Chapman algorithm

This algorithm (Equation 3) was developed by Chapman (1991). It utilises the recession constant as the filter parameter, k.

Chapman (1991) that this method produces a more realistic baseflow series than the Lyne-Hollick filter. However, in applying the algorithm to the test sites using hourly data, it was determined that the baseflow derived was significantly lower than realistic for many of the events. In a number of cases, the baseflow did not rejoin the streamflow at all. A similar effect was found by Mau and Winter (1997).

Applying a least squares fit and objective function to fit the recession periods of the calculated baseflow to the recession periods of the streamflow, as in Chapman (1999) is likely to improve the result. Since the baseflow constant would need to be determined for each site, and possibly be varied depending on event size, this method would be more complex to automate. In addition, the single parameter algorithm has been found to produce less satisfactory results than the two-parameter version by both Chapman (1999) and the results of this study.

Boughton two parameter algorithm

A second approach (Equation 4) was created by replacing the (1-k) in the Chapman algorithm with a second parameter, C, as used in the AWBM model (Boughton, 1993). The parameter C is to be

selected on a trial and error basis (Chapman and Maxwell, 1996), which makes automation difficult and the results subjective, since an optimisation technique cannot be applied. This poses a significant problem for applying the method across a large number of catchments and events.

The two-parameter algorithm produced the most satisfactory baseflow series of the Chapman, Boughton and Jakeman and Hornberger methods. On daily data, the same parameter values could be used on multiple sites, and produced plausible results. However, on hourly data the baseflow series was more sensitive to changes in parameter values, with a single parameter value no longer applicable over many sites. Similarly to both the IHACRES and single-parameter Chapman algorithms, using an hourly timestep either reduced the smoothing effect and produced unrealistically high baseflow peak, or created very low baseflow series which did not rejoin streamflow, even once the runoff had ceased.

Jakeman and Hornberger three parameter algorithm

The IHACRES three parameter algorithm (Equation 5) was found by Chapman (1999) to produce sharper peaks than would be considered realistic. When applying this method in this study, the daily data was found to produce acceptable results, however using hourly data further reduced the smoothing effect of the algorithm.

A significant drawback of this method is the increasing complexity with a greater number of parameters. As such, there is less confidence in the resulting baseflow series, both in terms of the best combination of parameters and the most appropriate shape of the series. With an increase in the number of parameters there is a greater range of shapes that can be created with combinations of values, of which the best selection is subjective.

Fitting the IHACRES algorithm to hourly data, it was apparent that matching recession periods is difficult or not possible. This may be an effect of the lack of differentiation between baseflow and streamflow, when the method is applied on an hourly timestep. Chapman (1999) and Ye (1996) also found that the model could not be consistently fitted to a number of catchments.

Chapman (1999) notes that the optimisation method used in the one-parameter Chapman-Maxwell algorithm is unsuitable for both the 2 and 3 parameter algorithms. In the absence of a method to optimise the selection of parameter values, they are likely to be unsuitable for use in an automated method.
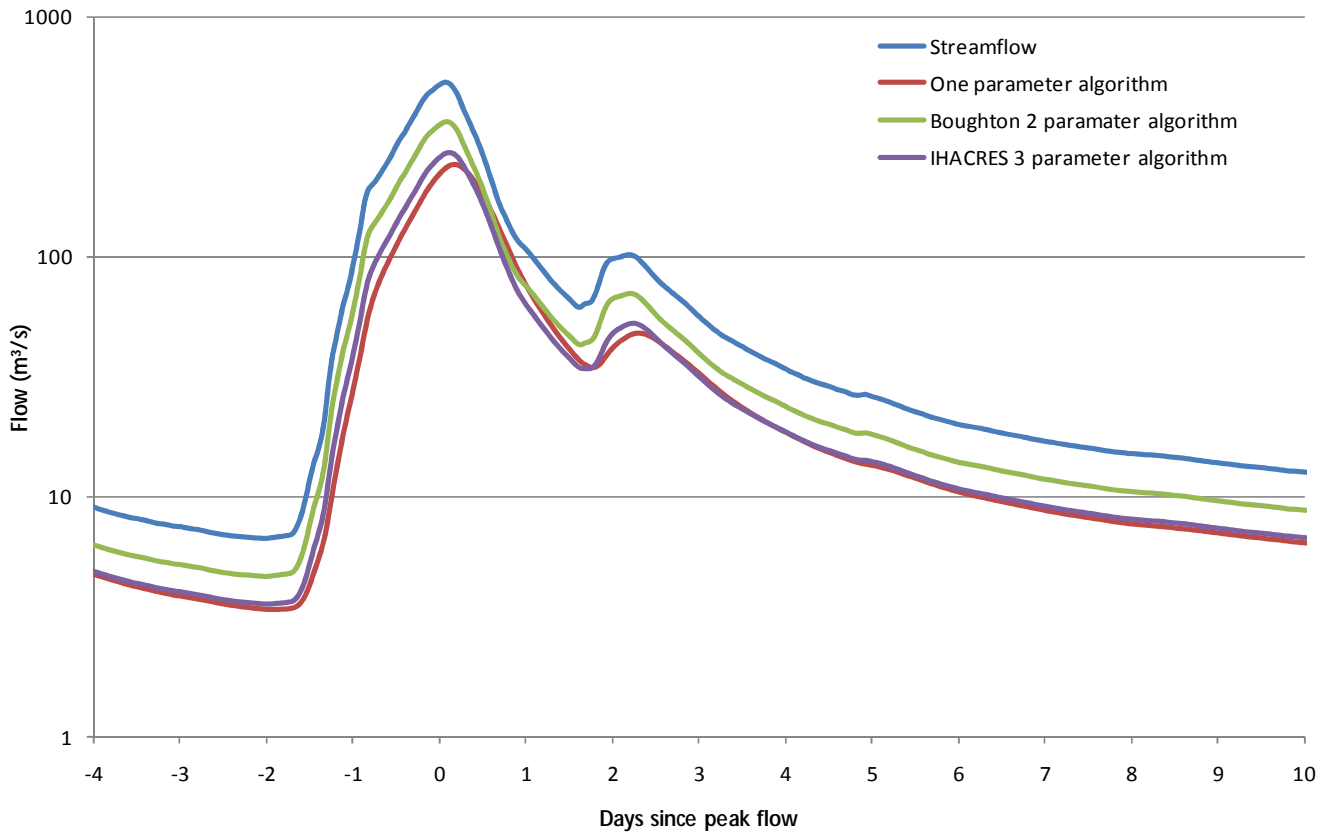
Figure 64 Hourly baseflow calculated using the 3 variations of the Chapman algorithm for 1 in 52 year event at Barron River at Picnic Crossing, Queensland (110003A)
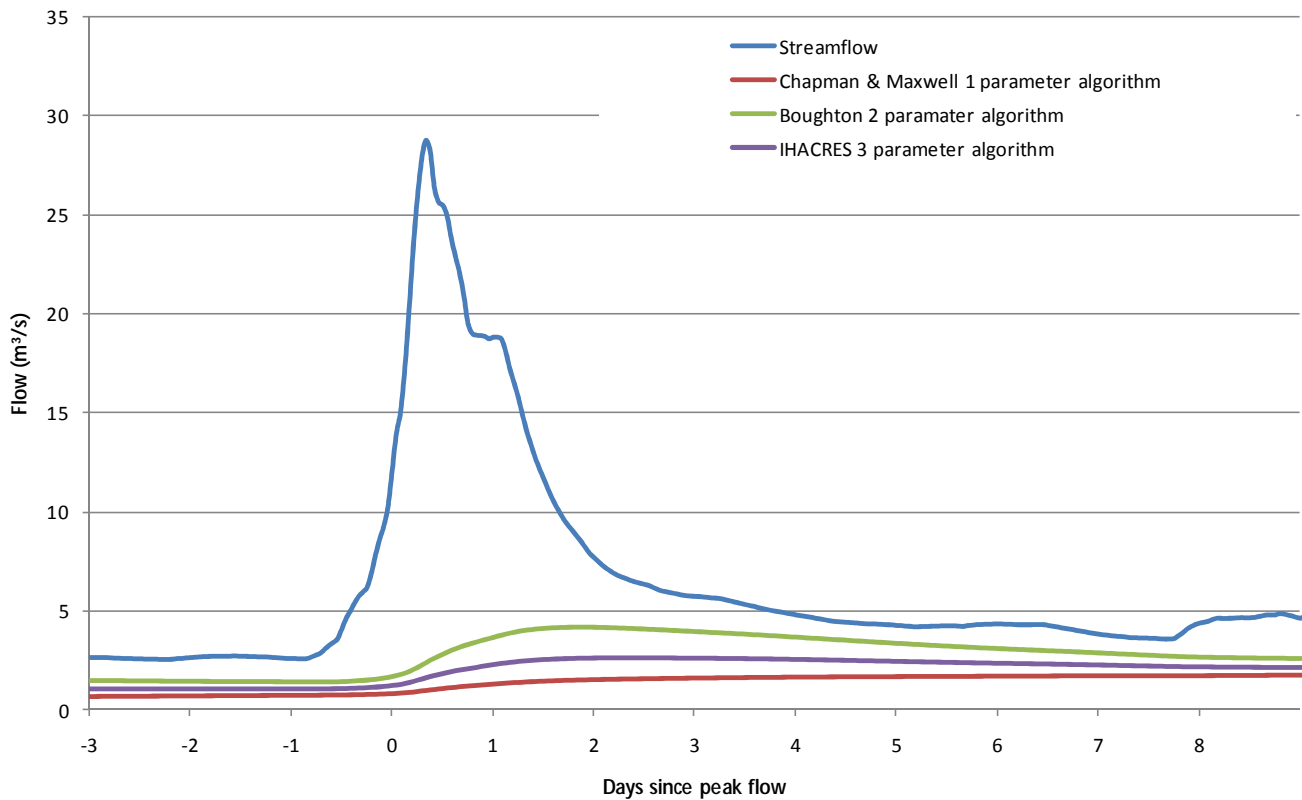
Figure 65 Hourly baseflow calculated using the three variations of the Chapman algorithm for the 1 in 30 year event at Little Yarra River, Victoria (229214)

Resclog

The computer program Recslog was developed to automate the implementation of the matching strip method of master recession curve analysis (Nathan and McMahon, 1990). The program allows the streamflow recessions of a number of hydrographs to be lined up, and which automatically adjusts to find the trend of best fit. The hydrographs are selected based on user defined minimum length of the recession period and the limits placed on the maximum and minimum flows for the recession. The recession constant, k, is estimated from the fitted relationship described by Equation 1. The recession constant calculated from this program can then be used in other digital baseflow separation algorithms.

Reservoir Inflow Sequence

The Reservoir Inflow Sequence (RIS) method (Mandeville, 2004) involves characterising flows by the flow (q) and the gradient of flow (dq/dt). The baseflow is removed from the streamflow record to determine the quickflow that forms a reservoir inflow. The technique focuses on determining a master recession curve for the catchment, which is then applied to the parts of the hydrograph that can be considered in 'pure recession'. The shape of the master recession curve is determined by comparing the gradient value and the flow value. A function of the form

$$\frac{dq}{dt} = j[q(t) + k]^l$$

Equation 13

is then fitted using the least squares method, where j, k and l are parameters to be fitted. A function is fitted to selection of events and the parameter values are averaged to create a generalised recession function. This approach of fitting a master recession curve is less subjective and easier than translating recession curves in time to find a common response.

A drawback of the RIS method is that the method can only be applied in periods of 'pure recession', which must be defined by other means. One of the principle issues with separating baseflows is hence still a problem in this method. The baseflow series during non-recession periods are filled by interpolation, as this method does not give technique for overall baseflow characterisation.

Frölich Method

The need to define the start and end of an event to characterise baseflow is a problem in many of the currently available baseflow separation methods. The method developed by Frolich et.al. (1994) uses the master recession curve to set the limits at which streamflow rejoins baseflow. This is achieved by applying an iterative algorithm to the streamflow series to find a lower limit for the baseflow series.

The rising limb of the hydrograph is considered the upper limit of baseflow. The equation of the master recession curve is applied backwards in time, until the master recession curve value at a point is calculated as greater than the streamflow at that point. The recession curve is then transposed to the limit of the point. This produces the lower limit of the baseflow hydrograph. The upper limit (represented by the streamflow) and this calculated lower limit are averaged to produce an approximate baseflow series. The strength of this method lies in its being easily automated and its objective application of the master recession curve to determine the baseflow across the whole event.

However, the baseflow that is determined is taken as simply the average of an upper and lower limit, which involves significant assumptions. This method also relies on the determination of a suitable Master Recession Curve, which requires dry periods in the series to be identified as pure baseflow. Frolich et.al. (1994) apply the method on a monthly timestep.

Tularam and Ilahee

This method is based on the application of Equation 11. In application of this method to hourly data the fraction of quickflow, α, was determined by trial and error. This poses similar problems as other subjective methods. Tularam and Ilahee attempted to create a generalised parameter value by calculating α on a number of events in a particular catchment, averaging them, and then applying the resulting parameter value on all events in the catchment. Figure 66 and Figure 67 show the difference in baseflow series created with an averaged parameter value and a subjectively determined value.

This method produces relatively satisfactory results for baseflow in the cases shown. However, the computational effort required to determine parameter values for a large number of catchments would be significant given the need to obtain a generalised parameter for a number of events at each site. The possibility of using a parameter value averaged across a number of catchments exists, but would likely result in increasingly less successful results.
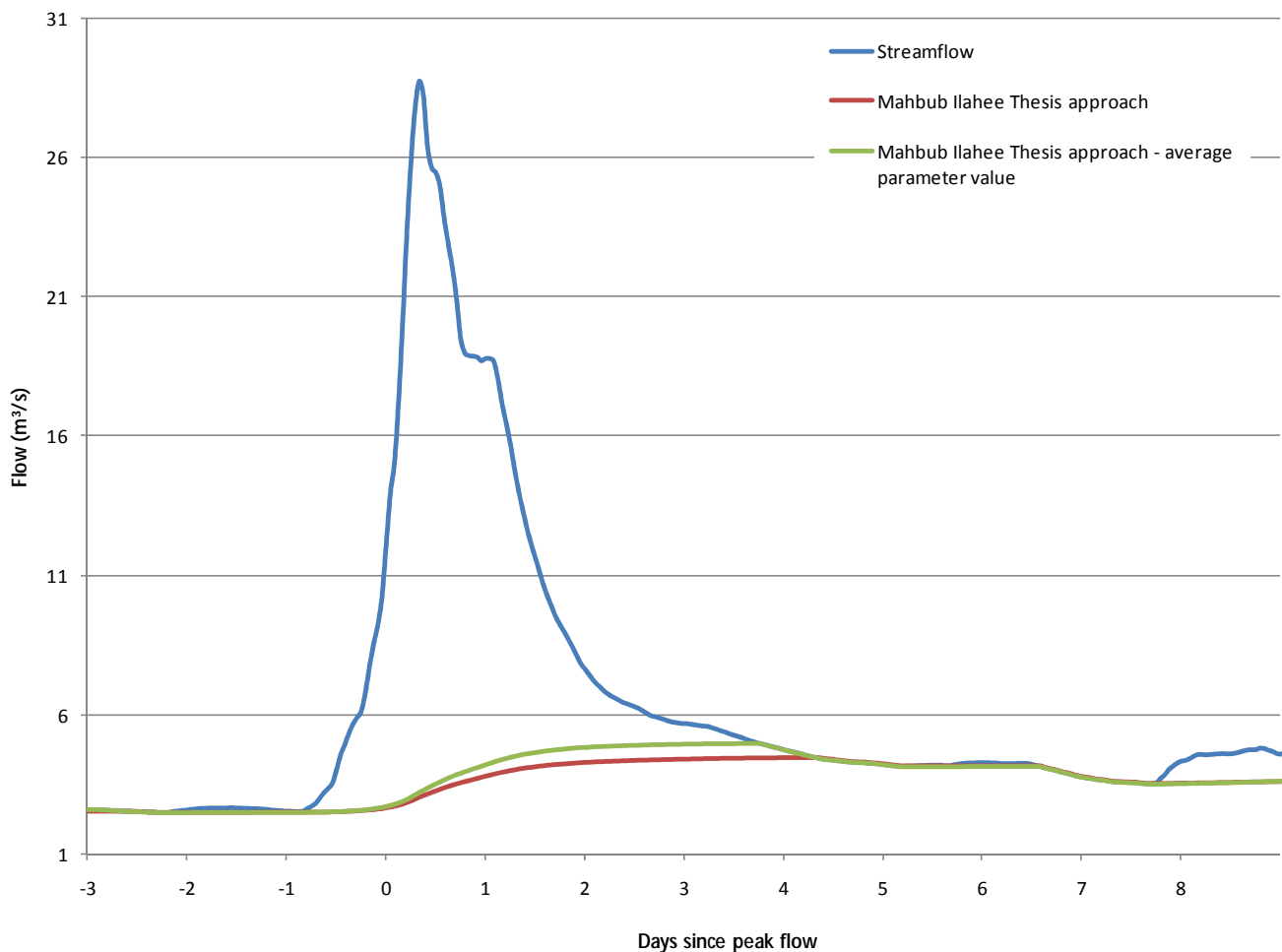
Figure 66 Mahbub Ilahee Thesis approach for 1 in 30 year event at Little Yarra River, Victoria, applied to hourly data
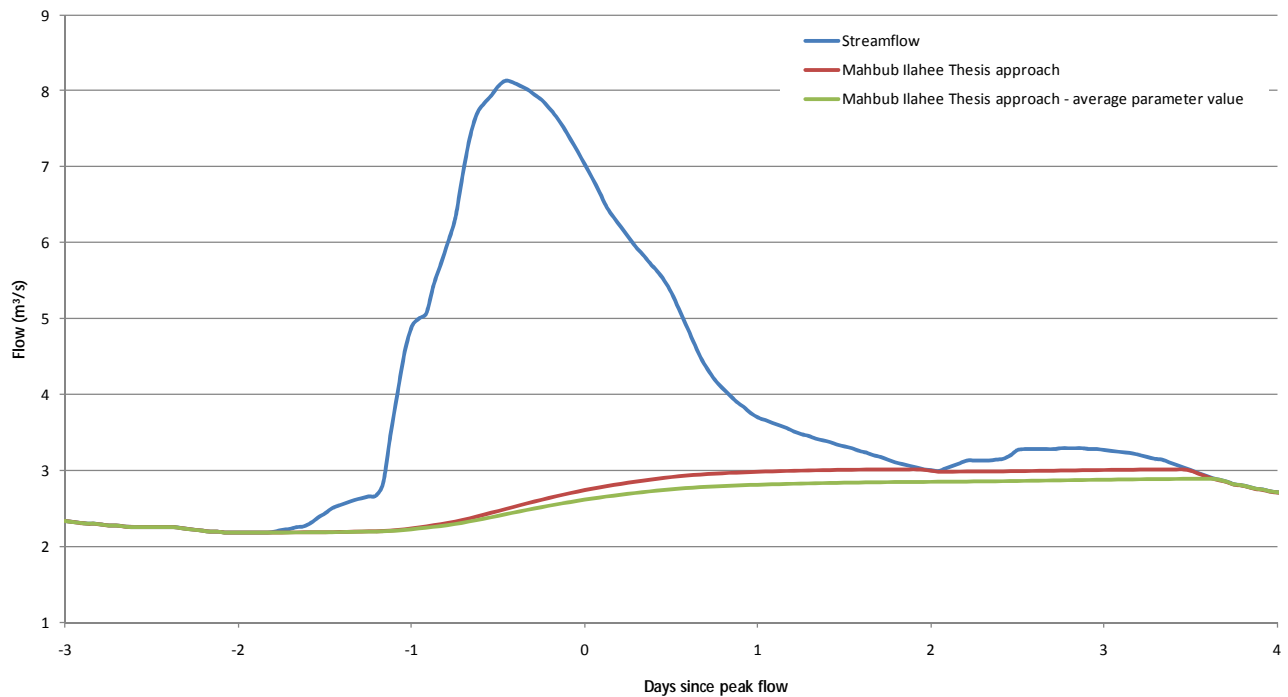
Figure 67 Comparison of baseflow techniques for 1 in 1 year event at Little Yarra River, Victoria using hourly data

Furey and Gupta algorithm

The Furey and Gupta algorithm utilises both streamflow and precipitation data series to determine a baseflow series that is based on physically meaningful parameters. This method also provides means by which parameters can be estimated, rather than selecting by trial and error.

The algorithm consists of four parameters, three of which are calculated from the data before application and the fourth which may be manipulated. The recession constant is one of the parameters, and is calculated using the rainfall series data. It is calculated by extracting the periods of streamflow over which no rainfall occurs, since these are assumed to consist of only baseflow. Of these periods, the days that have a higher streamflow than those before them are assumed to be affected by groundwater recharge or undetected precipitation and are removed from the recession analysis. The remaining periods that have at least 10 days since the last rainfall event are shown to have a narrow range of recession constants, and the mean of these is considered the recession constant for the basin. Thus, the baseflow series is estimated based on physical processes.
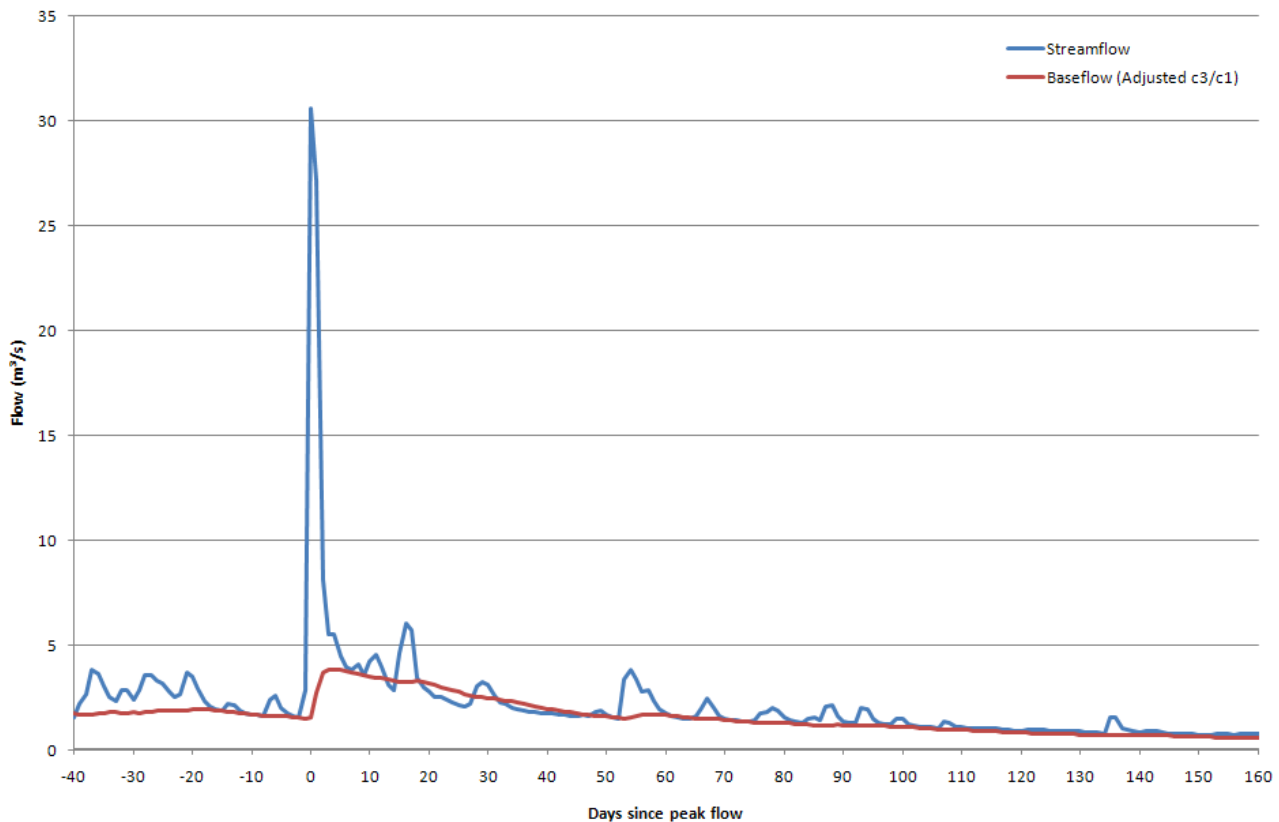
Figure 68 Furey and Gupta method (unconstrained) applied on daily timestep and with parameters manually adjusted, at Little Yarra River, Victoria

One particular feature of the Furey-Gupta method is that the algorithm is not constrained so that the baseflow is always lower than the streamflow. This maintains the parameters as strictly physically-based, but leads to unrealistic outcomes when the calculated baseflow is higher than the streamflow. This is observed in Figure 68, which produced a series where baseflow exceeded streamflow for a comparable proportion of timesteps as the results documented by Furey and Gupta (2001).

The paper also presents a case where one of the parameters usually calculated from the data is artificially adjusted to produce a better result. Manipulation of the data used to produce Figure 68 produces a better separation than that achieved by strictly applying the method, but still produces a significant proportion of time when baseflow is greater than streamflow. This is considered to be a serious problem for applying the method over many sites, since manual manipulation to correct results can be time consuming.

The Furey-Gupta method produced reasonable magnitudes of baseflow and retained many of the features of an idealised baseflow, such as a delayed peak. It is possible that this method and its physical basis may be an attractive option for development. However, it does not perform acceptably well to justify the significant increase in processing required to source and apply the method to hourly streamflow and rainfall data.

Wittenberg Method

This method has been applied for estimating the shallow groundwater balance in a semi-arid catchment in Western Australia (Wittenberg, 1999; Wittenberg and Sivapalan, 1999). It uses a

baseflow recession analysis to estimate a storage-discharge relationship for the groundwater aquifer. In addition, it places a greater weight than other methods on the role of seasonal evapotranspiration, which may be greater than baseflow in some arid conditions. Similar to most other methods, this method is empirically based.

The characterisation of the baseflow recession in this method is undertaken with the use of a single non-linear reservoir, with recession curve of the form:

$$Q_t = Q_0 \left[1 + \frac{(1-b)Q_0^{1-b}}{ab})t\right]^{1/(b-1)}$$

Equation 14

Where Q_t = Discharge at time, t

           Q_0 = initial discharge

           t = time

           a = coefficient relating to catchment properties

 b = dimensionless exponent

The parameters a and b are determined using a least squares fit, with a and b solved iteratively, where Q_t is equal to the observed recession curve. The set of a and b parameters that give the best fit to the recession curve are taken as being representative of the aquifer. In the application in this paper, the authors found that the values calculated as optimal for the recession curve were highly consistent for different parts of the recession curve.

The characterisation of the baseflow recession is seasonally based, calculated mostly using the parameter a, while the parameter b is maintained at a constant value of 0.5 in this case. b is found by calibration and has generally been found to be close to 0.5 for unconfined aquifers. This method has an increasing computational requirement compared to the other methods for determining baseflow recession. Any increase in accuracy gained from a more accurate seasonal recession characterisation will have to be considered against a significant increase in computational effort for each catchment.

Appendix B   Catchment Characteristics

Description	Unit	Catchment site number							
		110003	145018	204041	421018	223202	229214	803002	606001
Catchment area	km^2	231.2	80.7	1636.9	1247.5	902.6	154.0	440.0	436.6
Latitude of catchment centroid	decimal degrees	145.5	152.6	152.9	149.0	147.8	145.7	125.3	116.6
Longitude of catchment centroid	decimal degrees	-17.3	-28.3	-30.0	-33.0	-37.1	-37.8	-17.2	-34.6
Mean annual rainfall	mm/yr	1734.4	1350.7	1407.0	725.4	931.0	1350.3	919.8	997.4
Mean annual evaptranspiration	mm/yr	1155.1	827.2	862.1	684.7	701.7	703.5	739.9	946.7
Mean slope	degrees	3.9	9.6	4.6	2.8	9.4	8.1	6.0	1.5
Mean elevation	m	820.5	538.0	155.1	569.8	815.3	374.8	398.4	179.1
Total stream length in catchment	km	186.5	68.5	1376.3	972.8	661.4	109.7	400.2	231.6
Stream density in catchment	m/km^2	806.7	848.9	840.8	779.8	732.7	712.4	909.4	530.5
Number of stream junctions	no./km^2	33.0	14.0	239.0	162.0	132.0	21.0	92.0	36.0
Average soil depth	m	1.4	0.9	1.0	0.9	1.0	1.1	0.9	0.8
Proportion of woody vegetation	%	34.3	72.7	73.9	8.3	79.4	84.7	1.9	97.8
Average plant available water holding capacity	mm	191.2	118.3	102.8	92.8	133.0	139.3	128.7	144.9
Top soil layer nominal field water capacity	m	0.4	0.4	0.3	0.3	0.3	0.3	0.3	0.2
Top soil layer saturated hydraulic conductivity	mm/hr	216.5	162.3	106.8	215.8	175.4	268.8	205.9	299.3
Top soil layer saturated volumetric water content	m	0.6	0.5	0.4	0.5	0.5	0.5	0.5	0.4
Top soil layer thickness	m	0.2	0.2	0.3	0.2	0.3	0.3	0.2	0.6
Top soil layer nominal wilting point water capacity	m	0.2	0.2	0.1	0.2	0.2	0.1	0.2	0.1
Lower soil layer nominal field water capacity	m	0.4	0.4	0.4	0.4	0.4	0.3	0.3	0.2
Lower soil layer saturated hydraulic conductivity	mm/hr	71.2	51.9	20.2	75.4	55.1	89.5	120.8	299.0
Lower soil layer saturated volumetric water content	m	0.5	0.4	0.4	0.4	0.5	0.4	0.4	0.4
Lower soil layer thickness	m	1.1	0.7	0.7	0.6	0.7	0.7	0.8	0.5
Lower soil layer nominal wilting point water capacity	m	0.3	0.3	0.3	0.3	0.3	0.2	0.2	0.1
Weighted average conductivity based on proportion of catchment with each geology type	m/day	3.1	0.2	0.3	1.5	0.3	0.1	0.3	0.2
Weighted storage ranking based on proportion of catchment with each geology type	%	3.7	1.1	1.1	2.3	1.2	1.3	1.0	1.6
Weighted average conductivity based on proportion of river reach intersecting with each geology type	m/day	3.0	0.2	0.3	1.3	0.2	0.2	0.2	0.2
Weighted storage ranking based on proportion of river reach intersecting with each geology type	%	3.9	1.1	1.2	2.1	1.2	1.7	1.0	1.6

## Appendix C   Additional results for case study catchments

Barron River at Picnic Crossing, Queensland (110003a)

$y = 0.3145x^{-0.378}$
$R^2 = 0.4614$

$y = 9.0734\ln(x) + 18.286$
$R^2 = 0.7325$
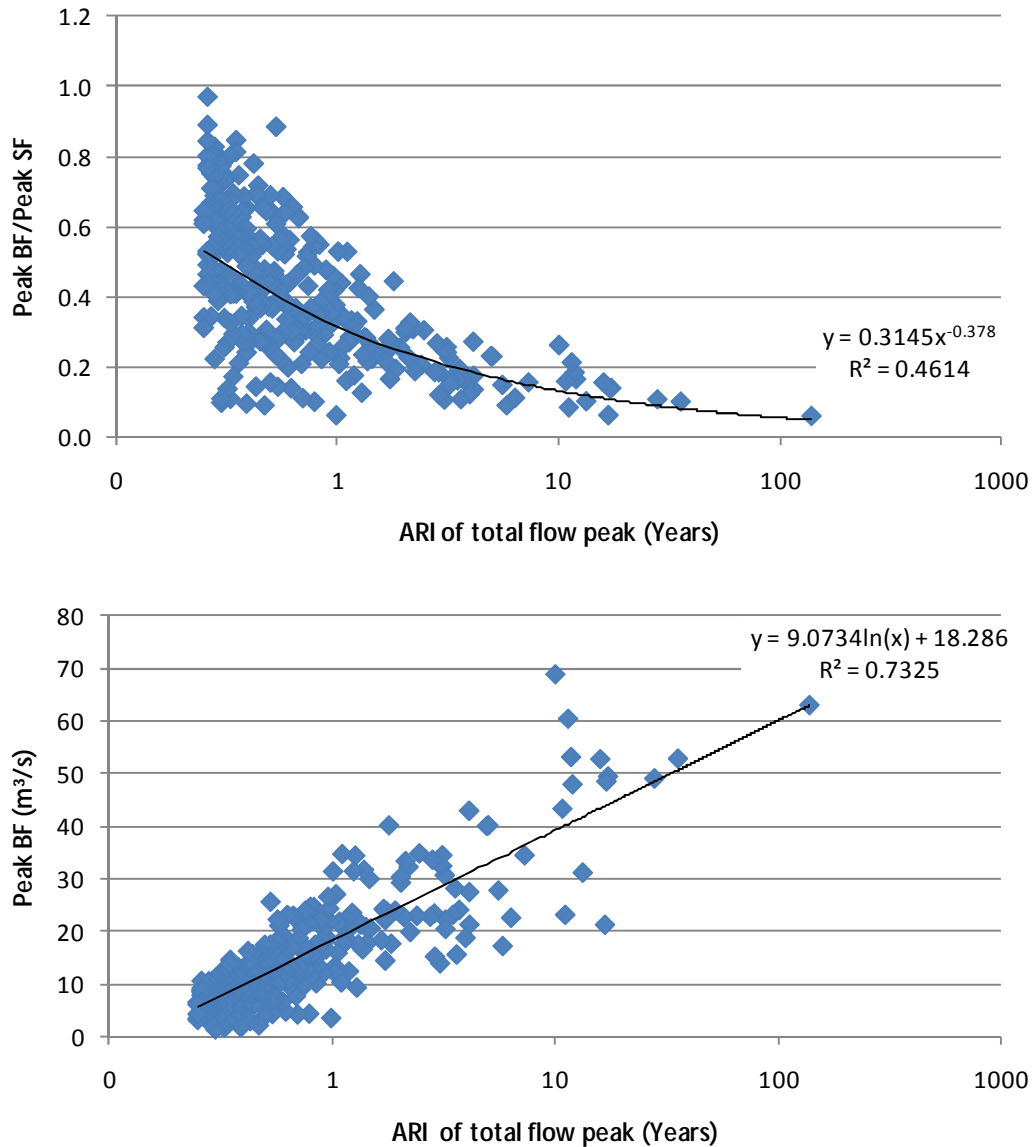
Figure 69 (a) Ratio of peak baseflow to peak streamflow, (b) Absolute magnitude of baseflow peak, Barron River at Picnic Crossing (110003a)

Burnett Creek upstream of Maroon Dam, Queensland (145018a)

$$y = 0.0329x^{-0.285}$$
$$R^2 = 0.0774$$

$$y = 1.2735\ln(x) + 1.8984$$
$$R^2 = 0.4615$$
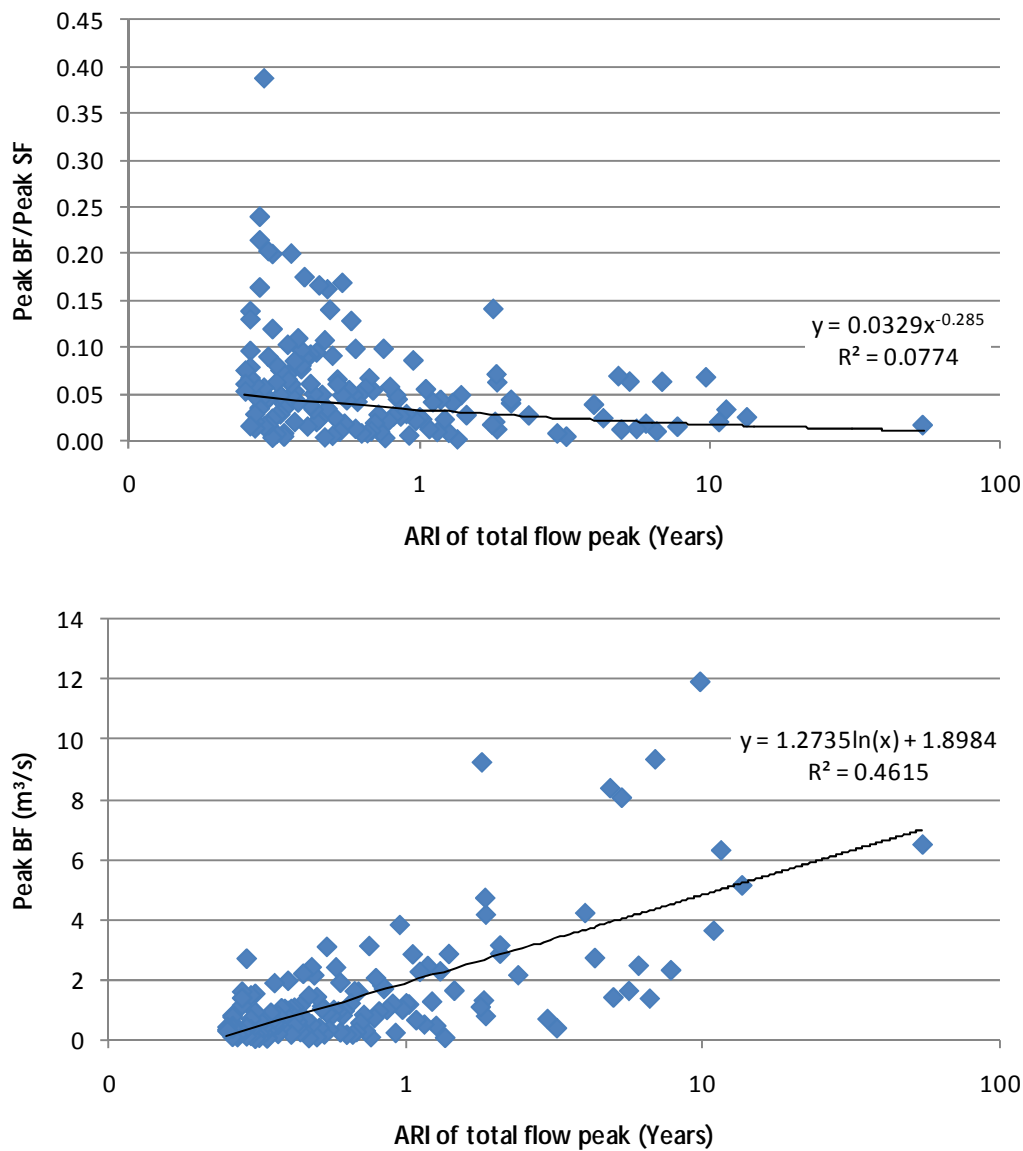
Figure 70 (a) Ratio of peak baseflow to peak streamflow, (b) Absolute magnitude of baseflow peak, Burnett Creek upstream of Maroon Dam (145018a)

Orara River at Bawden Bridge, New South Wales (204041)
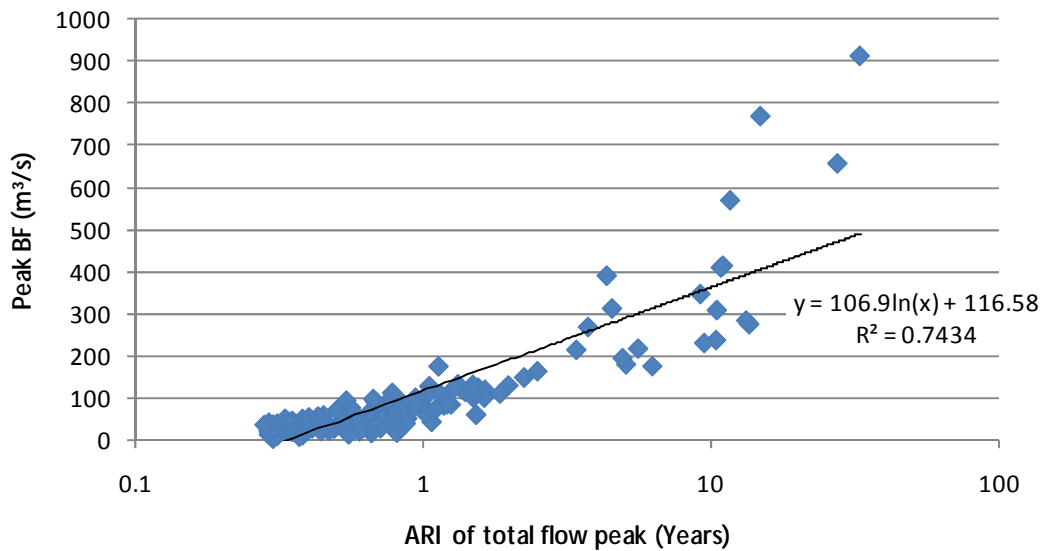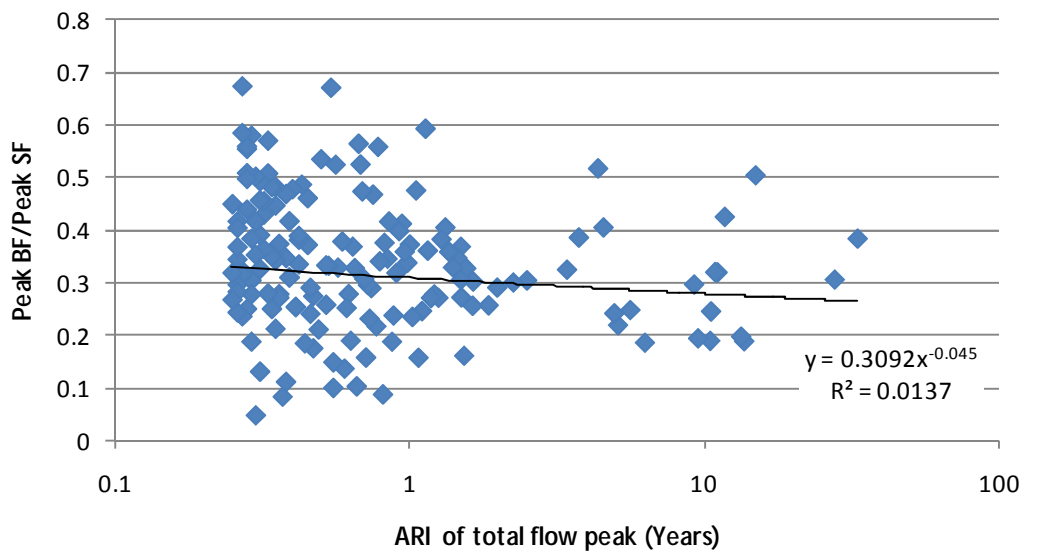
Figure 71 (a) Ratio of peak baseflow to peak streamflow, (b) Absolute magnitude of baseflow peak, Orara River at Bawden Bridge (204041)

Bell River at Newrea, New South Wales (421018)
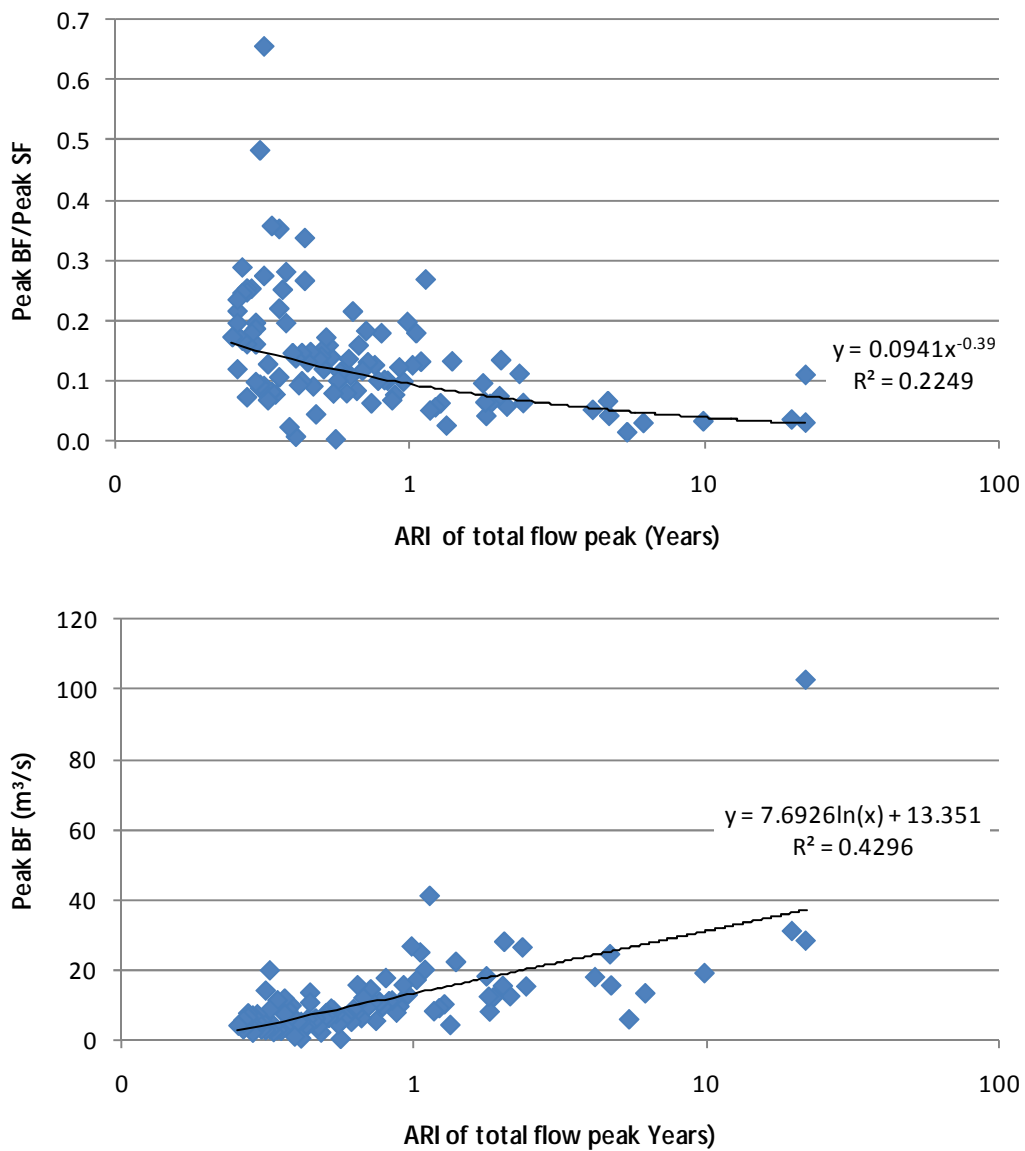
Figure 72 (a) Ratio of peak baseflow to peak streamflow, (b) Absolute magnitude of baseflow peak, Bell River at Newrea (421018)
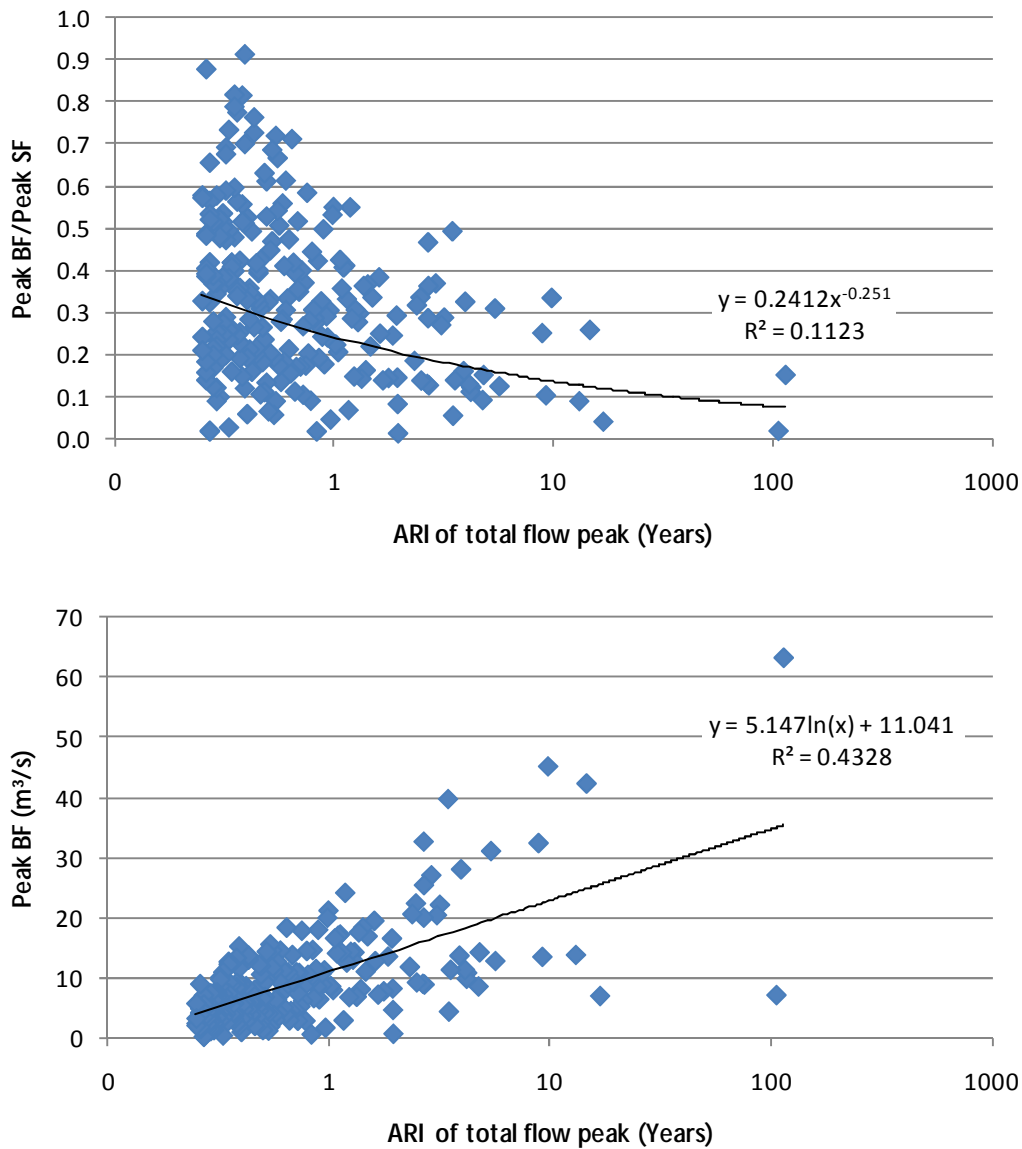
Tambo River at Swifts Creek, Victoria (223202)

Figure 73 (a) Ratio of peak baseflow to peak streamflow, (b) Absolute magnitude of baseflow peak, Tambo River at Swifts Creek (223202)

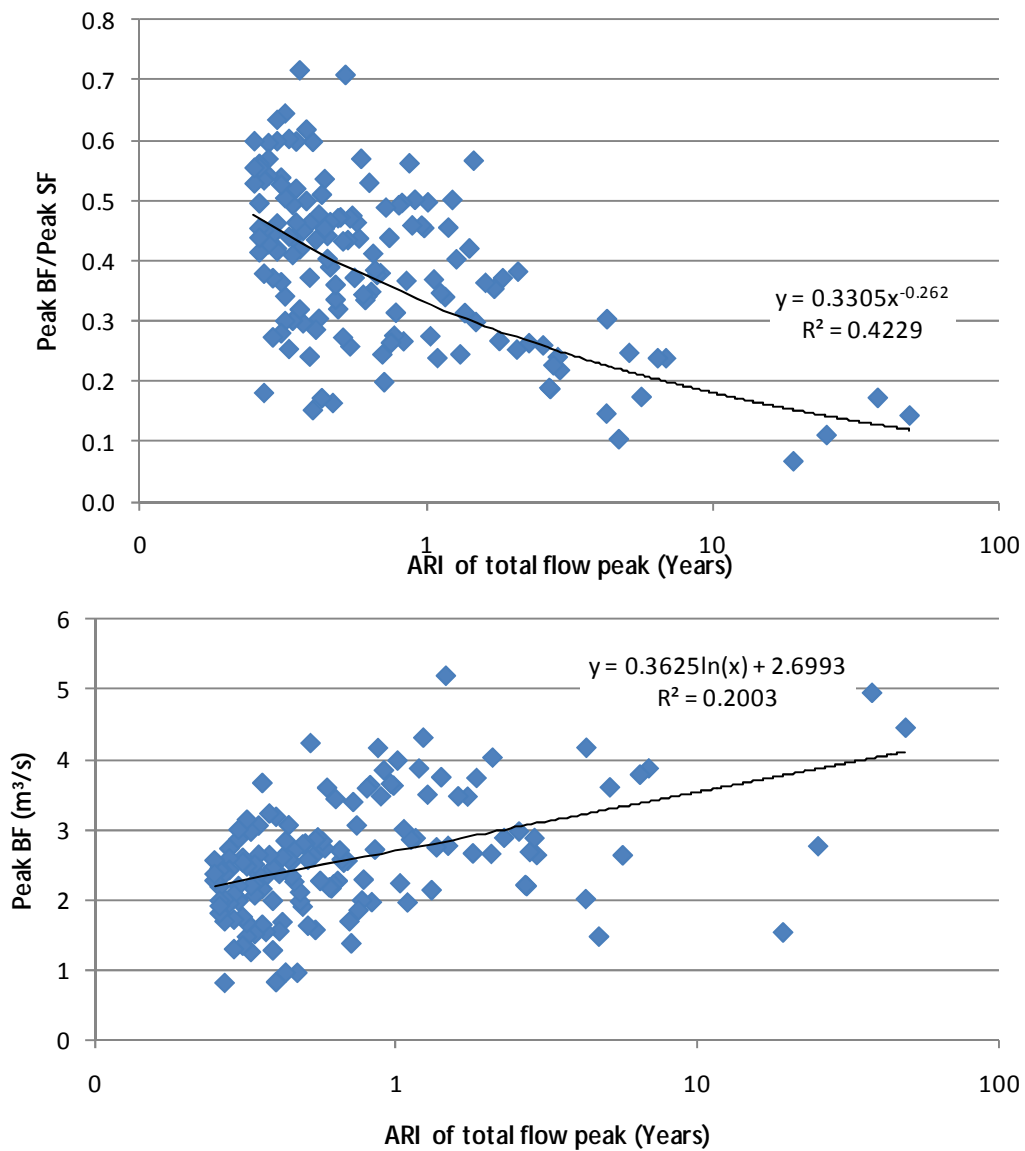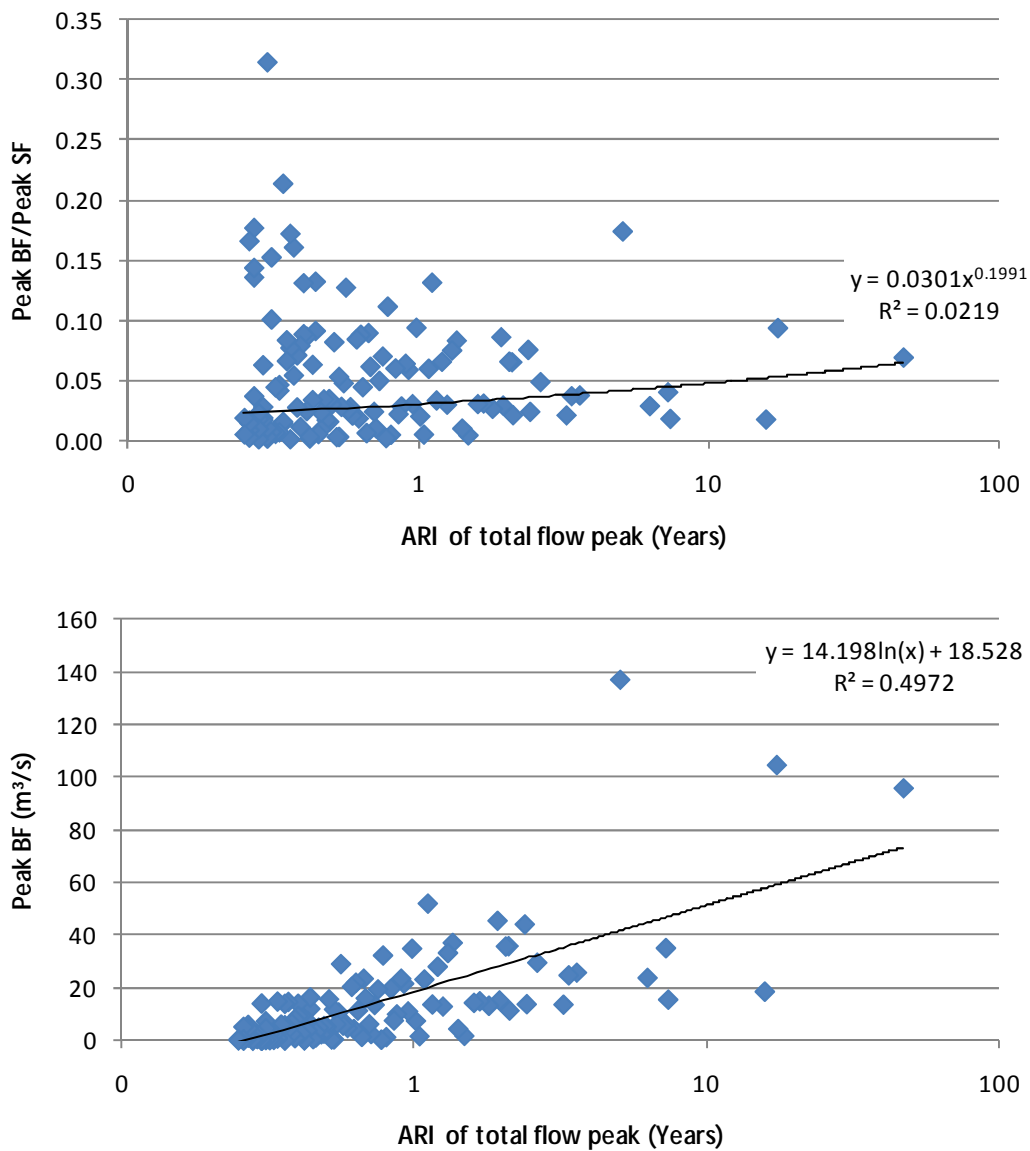## Little Yarra River at Yarra Junction, Victoria (229214)

Figure 74 (a) Ratio of peak baseflow to peak streamflow, (b) Absolute magnitude of baseflow peak, Little Yarra River at Yarra Junction (site 229214)

Lennard River at Mt Herbert, Western Australia (803002s)

Figure 75 (a) Ratio of peak baseflow to peak streamflow, (b) Absolute magnitude of baseflow peak, Lennard River at Mount Herbert (803002s)